Preface

The present Thesis is written in partial fulfilment of the requirements for the degree of *Doctor of Philosophy, Ph.D.,* from the *Technical University of Denmark*. The work was supported financially by a scholarship from the Technical University of Denmark and carried out at the *Department of Mathematical Modelling* under the supervision of Docent, dr. techn. Peter Leth Christiansen (main supervisor, Department of Mathematical Modelling), Professor, dr. sc. Alwyn C. Scott (Department of Mathematical Modelling and Department of Mathematics, University of Arizona), Lector, lic. techn. Mads Peter Sørensen (Department of Mathematical Modelling), and Senior Scientist, lic. techn. Jens Juul Rasmussen (Optics and Fluids Dynamics Department, Risø National Laboratory).

The work presented in this Thesis is the result of close collaboration with several scientists, and the main part of the work has been published before in the articles [1–17], and the conference proceedings [18–26] or is going to be published [27]. The most important 13 articles [1–13] form the core of the Thesis. The Thesis consists of a review, the purpose of which is to relate the 13 articles and summarize the results. Finally, the 13 articles will be given in their complete form.

Lyngby, February 1997

Kim Ø. Rasmussen

Abstract

This Thesis deals with nonlinear and stochastic dynamics in systems which can be described by nonlinear Schrödinger models. Basically three different models are investigated. The first is the continuum nonlinear Schrödinger model in one and two dimensions generalized by a tunable degree of nonlinearity. Various perturbations such as fluctuating forces, localized impurities, and dissipation are considered. The second kind of model is the discrete nonlinear Schrödinger model, which also is investigated in one and two dimensions. External perturbations similar to the continuum case are also considered in the discrete model. Finally, nonlinear Schrödinger continuum and discrete models with nonlocal dispersion are investigated.

In the introductory chapter the physical situation of energy transport on molecular aggregates in which the results applies is discussed in detail. This chapter also introduces the nonlinear Schrödinger model in one and two dimensions, discussing the soliton solutions in one dimension and the collapse phenomenon in two dimensions. Also various analytical methods are described.

Then a derivation of the nonlinear Schrödinger equation is given, based on a Davydov like system described by a tight-binding Hamiltonian and a harmonic lattice coupled by a deformation-type potential. This derivation results in a two-dimensional nonlinear Schrödinger model, and considering the harmonic lattice to be in thermal contact with a heat bath we show that the nonlinear Schrödinger equation must be augmented by a multiplicative noise term. The resulting stochastic model is investigated in the continuum limit and the behavior of the coherent excitations under the influence of the noise is studied. Similarly, we study the fluctuation effects on the two-dimensional collapse phenomenon. We find numerically and analytically that the collapse can be delayed and ultimatively arrested by the fluctuations. Allowing the system to reach thermal equilibrium we further augment the model by a nonlinear damping term and find that this prohibits collapse in the strict mathematical sense. However a collapse like behavior still persists in the presence of the nonlinear damping. Apart from the absence of the collapse in the strict mathematical sense we find that the nonlinear damping term has rather weak influence on the interplay between fluctuations and self-focusing. The study of the continuum model is concluded by an investigation of the dynamics of localized states in the vicinity of an impurity.

Studying the discrete nonlinear Schrödinger model, we first analyze the in-

trinsically localized excitations supported by this model in one dimension. This analysis is accomplished using analytical methods developed for nonlinear maps. It is demonstrated how the nonanalyticity of the map through homoclinic and heteroclinic connections permits the existence of localized states on the lattice. The pinning effect of the discrete lattice is also investigated, constructing a Melnikov function describing qualitatively the difference between on-site and inter-site states.

Since the intrinsically localized excitations are rather robust we further study the implications of fluctuations and nonlinear damping in this discrete model. The fluctuations are found always to destroy the localized states.

Existence and dynamics of the intrinsically localized excitations in the two-dimensional discrete model are also studied. It is found that in two dimensions a bistability phenomenon of the localized states appears. The bistability expresses itself by allowing localized states of various width to have equal norms. We find in the two-dimensional discrete model that the interplay of the collapse effect and the discrete pinning allows dynamical creation of a spatially distributed set of localized states from a broad initial excitation.

The last kind of models studied in the Thesis is nonlinear Schrödinger models with nonlocal dispersive interaction. First a continuum model with an exponential dependence of dispersive interaction is studied. This model shows in contrast to the ordinary continuum nonlinear Schrödinger models that the nonlocality imposes an upper bound on the norm of a possible localized excitation. The model is also shown to support a cusp soliton. A similar discrete nonlocal model is discussed. This model has an algebraic dependence of the dispersive interaction. There exists no upper limit of the norm in the discrete model, but the possibility of a bistability phenomenon similar to that of the two-dimensional model is shown to occur.

Finally, we show that a two-dimensional Kronig-Penney model describing for example propagation of electromagnetic waves in photonic bandgap materials can be reduced to a one-dimensional nonlocal nonlinear Schrödinger model, which is similar to the nonlocal models considered previously.

Dansk resumé

Nærværende afhandling omhandler ikke-lineær og stokastisk dynamik af systemer, som kan modelleres ved hjælp af den ikke-lineære Schrödingerligning. Tre forskellige modeller studeres. Den første er kontinuumsversionen af den ikke-lineære Schrödingermodel i henholdsvis én og to dimensioner. Modellen er generaliseret således, at muligheden for en regulerbar grad af ikke-linearitet er medtaget. Forskellige perturbationer såsom fluktuerende eksterne kræfter, lokaliserede urenheder og dissipation er betragtede. Den anden form for model, som er betragtet i afhandlingen, er den diskrete ikke-lineære Schrödingermodel i én såvel som i to dimensioner. Også i den diskrete version er effekter af de ovenfor nævnte eksterne perturbationer betragtede. Endelig studeres som den tredie art model kontinuumsversioner og diskrete versioner af ikke-lineære Schrödingermodeller med ikke-lokale dispersive led.

Indledningsvis beskrives fysiske situationer, hvor de opnåede resultater finder anvendelse. Endvidere introduceres den ikke-lineære Schrödingerligning ved en diskussion af solitonløsningerne af den éndimensionale version og kollapsfænomenet i den todimensionale version. Kapitlet beskriver også forskellige analytiske metoder, som anvendes i forbindelse med den ikke-lineære Schrödingerligning.

Udledningen af den ikke-lineære Schrödingerligning, som den forekommer i afhandlingen, er baseret på et system som ligner Davydovsystemet. Dette system er beskrevet ved en tight-binding Hamiltonfunktion og ved et harmonisk gitter, hvor tight-binding systemet og gitteret er koblet sammen via et deformationspotentiale. Idet vi betragter det harmoniske gitter som værende i termisk kontakt med et varmereservoir, vises det, at den ikke-lineære Schrödingerligning skal modificeres med et multiplikativt støjled. Den resulterende stokastiske model undersøges i kontinuumsgrænsen, hvor udviklingen af kohærente excitationer under støjpåvirkningen analyseres. Ligeledes er støjpåvirkningen af det todimensionale kollaps studeret. Vi finder ved analytiske og numeriske metoder, at kollapset bliver forsinket og ultimativt ophører med at eksistere som følge af støjen. Det vises, at modellen yderligere må modificeres med et ikke-lineært tabsled, hvis systemet skal kunne opnå termisk ligevægt. Det ikke-lineære tabsled medfører, at kollapset i matematisk stringent forstand ikke længere kan forekomme i modellen, hvorimod den modificerede model opretholder muligheden for en kollapslignede effekt. Bortset fra at kollaps ikke eksisterer i stringent matematisk forstand, viser det sig, at det ikke-lineære tabsled ikke har nogen

afgørende betydning for samspillet mellem fluktuationerne og selvfokuseringseffekten. Studiet af kontinuumsmodellen afsluttes med en undersøgelse af den dynamik, som udvises af lokaliserede excitationer, når de befinder sig i umiddelbar nærhed af en urenhed.

Hvad angår den diskrete ikke-lineære Schrödingermodel, undersøger vi indledningsvis de intrinsisk lokaliserede excitationer, som denne model understøtter i én dimension. Denne undersøgelse udføres ved anvendelse af analytiske metoder, som er udviklet til brug ved analyse af ikke-linære afbildninger. Vi demonstrerer, hvordan den ikke analytiske afbildning svarende til den diskrete ikke-lineære Schrödingermodel gennem homokline og heterokline forbindelser muliggør eksistensen af lokaliserede excitationer på det diskrete gitter. Desuden konstrueres en Melnikovfunktion til kvantitativ beskrivelse af den diskrete pinning-effekt, som stærkt lokaliserede excitationer udsættes for på gitteret.

Eftersom de intrinsisk lokaliserede excitationer synes at være usædvanligt robuste, undersøger vi, hvordan disse påvirkes af et ikke-lineært tab kombineret med fluktuationer. Det viser sig, at fluktuationerne altid destruerer de lokaliserede excitationer.

Endvidere studeres eksistensen og dynamikken af intrinsisk lokaliserede excitationer i den todimensionale diskrete model. Vi finder, at der i denne model forekommer et bistabilitetsfænomen af de lokaliserede løsninger. Dette bistabilitetsfænomen giver sig til kende ved at tillade to forskellige løsninger at have den sammen norm. Desuden giver den todimensionale diskrete model ved at kombinere kollapseffekten og pinning-effekten mulighed for dynamisk at skabe et antal rumligt distribuerede lokaliserede excitationer ud fra en delokaliseret excitation.

Endeligt studeres ikke-lineære Schrödingermodeller med ikke-lokale dispersive effekter. Først studeres en kontinuumsmodel, hvor den dispersive kobling afhænger eksponentielt af koblingsafstanden. Denne model viser i kontrast til almindelige kontinuums ikke-lineære Schrödingermodeller, at der pga. ikke-lokaliteten er en øvre grænse for normen af de lokaliserede excitationer. En lignende diskret model, hvor den ikke-lokale kobling afhænger algebraisk af koblingsafstanden, er også diskuteret. I dette diskrete tilfælde er der ingen øvre grænse for normen, men der optræder et bistabilitetsfænomen ækvivalent til det, der forekommer i den diskrete todimensionale model.

Til sidst vises det, hvordan en todimensional Kronig-Penney-model, som bl.a. beskriver udbredelsen af elektromagnetiske bølger i dielektriske supergitre, kan reduceres til en éndimensional ikke-lokal model.

Acknowledgements

The work presented in this Thesis is a result of collaboration, and it is difficult to imagine the work without the help and support of a number of people. For this reason, I write "we" throughout the Thesis.

During the three years of Ph.D. study I have learned tremendously much and I would like to thank everyone who has contributed in making these three years a challenging, stimulating and rewarding time.

First, I would like to express my sincere gratitude to my four supervisors, Peter L. Christiansen, Jens Juul Rasmussen, Alwyn C. Scott, and Mads Peter Sørensen.

Special thanks go to Peter L. Christiansen for his dedication in my work and for having the patience to try to teach me the virtue of being precise. I am also grateful that he has provided me with many possibilities of working abroad and with numerous valuable contacts from which I have highly benefited.

Also, a special thanks to Jens Juul Rasmussen for his never failing interest in my work, and for the many stimulating discussions we have had.

A very special thanks go to Yuri B. Gaididei who has visited MIDIT several times during my study and with whom I done a large part of the work included in the Thesis. I am grateful to Yuri for having the patience to teach me very many things about nonlinear physics.

I am also grateful to Ole Bang for getting me started and for the much encouragement he has given me.

A special thanks also go to Nikos Lazarides for his warm friendship and for his encouragements.

I have also a special thanks to Magnus Johansson for sharing his large knowledge on discrete systems and numerical methods and for the many fruitful discussions. Furthermore, I wish to thank Magnus for his effort in proof reading the Thesis and for his many valuable suggestions for improvements.

Volodja Mezensev and Luc Bergé are also thanked for sharing their large knowledge of nonlinear systems and for the many rewarding and entertaining discussions we have had.

I also whish to thank my fellow Ph.D. students: Svend Bischoff, Carl B. Clausen, Michel R. Schmidt, and Jens Trandum for the many stimulating discussions.

Lise Gudmandsen, our secretary at MIDIT, is thanked for her never failing cheerfulness and for making things work out.

In my three years at MIDIT there has been a never ceasing flow of visitors, far too many to mention everybody by name, but I wish to thank them all for spending the time and the effort to discuss with me.

I have spend more than seven month of the three years abroad and in this connection I wish to thank the following people:

George Tsironis for always having time to discuss and for his never failing enthusiasm during my two months stay in the Department of Physics at The University of Crete.

Luis Vázques for making my three week's stay in the Department of Theoretical Physics at the Universidad Complutense very pleasant.

Dirk Hennig and Helmut Gabriel for two rewarding visits to the Department of Theoretical Physics at the Free University of Berlin. Especially I wish to thank Dirk for his warm friendship and for having the patience to share some of his large amount of knowledge on dynamical systems with me. I thank Dirk for the very many things he has taught me and for the many pleasant hours I have spent in company with him, and his family.

Niels Grønbech-Jensen, Peter Lomdahl and Alan Bishop for making my two months stay in The Center of Nonlinear Studies at the Los Alamos National Laboratory possible, and for making it a very rewarding stay. In this connection I specially wish to thank David Cai for sharing his large amount of knowledge on nonlinear systems and for the many rewarding discussions. I also wish to thank David for the many pleasant hours we spend together after work. It is fair to say that David showed me aspects of New Mexico I would never have seen without him.

Last but certainly not least I wish to give my thanks and love to Annette, who have shown me endless amounts of love and affection, despite the time, effort and energy I have spent on this work.

Contents

Preface **i**

Abstract **iii**

Dansk resumé **v**

Acknowledgements **vii**

1 Introduction **1**
1.1 Overview and strategy 1
1.1.1 List of papers 2
1.2 Physical context 4
1.2.1 Scheibe aggregates 8
1.3 The Nonlinear Schrödinger Equation 12
1.3.1 Properties in one dimension 12
1.3.2 Properties in two dimensions 15

2 Continuum models **21**
2.1 Introduction 21
2.2 Effects of fluctuations 21
2.3 Effects of nonlinear damping 30
2.4 Effects of impurities 33
2.5 Conclusion 37

3 Discrete models **39**
3.1 Introduction 39
3.2 Discrete nonlinear Schrödinger equations 39
3.3 Solitonlike solutions 42
3.4 Noise effects on discrete solitonlike excitations 49
3.5 Two-dimensional effects 52
3.6 Conclusion 56

4 Nonlocal models **57**
4.1 Introduction 57
4.2 Physical origin 57
4.3 Continuum description 58
4.4 Discrete description 61
4.5 Two-dimensional Kronig-Penney model 66
4.6 Conclusion 68

Index **69**

Bibliography **69**

5 Paper I **83**

6 Paper II **95**

7 Paper III **109**

8 Paper IV **117**

9 Paper V **123**

10 Paper VI **131**

11 Paper VII **145**

12 Paper VIII **153**

13 Paper IX **169**

14 Paper X **179**

15 Paper XI **193**

16 Paper XII **199**

17 Paper XIII **211**

Chapter 1

Introduction

1.1 Overview and strategy

The present Thesis is a collection of work illuminating different aspects of the most generic and universal simple nonlinear model: *The nonlinear Schrödinger equation*.

The physical subject which formed the foundation of the thesis work is described in the following section (section 1.2) while an introduction to the mathematics of the nonlinear Schrödinger equation will be the subject of the final section (section 1.3) of this introduction. Section 1.3 shall also introduce the analytical methods which are essential for the remaining part of the Thesis.

The work divides naturally into three parts. The first part presented in chapter 2 (Paper I-Paper VII) deals with the continuum nonlinear Schrödinger equation as a model of molecular aggregates. This part studies the coherence of an excitation in the presence of noise and it also studies the collapse phenomenon in the presence of noise.

Chapter 3 (Paper VIII-Paper X) presents the second part of the Thesis, which deals with one and two-dimensional discrete nonlinear Schrödinger equations. The existence and stability properties of localized excitations in these models are studied. This part also studies the behavior of localized excitations in the one-dimensional discrete nonlinear Schrödinger equation in the presence of noise and nonlinear damping.

The review part of the Thesis ends with chapter 4 (Paper XI-Paper XIII) which deals with continuum and discrete nonlinear Schrödinger equations with nonlocal dispersive interaction. The existence and stability properties of localized excitations in the presence of nonlocal dispersive interactions are studied.

Finally, chapter 5-17 contains the 13 articles in their full extent.

The spirit in which the Thesis is written is that of a review paper, which first presents in short form the physical context and the basic knowledge required. Then it proceeds to give a concentrated description of the new work of the

13 articles forming the core of the Thesis. The material of the 13 articles is presented in review form in the chapters 2-4. Review form implies that only the main results are commented on and they are given almost without details of analytics and numerics. This is meant to give a continuous and coherent presentation of the results. Effort has been made to relate the results to each other and to show the logic and reason of the next step in the investigation. Apart from the results, background knowledge and extensive reference to the results of other researchers has been provided in proper relations. Therefore all the main points of the thesis work can be found in the first four chapters while all the many details must be sought in the specific article. Making this possible this overview shall conclude by defining the names of the articles directly contained in the Thesis. The names Paper I-Paper XIII will below each be connected to an article and all the way through the Thesis this name will be applied when referring to one of these article, in contrast to the articles cited in the reference list which will be referred to by a number in square brackets.

The outlined strategy presents however the technical difficulty that the notation changes slightly from article to article. In the three following chapters one certain notation is chosen and is maintained throughout these chapters, and whenever a new notation or quantity is introduced an appropriate explanation is given. The notation of the next three chapters may however occasionally conflict with the notation of the articles. In particular Paper IV has a conflicting notation.

1.1.1 List of papers

Paper I [1]: O. Bang, P. L. Christiansen, F. If, K. Ø. Rasmussen, and Yu. B. Gaididei, "Temperature effects in a nonlinear model of monolayer Scheibe aggregates", Phys. Rev. E **49**, 4627 (1994).

Paper II [2]: O. Bang, P. L. Christiansen, F. If, K. Ø. Rasmussen, and Yu. B. Gaididei, "White noise in the two-dimensional nonlinear Schrödinger equation", Applicable Analysis, **57**, 3 (1995).

Paper III [3]: K. Ø. Rasmussen, Yu. B. Gaididei, O. Bang, and P. L. Christiansen, "The Influence of Noise on the Critical Collapse in the Nonlinear Schrödinger equation", Phys. Lett. A, **204**, 121 (1995).

Paper IV [4]: P. L. Christiansen, K. Ø. Rasmussen, O. Bang, and Yu. B. Gaididei, "The temperature-dependent collapse regime in a nonlinear dynamical model of Scheibe aggregates", Physica D **87**, 321 (1995).

Paper V [5]: P. L. Christiansen, Yu. B. Gaididei, M. Johansson, K. Ø. Rasmussen, and I. I. Yakimenko, "Collapse of solitary excitations in the nonlinear Schrödinger equation with nonlinear damping and white noise" Phys. Rev. E **54**, 924 (1996).

Paper VI [6]: Yu. B. Gaididei, K. Ø. Rasmussen, P.L. Christiansen, "Nonlinear excitations in two-dimensional molecular structures with impurities", Phys. Rev. E **52**, 2951 (1995).

Paper VII [7]: Yu. B. Gaididei, K. Ø. Rasmussen, P. L. Christiansen, "Dipole-like nonlinear excitations in an inhomogeneous two-dimensional system", Phys. Lett. A **203**, 175 (1995).

Paper VIII [8]: D. Hennig, K. Ø. Rasmussen, H. Gabriel and A. Bülow, "Solitonlike solutions of the generalized discrete nonlinear Schrödinger equation", Phys. Rev. E **54**, 5788 (1996).

Paper IX [9]: P. L. Christiansen, Yu. B. Gaididei, M. Johansson, and K. Ø. Rasmussen, "Breatherlike excitations in discrete lattices with noise and nonlinear damping", Phys. Rev. B **55**, 5759 (1997).

Paper X [10]: P. L. Christiansen, K. Ø. Rasmussen, Yu. B. Gaididei, V. K. Mezentsev, and J. Juul Rasmussen. "Dynamics in discrete two-dimensional nonlinear Schrödinger equations in the presence of point defects" Phys. Rev. B **54**, 900 (1996).

Paper XI [11]: Yu. B. Gaididei, P. L. Christiansen, S. F. Mingaleev, and K. Ø. Rasmussen, "Effect of nonlocal dispersion on self-interacting excitations" Phys. Lett. A **222**, 152 (1996).

Paper XII [12]: Yu. B. Gaididei, P. L. Christiansen, S. F. Mingaleev, and K. Ø. Rasmussen, "Effects of Nonlocal Dispersive Interactions on Self-Trapping Excitations", Phys. Rev. E **55**, 6141 (1997).

Paper XIII [13]: Yu. B. Gaididei, P. L. Christiansen, K. Ø. Rasmussen and M. Johansson, "Two-dimensional effects in nonlinear Kronig-Penney models", Phys. Rev. B **55**, R13365, (1997).

1.2 Physical context

Although the concrete physics of the Thesis is modelling the energy transfer in Scheibe aggregates the model which will appear (the derivation is described in Sec. 2.2) is a very general and generic model which turns the obtained results into results of general interest in a variety of physical contexts. A review of alternative physical systems where the results may find applications will therefore be given in here.

Before discussing specific physical contexts we shall in general terms describe the generic nature of the nonlinear Schrödinger (NLS) equation.

The NLS equation in the form

$$\frac{2ik_c}{\omega'}\left(\frac{\partial\psi}{\partial t}+\omega'\frac{\partial\psi}{\partial z}\right)+\nabla_\perp^2\psi+\frac{\omega''k_c}{\omega'}\frac{\partial^2\psi}{\partial z^2}+2k_c^2n(|\psi|^2)\psi=0, \tag{1.1}$$

describes the propagation of the scalar envelope $\psi(x,y,z,t)$ of the field $\vec{E}=\mathrm{Re}[\vec{e}\,\psi(x,y,z,t)\exp i(k_cz-\omega_0t)]$ of an almost monochromatic wave in a weakly nonlinear dispersive medium.

The equation (1.1) can be obtained by a multiple scale expansion of the high-frequency carrier wave equation permitting description of the slowly varying envelope of the beam. This implies that $\omega'=\partial\omega/\partial k|_{k_c}$ and $\omega''=\partial^2\omega/\partial k^2|_{k_c}$ is the group velocity and the dispersion coefficient (group velocity dispersion) along the propagation axis z, respectively. The diffraction of the wave in the transverse plane (x,y) perpendicular to the propagation axis is represented by $\nabla_\perp^2=\partial_x^2+\partial_y^2$. The nonlinearity $n(|\psi|^2)$ arises from the response of the medium to the wave amplitude. Assuming the response to be instantaneous it can simply be approximated by a first order Taylor expansion in powers of the beam intensity, $n(|\psi|^2)\propto|\psi|^2$.

An equivalent way to obtain Eq.(1.1) is by formally taking the Fourier transform in space and time of the expansion of the nonlinear dispersion law $\omega=\omega(k,n(|\psi|^2))$. The expansion must be in the components of the wave number k centered around the carrier wave number k_c of the unperturbed incident wave ($\omega_0=\omega(k_c)$) and in the variations of the refractive index $n(|\psi|^2)$ of the nonlinear medium.

In this manner Eq.(1.1) arises in various branches of physics concerned with the description of a high-frequency carrier wave slowly modulated.

One of the earliest applications of this sort was in nonlinear optics, which is still one of the branches of nonlinear science most accessible to experiments and theoretical analysis. Within nonlinear optics, Eq.(1.1) describes the influence imposed on the wave envelope by the refractive index n of the medium. Commonly the refractive index depends on the wave intensity via the so-called Kerr effect: $n=n_0+n_2|\psi|^2$. As given in Ref. [28] the nonlinear term simply becomes $2k_c^2n_2/n_0|\psi|^2\psi$ in this case. In the context of nonlinear optics, the variable t often refers to the longitudinal distance along the beam propagation axis, whereas the z occuring in the space derivatives corresponds to the retarded time $\tilde{t}=t-z/\omega'$. This means that the variables t and z are

interchanged in the context of nonlinear optics. Thus, the term $\partial^2\psi/\partial z^2$ in Eq.(1.1) represents temporal dispersion in nonlinear optics. The effect is often termed *group velocity dispersion* because of the coefficient $\omega'' k_c/\omega'$. Depending on the dispersive properties of the medium this coefficient can either be positive in the case of *anomalous* dispersive medium or negative in the case of *normal* dispersive medium. That the behavior of a beam crucially depends on whether the medium has normal or anomalous dispersion has been verified theoretically [29, 30] as well as experimentally [31]; normal dispersion causes filamentation of the beam while anomalous dispersion leads to self contraction and ultimatively collapse. In some cases, as for example when the temporal width of the beam is large, the temporal dispersion can be neglected causing the beam dynamics, at least initially, to be determined by a two-dimensional NLS equation.

At present a technologically important application of the NLS equation within optics is the description of optical pulse propagation along optical fibers. In this context the relevant NLS equation is one-dimensional and the derivation is similar to the above sketched. This application and the potential advantages of the soliton solution was first noted 1973 by Hasegawa and Tappert [32]. The purpose of applying the soliton property in optical communication was at that time apparently the possibility of letting the nonlinearity counter balance the invalidating pulse spreading effects caused by the dispersion. However, due to the development of the dispersion shifted fibers the soliton effect has become an appropriate way of dealing with the inevitable nonlinear effects. In any case the application of the NLS equation in optical communication remains one of its primary applications and a lot of research effort has been invested in investigating this field. A recent exposition of the development of the optical communication application is given by Hasegawa and Kodama [33]. Since first order nonlinear effects are intrinsically absent in optical fibers due to the inversion symmetry of SiO_2 and since the fibers are nearly completely transparent the specific example of pulse propagation on optical fibers probably is the one example where the NLS equation provides the most accurate description. In spite of this, the description can be improved by including terms which account for higher order effects as third order dispersion ψ_{ttt}, self-steepening $(|\psi|^2\psi)_t$ and self-frequency shift via stimulated Raman scattering $(|\psi|^2)_t\psi$ [34]. Note that the terms are given in the framework of optics and not in the notation used in Eq.(1.1). Augmented by such terms the NLS equation shows some rather interesting features, and in some special cases exact soliton solutions can still be found [35–37].

Also discrete versions of the NLS equation find application in nonlinear optics. For weakly coupled optical waveguides, coupled mode theory yields [38, 39] that the envelope ψ_n of the field in guide n obeys

$$i\partial_z\psi_n + (\psi_{n+1} - 2\psi_n + \psi_{n\perp 1}) + \beta''\partial_{tt}\psi_n + 2|\psi_n|^2\psi_n = 0, \qquad (1.2)$$

where the term $\partial_{tt}\psi_n$ as described above is due to the group velocity dispersion and the coefficient β'' can have both signs or be neglected depending on the actual situation. This description can quite naturally be extended to include two-dimensional fiber arrays just by extending the discrete derivative in

Eq.(1.2) to two dimensions. Since these equations are two-dimensional (three-dimensional) NLS equations which simultaneously are continuum and discrete, quite interesting effects arise [40].

Plasma physics is another branch of physics where the NLS equation appeared very early. It was first derived in this context from hydrodynamical equations using the so-called reductive perturbation method [41, 42]. The description of the coupling of a light wave into electron plasma waves by density fluctuations is also accomplished by a NLS equation in the form (1.1). It is possible for an excited plasma wave to beat with the imposed light wave creating variations in the electric field intensity. This gradient in the field intensity produces a force (the pondermotive force), which acts back on the plasma creating ion density fluctuations. Clearly this is a nonlinear effect and the fact that the pondermotive force is proportional to the field intensity leads to the cubic nonlinearity in the description. The final application in plasma physics we mention here is that the NLS equation can emerge from the Zakharov equations [43]. These equations describe the slowly varying Langmuir electric field amplitude coupled to the low frequency fluctuations of the electron density. In the limit where the ion inertia is neglected the Zakharov equations reduce to a NLS equation governing the envelope of the high frequency field. Naturally the NLS equation usually only yields idealized and approximative analysis, and therefore a variety of perturbations has to be considered to improve the description (see [44] e.g.).

The traditional application of discrete NLS models is in condensed matter physics, and we shall here give a brief explanation of how it appears and what it describes in this branch of physics.

The *tight-binding* approach is a traditional way [45] of calculating energy bands and electron wave functions for bands arising from weakly overlapping atomic orbitals in periodic solids. The tight-binding model is a one-electron model neglecting electron-electron interaction, and disregarding the coupling between orbitals belonging to different bands. Assuming further that each atom contributes only with one orbital, the tight-binding Hamiltonian can in second quantized form be written as

$$H = \sum_n V_n a_n^\dagger a_n + \sum_{n,m} J_{n,m} a_n^\dagger a_m \tag{1.3}$$

describing a periodic crystal with the on-site potential V_m and the hopping integral $J_{n,m}$. In Eq.(1.3) n and m are lattice site indices and $a_n^\dagger$ (a_n) is the creation (annihilation) operator for an orbital centered around site n. A moving electron can be described by $|\Psi\rangle$ whose time evolution is governed by the Hamiltonian (1.3) through the standard Schrödinger equation

$$i\hbar \frac{d|\Psi>}{dt} = H|\Psi> . \tag{1.4}$$

Expanding $|\Psi\rangle = \sum_m \psi_m |m\rangle$ and multiplying the resulting equation by a Wan-

nier localized state $\langle m|$, one obtains

$$i\hbar \frac{d\psi_m}{dt} = \sum_n J_{n,m}\psi_n + V_m\psi_m, \tag{1.5}$$

for the amplitudes ψ_m. In the presence of vibrations, V_m (and in principle also $J_{n,m}$) depends on the vibrational coordinates u_m. A simple and reasonable assumption is that V_m depends linearly on u_m. Considering only optical phonons it is reasonable that the lattice in absence of the interactions are harmonic oscillators, oscillating with the frequency ω. This makes it natural that u_m in the presence of interactions obeys

$$\frac{d^2u_m}{dt^2} + \omega^2 u_m = \text{const.} \times |\psi_m|^2. \tag{1.6}$$

Hence, the equilibrium position of the oscillator is changed by an amount proportional to the occupation probability at the respective site.

Now assuming the vibrations of the lattice to be faster than the time scale of the electron evolution, such that the vibrations are slaved by the probabilities, it is permissible to ignore the time derivatives in Eq.(1.6). This leaves the vibrational coordinate proportional to the occupation probability, and the discrete NLS equation is obtained for the occupation probability

$$i\hbar\dot{\psi}_m = \sum_n J_{n,m}\psi_n + \gamma|\psi_m|^2\psi_m, \tag{1.7}$$

where γ is a constant specified by the coupling between the lattice and the electron. The same result could have been reached starting from a Hamiltonian describing the particle, the vibrating lattice, and the interaction. The essential steps, originally given by Holstein [46], being to neglect the kinetic energy terms and expanding the wave function in Wannier states as above.

The discussion of the appearance of the discrete NLS equation in condensed matter physics given above is of course not very precise but it hopefully conveys the essential physical content. A more thorough derivation including the microscopic subtleties can be found e.g. in [47]. A nice account of the many applications the discrete NLS equation has in condensed matter physics has been given by Kenkre [48].

The Davydov model of energy transport on α-helix proteins is also an example which under assumptions similar to those of Holstein [46] reduces to a NLS equation. This model is quite similar to the model which is discussed in Sec.2.2 of this Thesis so we shall postpone the discussion to that section, and here only mention that many details on Davydov's theory of proteins and its relation to the NLS equation can be found in [49–52].

More exotically the NLS equation occurs in dynamics of quasi one-dimensional ferromagnets with easy-axis anisotropy [53] and applications related to nonideal Bose gas with attraction [54].

The discussion of this section on the various applications of the NLS equation should make it clear that it is an extremely general and generic model which

has applications in very many branches of modern physics. Thus, although the results reviewed in this Thesis as a rule refer to the physical example of the molecular aggregates given in Sec.1.2.1, they certainly pertain to a large number of alternative physical problems and using the results in these situations is merely a matter of changing terminology and notation.

1.2.1 Scheibe aggregates

Scheibe aggregates [55] are a special kind of ordered molecular systems, which experimentally exhibits highly efficient energy transfer which possibly can be explained through nonlinear dynamical effects inherent to the system.

Scheibe aggregates are found in nature, where they function as energy funnels for sunlight to be used in photochemical processes [56], but they may also be produced artificially in the laboratory by the Langmuir-Blodgett technique [57]. In this way Langmuir-Blodgett Scheibe aggregates may be used to study the important process of photosynthesis, and may also be used technologically to identify the combination of molecules resulting in the most efficient energy transfer.

Scheibe aggregate formation of monolayer Langmuir-Blodgett films may be obtained by mixing dye molecules with inert molecules in the molar ratio 1:1 [58]. The aggregated structure of such a film is sketched in Fig.1.1 (right), showing how the chains of the inert molecular filler (in this case octadecane) occupies the holes left by the hydrophobic chains of the dye (in this case oxacyanine). This compact packing structure results in a large intermolecular binding energy [58]. In films where the molecular structure is less ordered and compact, the Scheibe band, which gives this kind of Langmuir-Blodgett film its special and interesting properties, will not arise (e.g. mixing ratios dye:filler other than 1:1).

The absorption and fluorescence bands of the chromophores in the Scheibe aggregates are mainly determined by the π-electron portion between the nitrogen atoms. Due to these strong narrow coinciding absorption and fluorescence bands the Langmuir-Blodgett Scheibe aggregates, have unique energy transfer properties. Furthermore, Langmuir-Blodgett films are particularly suited for studies of energy transfer, since the positions and orientations of the molecules are fixed, and by appropriate planning of the assembly procedure the architecture of the aggregates can be varied systematically.

Confirmation of highly efficient energy transfer over unusually large distances in Langmuir-Blodgett Scheibe aggregates was first obtained by Möbius and Kuhn in 1979 [59]. The monolayer Langmuir-Blodgett Scheibe aggregate studied by Möbius and Kuhn consists of an oxacyanine dye (donors) doped with a thiacyanine dye (acceptors) with a donor:acceptor ratio as high as 10^4. The terminology acceptor and donors arise from the fact that the acceptor molecules have a slightly lower excitation energy than the donors, allowing energy transfer from donor molecules to acceptor molecules. Sterically, the thiacyanine acceptor molecules are very similar to oxacyanine donor molecules, and it is therefore assumed simply to substitute a donor molecule in the brickstone work lattice, in which the donors are arranged. The brickstone work model of the aggregate

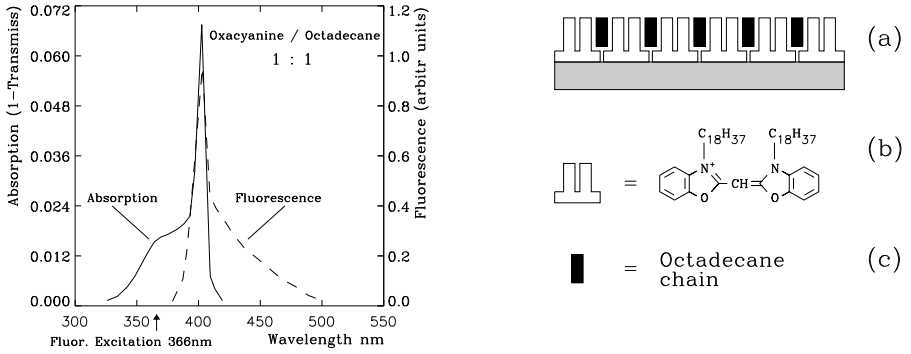

Figure 1.1: Left: Absorption and fluorescence spectra of a monolayer LB Scheibe aggregate of an oxacyanine dye mixed with octadecane, acting as inert molecular "filler". Molar mixing ratio 1:1, T=300K. Taken from Ref. [58]. Right: (a) Aggregated structure of the film, where octadecane chains occupies the holes left by the oxacyanine dye molecules, resulting in a closest packing structure. (b) Representation of oxacyanine molecules. (c) Representation of octadecane chains.

is depicted in Fig. 1.2, where also the excitation and movement of the so-called *coherent exciton* domain is sketched. Coherent exciton or simply exciton is the name usually applied for the localized wave function describing the excitation of the π-electrons in the aggregate. Möbius and Kuhn found the efficiency of energy transfer to be proportional to the temperature in the range 20K-300K [59]. In Langmuir-Blodgett films with less ordered and compact molecular structures than the Scheibe aggregates, the energy transfer is less efficient, and no temperature dependence is observed in the range 20K-300K [59]. In later studies the energy transfer was found to be up to ten times more efficient when donors and acceptors are situated in the same layer, than if situated in adjacent layers [60]. Therefore we shall concentrate our interest on monolayer Langmuir-Blodgett Scheibe aggregates. They seem to have the best energy transfer properties and may model the processes of energy harvesting and transfer in photosynthesis. Furthermore, limiting ourselves to monolayers reduces the dimension of the relevant model from three dimensions to two dimensions. The main experiments of Möbius and Kuhn on such films are presented in References [59, 60].

Theoretically, Möbius and Kuhn found that a coherent exciton model could explain their experimental results [59, 60]. In their model it is assumed that on excitation of the aggregate a coherent exciton, extending over a certain number of molecules, is created. Since the decay rate associated with a single donor molecule is constant, this results in a radiative decay rate of the exciton which is proportional to its domain size. Experimentally the radiative decay rate of the exciton was found to be inversely proportional to the temperature implying

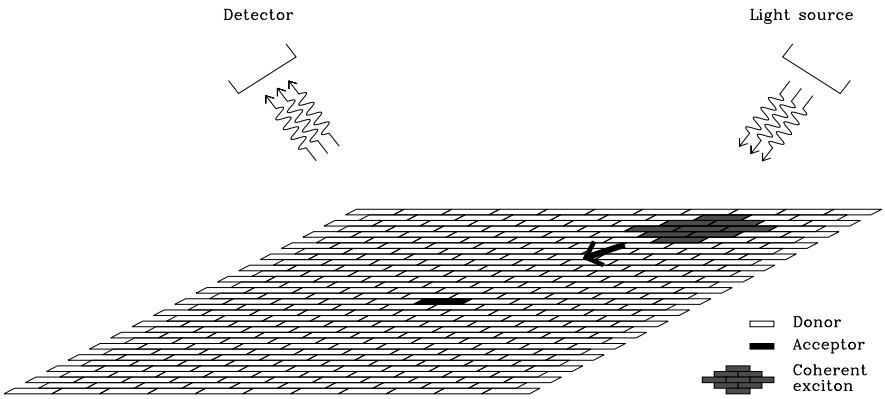

Figure 1.2: Brickstone work model of a monolayer LB Scheibe aggregate, where each brick represents a cyanine dye molecule. The excitation of a coherent exciton extending over 9 molecules, and moving over the aggregate towards an acceptor molecule, is sketched.

that the domain size of the coherent exciton is also inversely proportional to the temperature [59, 60]. The exciton then moves across the aggregate with its domain size remaining constant. Occasionally it will reach the vicinity of an acceptor molecule, with a certain probability of transferring its energy depending on its domain size. This explains the measured temperature dependence of the energy transfer efficiency.

It is important to note that the coherent exciton model suggested by Möbius and Kuhn displays mean behavior. It does not state anything about the dynamics. On the average the exciton, which has a certain domain size, must travel with a certain velocity (higher than the speed of sound in the aggregate), since it is supposed to reach an acceptor molecule during its life time. It seems likely that, e.g., the domain size will be a decreasing function of time, due to destruction of coherence through thermal fluctuations.

In summary, the main experimental results of Möbius and Kuhn on cyanine Scheibe aggregates are that on illumination of the film

1) a coherent exciton extending over a domain of molecules is excited,
2) the domain size is inversely proportional to temperature,
3) the exciton stays coherent during its life time,
4) the exciton life time is proportional to temperature,
5) the efficiency of energy transfer from donor to acceptor molecules, is inversely proportional to temperature.

The temperature-dependent radiative decay rate of excitons in pseudoisocyanine Scheibe aggregates both in solutions, and in monolayer Langmuir-Blodgett films has been studied by Dorn and Müller [61]. They verified that the fluores-

cence life time was an increasing function of temperature, indicating a progressive destruction of cooperativity (decreasing domain size of Möbius and Kuhn's coherent exciton). Similar conclusions were drawn by De Boer and Wiersma from studies of pseudoisocyanine bromide Scheibe aggregates [62], by Itoh *et al.*, who studied the fluorescence life time of excitons in CuCl microcrystals [63], and by Feldman *et al.* [64], who studied the same effect in GaAlAs quantum wells. Thus the experimental results of Möbius and Kuhn seem well supported.

Langmuir-Blodgett films and molecular architecture have many technological applications in electronics (dielectric layers in semiconductors, capacitors, etc.), and especially optoelectronics (photoresistors, photodiodes, photomemory, gratings, 2nd harmonic generation, etc.). They may also serve as model systems for fundamental investigations of exciton processes as well as of structure and function in two-dimensional and three-dimensional molecular systems in general. For a broader overview, interested readers are referred to, e.g., the review articles by Blinov [65] and by Tredgold [66].

While in the past much work on Scheibe aggregates was aimed at understanding the spectroscopy, the focus has recently changed towards comprehending their dynamical properties. Thus Mukamel and co-workers [67, 68] have established the existence of a temperature dependent coherence size of the exciton from numerical calculations in one-dimensional, provided that the exciton dephasing time scale is much shorter than the fluorescence life time, and that the exciton-phonon coupling is weak. When the coupling is strong, purely incoherent motion is observed, with an effective coherence size of only one molecule, independent of temperature.

The conclusion that the experimental results may only be reproduced if the exciton-phonon coupling is weak was also reached by Bartnik *et al.*, who studied a purely quantum mechanical model of Scheibe aggregates [69–72]. Incorporating an acceptor molecule among the donor molecules, the acceptor was found to act as an energy trap, provided the parameter values satisfy certain constraints. Furthermore, it is proposed that both coherent and incoherent (diffusive) exciton motion may participate in the energy transfer, initially being coherent, but eventually becoming incoherent.

Huth *et al.* [73] first proposed a nonlinear model of Scheibe aggregates, where the coherent domain observed experimentally is assumed to arise from nonlinear dynamical effects in the aggregate. The model is based on the cubic nonlinear Schrödinger (NLS) equation allowing energy transfer to occur through solitary waves. Initially formulated in one dimension the model was later supposed to be applicable also in two dimensions, with the initial conditions becoming ring waves. In two dimensions the NLS equation is no longer integrable, and thus the ring wave may collapse at the center. Christiansen and co-workers [74, 75] used this collapse of the ring waves in the nonlinear model to predict the exciton life time at room temperature.

The nonlinear model of Huth *et al.* requires a strong coupling between excitons and phonons. This contrasts the result obtained by Mukamel, Bartnik, and their collaborators, that the coupling must be weak. It is noted that the definition of weak and strong coupling is not yet clear in this connection. Fur-

thermore, the model does not take thermal effects into account. Thus, as for the Davydov soliton in proteins [76], a natural question arises: For how long time can solitary waves exist in Scheibe aggregates at a certain temperature?

A model similar to that of Huth *et al.* is developed and investigated in the first part of the Thesis (Paper I-Paper V). This model will include thermal effects. The remaining part of the Thesis (chapters 3 and 4) continues to discuss different aspects of the model, however the connection to the physical context described above is not direct.

1.3 The Nonlinear Schrödinger Equation

As is evident at this point the mathematical theme of this Thesis is nonlinear Schrödinger equations in various forms and dimensions. Therefore it is appropriate to give a short summary of the properties of this equation. This will be the scope of this section, and it will be divided into a subsection on one-dimensional results where the unperturbed NLS equation is integrable, and a subsection on two-dimensional results where the integrability is lost and the collapse phenomenon appears. The two subsections of this section shall also introduce the most relevant analytical methods which are to be applied in the thesis.

1.3.1 Properties in one dimension

The one-dimensional nonlinear Schrödinger equation

$$i\psi_t + \psi_{xx} + |\psi|^2\psi = 0, \tag{1.8}$$

is in the sense of Calogero [77] completely S-integrable, which means that the evolution of any initial wave can be found analytically via the inverse scattering transform (IST).

The IST was first introduced for the Korteweg-de Vries (KdV) equation in the paper by Gardner, Green, Kruskal and Miura [78]. The method was further developed by Lax [79], Zakharov and Shabat [80], and Ablowitz *et al.* [81, 82]. Today the method is well developed for a number of nonlinear evolution equations and detailed accounts are given by several authors [83–89]. The basic idea of the IST is to represent a nonlinear evolution equation for a function $\psi(x,t)$ in the form of the so-called Lax-pair [79] (L, A)

$$L_t + [L, A] = 0, \tag{1.9}$$

where the linear operators L and A have coefficients which depend on the function $\psi(x,t)$ and its derivatives. Thereby the evolution equation for $\psi(x,t)$ appears as the compatibility condition of the auxiliary linear equations

$$L\Psi = \lambda\Psi, \tag{1.10}$$

$$\Psi_t = A\Psi, \tag{1.11}$$

where λ is a spectral parameter and the auxiliary function Ψ is the so-called *Jost function*. The first step in applying the IST is to solve the direct scattering problem which involves determining the eigenfunctions of the spectral problem (1.10). Since the operator L depends on $\psi(x,t)$, the *scattering data* of (1.10) will depend on this function. The scattering data will in general consist of two components $S(\lambda)$ and S_n defining the continuous and discrete spectrum, respectively. n is the index labeling the discrete eigenvalues. Via (1.11) the temporal evolution of the scattering data generates the temporal evolution of $\psi(x,t)$. A crucial point here is that the evolution of the scattering data is trivial since they generally obey equations of the form

$$\frac{\partial S(\lambda,t)}{\partial t} = i\gamma(\lambda)S(\lambda,t), \tag{1.12}$$

$$\frac{dS_n(t)}{dt} = \gamma_n(\lambda)S_n(t), \tag{1.13}$$

where the coefficients $\gamma(\lambda)$ and $\gamma_n(\lambda)$ may be zero. Solving the initial value problem of the evolution equation (Eq.(1.8) e.g.) one should first find the initial scattering data $S(\lambda, t=0)$ and $S_n(t=0)$ corresponding to an initial condition $\psi(x, t=0)$, i.e., solve *the direct scattering problem*, then find $S(\lambda,t)$ and $S_n(t)$ (for any $t>0$) form the evolution equations (1.12) and (1.13). Finally, $\psi(x,t)$ should be reconstructed based on $S(\lambda,t)$ and $S_n(t)$, i.e., *the inverse scattering problem*, must be solved. The discrete spectrum of the scattering data always corresponds to solitons (the nonlinear part of the solution) while the continuous spectrum of the scattering data always corresponds to radiation (the linear part of the solution).

For Eq.(1.8) the Lax pair (L, A) has matrix form and was first found by Zakharov and Shabat [80]. Using these operators and the IST procedure described above the soliton solutions of Eq.(1.8) can be found. In particular the one soliton solutions are given as

$$\psi_s(x,t) = \sqrt{2}\eta\,\mathrm{sech}[\eta(x-\zeta)]\,\exp[-2i\xi x - i\phi], \tag{1.14}$$

where

$$\phi = 4(\xi^2-\eta^2)t + \phi_0, \quad \zeta = -4\xi t + \zeta_0. \tag{1.15}$$

ϕ_0 and ζ_0 are arbitrary constants; the amplitude η and velocity ξ are in general defined by the initial data. The general expression for the N soliton solution is given by Satsuma and Yajima [90].

Being S-integrable Eq.(1.8) additionally possesses an infinite number of conserved quantities, of which we here shall show the three most fundamental.

i) The norm N which has different names in different physical contexts, *power* in optics, *number of particles* in plasma physics and *excitation number* in the Davydov theory, is defined as

$$N = \int_{\perp\infty}^{\infty} \mathcal{N}dx = \int_{\perp\infty}^{\infty} |\psi|^2 dx. \tag{1.16}$$

ii) The Hamiltonian H, whose name stems from the fact that Eq.(1.8) is given as $i\psi_t = \frac{\partial \mathcal{H}}{\partial \psi^*}$, is defined as

$$H = \int_{\perp\infty}^{\infty} \mathcal{H} dx = \int_{\perp\infty}^{\infty} \left(|\psi_x|^2 - \frac{1}{2}|\psi|^4 \right) dx. \tag{1.17}$$

iii) Finally, the momentum P is given as

$$P = \int_{\perp\infty}^{\infty} \mathcal{P} dx = i \int_{\perp\infty}^{\infty} \left(\psi_x \psi^* - \psi \psi_x^* \right) dx. \tag{1.18}$$

Since the quantities are conserved they fulfill $\dot{N} = \dot{H} = \dot{P} = 0$ where the overdot denotes the derivative with respect to time.

Various physical systems (see [44] e.g.) are of the form

$$i\psi_t + \psi_{xx} + |\psi|^2 \psi = \epsilon R[\psi]. \tag{1.19}$$

where $\epsilon R[\psi]$ can be considered small. This suggest the usefulness of developing perturbational schemes. Since the unperturbed equation is completely integrable the most powerful perturbative technique is based on the IST. Perturbation theory based on the IST was introduced by Kaup [91] and independently by Karpmann and Maslov [92, 93], also Kaup and Newell [94] contributed importantly to the development of this method. In the framework of the IST the solitonic and radiative (discrete and continuous spectra) parts separate naturally, suggesting an analogous separation in the presence of perturbations. One possible way of exploiting this is merely to take into account the evolution Eq.(1.13) for the scattering data forming the discrete spectrum leading to evolution equations for the solitonic parameters η and ξ. This approach is often referred to as *adiabatic* perturbation theory. It is of course only an approximate treatment but it can be shown [93] that the effects of the radiation emitted from the soliton appears only in the second order perturbation result, which provides us with the theoretical support for applying the adiabatic theory.

An alternative adiabatic approach applicable for equations of the form (1.19) has been proposed by Bondeson, Lisak and Anderson [95] and is an extension of the averaged variational principle given by Whitham [96]. We will describe the method as it appears in connection with Eq.(1.19) even though it is generally applicable for integrable systems with perturbations.

The unperturbed evolution equation (1.8) can be derived from the Lagrangian density $\mathcal{L}$

$$\mathcal{L} = \frac{1}{2} i \left(\psi^* \psi_t - \psi \psi_t^* \right) - |\psi_x|^2 + \frac{1}{2}|\psi|^4 \tag{1.20}$$

such that Eq.(1.8) is given as

$$\frac{\delta \mathcal{L}}{\delta \psi^*} = \frac{d}{dt}\frac{\partial \mathcal{L}}{\partial \psi_t^*} + \frac{d}{dx}\frac{\partial \mathcal{L}}{\partial \psi_x^*} - \frac{d\mathcal{L}}{d\psi^*} = 0. \tag{1.21}$$

The assumption of adiabaticity implies that only the soliton parameters are going to be time dependent as a result of the perturbation, implying that the solution can be expressed as $\psi = \psi(x, t, p_j(t))$ where $p_j(t)$ are parameters characterizing the soliton. For non-Hamiltonian external perturbative forces, the Euler-Lagrange equations have to be modified. This modification can be obtained following Whitham [96] in using the action $L = \int \mathcal{L} dx$ instead of the Lagrangian density. After a few simple manipulations it follows that the evolution of the parameters p_j is governed by

$$\frac{\partial L}{\partial p_j} - \frac{d}{dt}\frac{\partial L}{\partial \dot{p_j}} = \epsilon \left(\int_{\perp\infty}^{\infty} R \frac{\partial \psi^*}{\partial p_j} dx + c.c \right) \tag{1.22}$$

where c.c. denotes complex conjugated. If the perturbations are Hamiltonian, as will often be the case in the following, then the action L can be modified to L_{mod} which includes explicitly the perturbations. In such case the method results in the following equation for the parameters p_j

$$\frac{\partial L_{\text{mod}}}{\partial p_j} - \frac{d}{dt}\frac{\partial L_{\text{mod}}}{\partial \dot{p_j}} = 0. \tag{1.23}$$

In some cases the action can be modified to account also for non-Hamiltonian perturbations, examples of this are given in [15] and [97]. A slightly modified version of the described methods is to exploit the conserved quantities of the unperturbed system instead of the Lagrangian. Examples of this are given in [98] (KdV) and in [99] (NLS).

The variational methods described above are often referred to as *methods of collective coordinates* [15, 100] where the parameters p_j are thought of as the collective coordinates. As a method of analyzing nonlinear phenomena the methods of collective coordinates has proven to be very powerful and it has been used by many authors in several contexts of nonlinear physics and mathematics [100–109] (the list of citations is not complete and not meant to be but meant to illustrate the variety of applications of the method). Also in the work presented in this Thesis the method of collective coordinates or related methods are applied very frequently (see Paper II - Paper V, Paper IX and Paper XI - Paper XII).

1.3.2 Properties in two dimensions

In two spatial dimensions the NLS equation

$$i\psi_t + \psi_{xx} + \psi_{yy} + |\psi|^2\psi = 0, \tag{1.24}$$

loses its integrability, which of course means that no inverse scattering transform exists for this equation and equivalently Eq.(1.24) possesses only a finite number of conserved quantities. However, the norm, Hamiltonian and the momentum which are trivial extensions into two dimensions of the quantities given in Eqs.(1.16), (1.17) and (1.18) are still conserved under the evolution of Eq.(1.24).

In spite of the non integrability "soliton" solutions or at least localized solutions are possible. Assuming radially symmetric solutions of the form

$$\psi(r,t) = \lambda\, R(\lambda\, r)\exp(i\lambda^2\, t) \tag{1.25}$$

where λ is a parameter (frequency) then the real valued profile $R(r)$ must satisfy

$$\frac{d^2R}{dr^2} + \frac{1}{r}\frac{dR}{dr} - R + R^3 = 0,\ R'(0) = 0,\ R(\infty) = 0. \tag{1.26}$$

The unique positive solution of this equation is monotonically decreasing. It was found numerically by Chiao, Garmire and Townes [110] and is often called the *Townes soliton* [111, 27]. The norm, N_T, of the Townes soliton is

$$N_T = 2\pi\int_0^\infty R^2 r dr \simeq 11.69. \tag{1.27}$$

Discussing the stability of the Townes soliton it is advantageous to consider a slightly more general equation than (1.24)

$$i\psi_t + \nabla^2\psi + |\psi|^{2\sigma}\psi = 0 \tag{1.28}$$

where the Laplacian can take any dimension, d. The nonlinearity $|\psi|^{2\sigma}$ is a good approximation in several physical situations (see, e.g., [112–114]), and is also convenient for numerical simulations (see [15] and Paper III). This kind of nonlinearity has also been used to obtain some quite surprising results in discrete systems [115–117].

We are interested in the stability of stationary spatially localized solutions of the form

$$\psi(r,t) = \lambda^{1/\sigma}\, R(\lambda\, r)\exp(i\lambda^2\, t). \tag{1.29}$$

The standard approach of the soliton theory is to analyze the linear stability of the stationary, spatially localized solutions. In this context stability is signifying that the localized solution during the evolution remains (neither disperses nor collapses) localized even in the presence of small perturbations. For the generalized NLS equation (1.28) the soliton stability is determined by the well known *Vakhitov-Kolokolov criterion* [118, 119]. Thus, monotonically decreasing stationary solutions are stable whenever

$$\frac{dN}{d\lambda} > 0. \tag{1.30}$$

Sketching how the criterion arises we consider

$$\psi = [\psi_s + (u + iv)\exp(\Omega t)]\exp(i\lambda^2 t) \tag{1.31}$$

where $\psi_s(x,y)$ is the monotonically decreasing solution to Eq.(1.28) ($\psi_s(x,y)$ is without loss of generality assumed to be real) and $(u(x,y) + iv(x,y))\exp(\Omega t)$ is a perturbation. Assuming u and v are small we have to first order

$$\Omega u = L_+ v, \tag{1.32}$$

$$\Omega v = -L_\perp u, \tag{1.33}$$

where

$$L_\perp = \lambda^2 - \nabla^2 - \psi_s^{2\sigma}, \text{ and } L_+ = L_\perp - 2\sigma\psi_s^{2\sigma}. \tag{1.34}$$

Eliminating v from Eqs.(1.32) and (1.33) we arrive at the eigenvalue problem

$$-\Omega^2 u = L_+ L_\perp u. \tag{1.35}$$

Clearly, the stability is determined by the sign of the largest eigenvalue satisfying Eq.(1.35). Several authors [118, 119, 116] (Ref. [116] deals with the equivalent discrete problem) have shown that for the simple monotonically decreasing solution the sign of the largest eigenvalue is the same as the sign of the quantity

$$\zeta = \int_{\perp\infty}^{\infty} \psi_s L_\perp^{\perp 1} \psi_s \, dxdy. \tag{1.36}$$

Differentiating Eq.(1.28) with respect to λ^2 it follows straightforwardly that

$$\psi_s + L_\perp \frac{\partial \psi_s}{\partial \lambda^2} = 0, \tag{1.37}$$

and thus

$$-\frac{\partial \psi_s}{\partial \lambda^2} = L_\perp^{\perp 1} \psi_s \, . \tag{1.38}$$

Applying this in Eq.(1.36) we immediately obtain

$$\zeta = -\frac{1}{2}\frac{\partial}{\partial \lambda^2} \int_{\perp\infty}^{\infty} \psi_s^2 dxdy = -\frac{1}{4\lambda}\frac{\partial N}{\partial \lambda}. \tag{1.39}$$

Stability is obtained when the largest eigenvalue is negative ($\zeta < 0$) i.e. for $dN/d\lambda > 0$ as claimed in Eq.(1.30). It should be noted that the derivation is only sketched the details can be found in Ref. [119] e.g.

Using the scaling properties of Eq.(1.28) we easily obtain

$$N = \lambda^{\frac{2-\sigma d}{\sigma}} \int R^2(y) d^d y, \tag{1.40}$$

where the integral is independent of the frequency λ. According to the Vakhitov-Kolokolov criterion it therefore follows that the localized solutions are stable (unstable) when $d\sigma < 2$ ($d\sigma > 2$). In particular the soliton solutions of Eq.(1.8) ($d = 1$, and $\sigma = 1$) are stable, while for the Townes soliton we have $\frac{dN}{d\lambda} = 0$. This suggests that the case $d\sigma = 2$ is a critical case.

The instability and marginal stability (see later) of the soliton for $d\sigma \geq 2$ manifest itself in the possibility of *collapse*. From the mathematical point of view, collapse means that the solution of the initial value problem for some nonlinear evolution equations (the NLS equation in our case) exists only for a finite time until some moment $t = t_c$ and can not be continued for $t > t_c$. At the moment $t = t_c$ the solution abruptly loses its initial smoothness and a singularity appears. In the mathematical literature the development of a singularity in finite time is mainly referred to as the *blow-up* of the solution.

Since the growth of amplitude is associated with a spatial contraction of the wave-packet, the phrase collapse is commonly used among physicists and shall therefore be used in the following although a different distinction between the phrases has been suggested previously [120]. Considering the quantity

$$\langle r^2 \rangle = \frac{1}{N} \int r^2 |\psi|^2 d\mathbf{r} \tag{1.41}$$

where $\mathbf{r} = (x_1, x_2, ..., x_d)$ and $r = \sqrt{\sum_{i=1}^{d} x_i^2}$, we can easily prove that collapse indeed is possible in Eq.(1.28). The evolution of $\langle r^2 \rangle$ can be shown [121] to be governed by the equation

$$N \frac{d^2 \langle r^2 \rangle}{dt^2} = 4(2H - (d\sigma - 2)Y), \tag{1.42}$$

where H is the Hamiltonian corresponding to Eq.(1.28)

$$H = X - Y = \int |\nabla \psi|^2 d\mathbf{r} - \frac{1}{1+\sigma} \int |\psi|^{2(1+\sigma)} d\mathbf{r}. \tag{1.43}$$

This equation is often called the *virial theorem* [121]. Goldman and Nicholson [122] first introduced this term due to the similarity with the virial theorem of classical mechanics. From Eq.(1.42) we can easily derive the following relation

$$\begin{aligned} I &= 4Ht^2 + C_1 t + C_0 \\ &+ 4(2 - d\sigma) \int_0^t dt' \int_0^{t'} dt'' Y(t'') \end{aligned} \tag{1.44}$$

where $I = N\langle r^2 \rangle$ and

$$C_1 = \dot{I}_{t=0} = 4\mathrm{Im} \int (\mathbf{r} \cdot \nabla \psi) \psi^* d\mathbf{r}, \; C_0 = I_{t=0}. \tag{1.45}$$

For $d\sigma \geq 2$ the last term in Eq.(1.44) is negative or zero. If the second degree polynomial in t consisting of the three first terms has a real positive root t_r, then there exists a t_c, $0 \leq t_c \leq t_r$ for which $\lim_{t \to t_c} I = 0$. Therefore sufficient conditions for collapse are for $d\sigma \geq 2$

$$H < 0 \tag{1.46}$$

or

$$H = 0, \quad \text{and} \quad C_1 < 0 \tag{1.47}$$

or

$$H > 0, \quad \text{and} \quad C_1 < -4\sqrt{HC_0}. \tag{1.48}$$

The sufficient condition for collapse $H < 0$ was first found by Vlasov, Petrishchev and Talanov [123] and is therefore often [124, 125] referred to as the VPT criterion. Since N is conserved a sufficient condition for collapse is also

a sufficient condition for blow-up. On the other hand, collapse is a sufficient condition for blow-up but not necessary. Thus blow-up may occur even if I remains bounded. Denoting by N_s the norm of the simple soliton solution (for $d = 2$ and $\sigma = 2$, $N_s = N_T$) Weinstein [126] has in the case ($d\sigma = 2$) proven the following relation

$$\left[1 - \left(\frac{N}{N_s}\right)^{\sigma}\right] X \leq H, \tag{1.49}$$

where X is defined in Eq.(1.43). Equation (1.49) excludes the opportunity of $H < 0$ when $N < N_s$. Additionally we have for $N < N_s$

$$\sqrt{X + N} \leq \sqrt{\frac{H}{1 - (N/N_s)^{\sigma}} + N} \tag{1.50}$$

which has been shown by Ginibre and Velo [127] to be sufficient to prevent collapse. It is therefore important to note that this means that in the critical case ($d\sigma = 2$) collapse is only possible for excitations with $N > N_s$.

It is now clear that for $d\sigma = 2$ the soliton is located on the boundary separating the collapse region from the non collapse region. Considering the following perturbed soliton

$$\psi = (1 + \epsilon)\psi_s \tag{1.51}$$

we obtain

$$N \simeq N_s + 2\epsilon N_s, \tag{1.52}$$

$$H \simeq -2\epsilon X. \tag{1.53}$$

For $\epsilon \to 0^+$ this yields $N > N_s$, $H < 0$ and hence collapse, while $\epsilon \to 0^{\perp}$ yields $N < N_s$, $H > 0$ implying no collapse. Hence, Eqs. (1.52) and (1.53) show the *marginal stability* of the soliton and in particular of the Townes soliton. This agrees with the discussion following Eq.(1.30). The discussion above shows that a reasonable terminology is to denote $d\sigma < 2$ as the *subcritical* case, $d\sigma = 2$ as the *critical* case and $d\sigma > 2$ the *supercritical* case.

Chapter 2

Continuum models

2.1 Introduction

Having introduced the physical context and reviewed the essential properties of the NLS equation in one and two dimensions, the present chapter shall continue to review the papers Paper I-Paper VII describing the development of the model of the molecular aggregates. The developed model will include thermal fluctuation effects and as a result stochastic differential equations are studied. The effects of the fluctuations on the coherence of the excitations will be investigated analytically and numerically (Paper I and Paper II), and also the effects on the collapse phenomenon will be described (Paper III-Paper V). Finally the chapter will review the work of Paper VI and Paper VII on impurity effects in the model.

2.2 Effects of fluctuations

The basic model equations are derived in Paper I and is closely related to the Davydov model of energy transport in α-helix protein [76] except that the present model is two-dimensional. The derivation is in many ways similar to the derivation given in Sec. 1.2 in connection with the discussion of the applicability of the NLS equation in condensed matter physics. The model is based on a quantum mechanical energy operator consisting of three terms

$$\hat{H} = \hat{H}_{\rm ex} + \hat{H}_{\rm ph} + \hat{H}_{\rm int}. \tag{2.1}$$

The first term

$$\hat{H}_{\rm ex} = \sum_n E_0 \hat{B}_n^\dagger \hat{B}_n - \sum_{n \neq p} \sum_p J_{np} \hat{B}_n^\dagger \hat{B}_p \tag{2.2}$$

is the exciton energy operator. n and p count molecules on the aggregate, $\hat{B}_n^\dagger$ ($\hat{B}_n$) is the creation (annihilation) operator of the exciton, while E_0 and

$-J_{np}$ are the molecular site energy and the dipole-dipole interaction energy, respectively. The phonon energy, which is treated classically, is given by

$$\hat{H}_{\rm ph} = \frac{1}{2} M \sum_n [\dot{u}_n^2 + \omega_0^2 u_n^2], \tag{2.3}$$

where M is the molecular mass and $u_n(t)$ denotes the elastic degree of freedom at site n. As is apparent from Eq.(2.3) the elastic degree of freedom is approximated by Einstein oscillators, having the trivial optical dispersion relation $\omega(k) = \omega_0$, ω_0 being a constant frequency. Finally, the exciton-phonon interaction is described by

$$\hat{H}_{\rm int} = \chi \sum_n u_n \hat{B}_n^\dagger \hat{B}_n \tag{2.4}$$

where χ is the exciton-phonon coupling parameter. Using standard techniques [128] Paper I describes how the model can be reduced to the following two equations governing the exciton wave function ϕ_n and the elastic degree of freedom u_n, respectively

$$i\hbar\dot{\phi}_n + \sum_{p \neq n} J_{np}\phi_p + \chi u_n \phi_n = 0, \tag{2.5}$$

$$M\ddot{u}_n + M\omega_0^2 u_n = \chi |\phi_n|^2. \tag{2.6}$$

A commonly chosen way [129–131] to model thermal fluctuations is to augment the equations with a randomly fluctuating term and a damping term turning the classical equations into *Langevin* equations [132]. Since fluctuation and dissipation physically are two different aspects of the same phenomenon the damping and the fluctuations have to be related quantitatively. The relation is obtained by the fluctuation-dissipation theorem [133] which relates the magnitude of the damping to the auto-correlation function of the fluctuating force. In Paper I the above described approach to the problem is chosen and leads to the following modification of Eq.(2.6)

$$M\ddot{u}_n + M\lambda\dot{u}_n + M\omega_0^2 u_n = \chi |\phi_n|^2 + \eta_n(t) \tag{2.7}$$

where the damping coefficient λ is related to the auto-correlation function of the fluctuating force $\eta_n(t)$ as

$$\langle \eta_n(t)\eta_{n'}(t')\rangle = 2M\lambda k_B T \delta(t-t')\delta_{nn'}, \tag{2.8}$$

in fulfilment of the fluctuation-dissipation theorem [129]. In Eq.(2.8) k_B is Boltzmann's constant and T is the absolute temperature. The fluctuating force, the noise, is chosen to be δ-correlated which is often called *white noise* because the spectrum (the Fourier transform of the auto-correlation function) is flat and there is an equal amount of power in each frequency component. The noise is chosen to be white mainly for mathematical convenience, and thus serve as a first approximation to physical fluctuations which in general will have a nonzero

correlation time. Finally, the distribution of the random variable η_n is assumed to be Gaussian in respect of the *central limit theorem*. This property also ensures that u_n will be continuous (see p. 83 of [129]) which is physically reasonable.

From this point a series of simplifying approximations are made, the most important being that the phonon system varies on a much faster time scale than the exciton system. Another important assumption is that $\lambda \ll 2\omega_0$, implying that the phonon system is strongly underdamped. These approximations lead to the governing equation for the exciton wave function, ϕ

$$i\hbar\phi_t + l^2 J_0 \nabla^2 \phi + l^2 V|\phi|^2\phi = -l^2\sigma\phi, \tag{2.9}$$

where the continuum limit has been taken for convenience. This approximation will be relaxed later in chapter 3 where the papers Paper VIII-Paper XI are described. As seen Eq.(2.9) is a perturbed two-dimensional NLS equation. The perturbation is $-l^2\sigma\phi$ where σ is a noise term which is no longer white noise. l is the lattice spacing, J_0 the dipole-dipole interaction energy in the continuum limit and $V = \chi^2/(M\omega_0^2)$ is the modified nonlinear coefficient. This concludes the derivation of the model equation which is to be studied in the remaining part of this chapter.

Paper I continues with a discussion of the appropriate model parameters and a discussion of how to approximate the now colored noise σ such that it can be handled conveniently in numerical simulations. Considering the Townes (see the previous section) soliton as the fundamental excitation of the two-dimensional NLS equation, the effect of disorder (time independent noise) on the evolution of this excitation is studied numerically. As expected the disorder tends to scatter the soliton. To quantify this scattering a coherence time t_{coh} is defined as the time where the center amplitude of the excitation has decreased by a factor e. Figure 2.1 (Fig. 7 of Paper I) displays the main result of Paper I which is the coherence time versus the temperature. The temperature dependence of the coherence time is found to

$$t_{\mathrm{coh}} \propto T^{\perp 0.24}. \tag{2.10}$$

An obvious demand to the exiton is that it is coherent at least up to the experimentally measured lifetime. On this background Paper I concludes at this point that the model with the chosen approximation of the noise only is appropriate for temperatures below $T \sim 3K$. However, as seen in the following the conclusion changes when more realistic noise is considered.

In Paper II the white noise approximation of the noise σ is investigated. The equation in normalized form is then

$$i\phi_t + \phi_{xx} + \phi_{yy} + |\phi|^2\phi = \eta\phi \tag{2.11}$$

where the noise, $\eta(x, y, t)$, is a Gaussian distributed random variable which is δ-correlated. Solving this equation numerically it is found, with the same definition of the coherence time, that the temperature dependence is

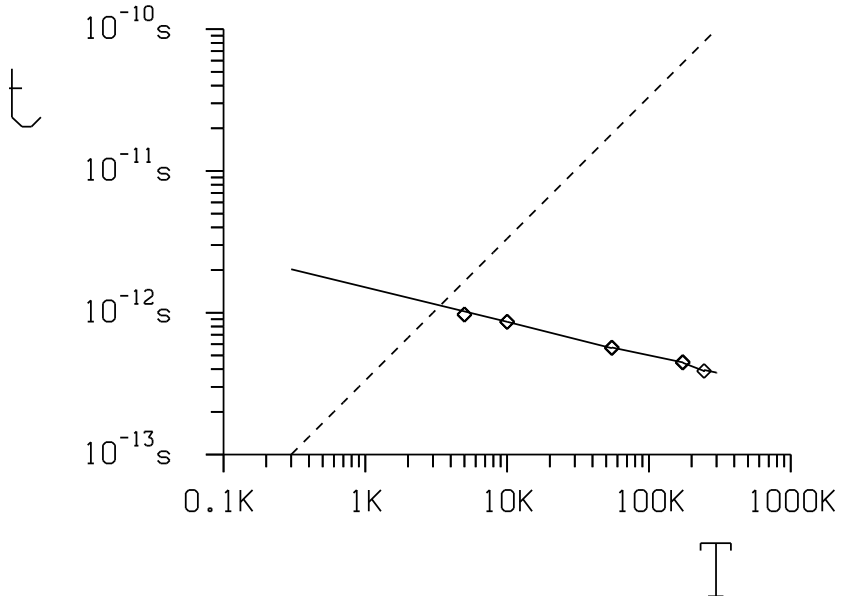

Figure 2.1: Coherence time (solid curve) found by numerical solution of Eq.(2.9), Experimentally [60] found lifetime (dashed curve) versus temperature (see Paper I for details).

$$t_{\rm coh} \simeq 4.0 T^{\perp 0.40}. \tag{2.12}$$

To gain some analytical understanding of this result a collective coordinate approach is applied, where radial isotropy is assumed for analytical convenience. Thus the equation is

$$i\phi_t + \frac{1}{r}\phi_r + \phi_{rr} + |\phi|^2\phi = \eta\phi \tag{2.13}$$

where $r = \sqrt{x^2+y^2}$ and the noise has the auto-correlation function

$$\langle \eta(r,t)\eta(r',t')\rangle = \frac{D}{r}\delta(r-r')\delta(t-t'), \tag{2.14}$$

where D is the noise variance which is proportional to the temperature T. The collective coordinate approach uses that Eq.(2.13) can be derived from the action

$$L = \int_0^\infty \{\frac{1}{2}{\rm Im}(\phi^*\phi_t) + |\phi_r|^2 - \frac{1}{2}|\phi|^4 + \eta(r,t)|\phi|^2\} r dr, \tag{2.15}$$

and the approach applies the trial function

$$\phi(r,t) = A(t)\ \mathrm{sech}(\frac{r}{B(t)})\exp\left(i\alpha(t)r^2 + i\beta(t)\right), \tag{2.16}$$

where the amplitude, A, width, B, and the phase functions, α and β, are the collective coordinates. Proceeding along the lines described in Sec. 1.3.1 the following equation governing the width B is obtained

$$B^3\ddot{B} = \Delta + \frac{4}{s_3}\int_0^\infty \left(1 - \frac{r}{B}\tanh(\frac{r}{B})\right)\mathrm{sech}^2(\frac{r}{B})\eta(r,t)rdr, \tag{2.17}$$

where the constant, Δ, is defined as

$$\Delta = \frac{4}{s_3}\left(s_1 - p_1 - \frac{p_1 N}{4\pi s_1}\right), \tag{2.18}$$

and the coefficients, s_m, and p_m, are given by

$$s_m = \int_0^\infty x^m \mathrm{sech}^2(x)dx, \quad p_m = \int_0^\infty x^m \mathrm{sech}^4(x)dx. \tag{2.19}$$

For $\eta = 0$ and $\Delta < 0$ ($N > N_T \simeq 11.69$, see definition of N_T one page 16) Eq.(2.17) clearly describes a collapse process, and has previously been derived for that purpose [102, 134]. In the case $\eta \neq 0$ Eq.(2.17) is a stochastic differential equation (Langevin equation), and the question of which interpretation of the stochastic integral to choose in the following arises.

Two different interpretations are commonly applied; the *Ito interpretation* and the *Stratonovich interpretation* . Dealing with a stochastic differential equation it is usually possible formally to integrate it. However, this involves an integration containing the stochastic variable and it is the definition of this integral which provokes the question of interpretation. Sense can be given to such a stochastic integral but the problem is that there is no unique way of defining it. The difference between the two definitions of the stochastic integral, connected with the names of Ito and Stratonovich is so profound that they in general give different results. Both integrals are defined, as in the case of a Riemann integral, by the limit of approximating sums. In contrast to the Riemann integral the result will depend on the choice of the evaluation point in the partition of the integration interval. Therefore the difference between the Ito and Stratonovich integrals resides in the choice of the evaluation point; Ito chooses the left hand point in the partition, whereas Stratonovich chooses the middle point. This can be shown [135] to leave the Stratonovich approach with some inherent correlation in contrast to the Ito approach. In applications, an important difference is that the Ito interpretation implies a special calculus while the Stratonovich interpretation implies standard calculus. The Ito interpretation is the most mathematically convenient due to the simple choice of evaluation point, for example most results of the Stratonovich interpretation are derived in the framework of the Ito interpretation. Because of the inherent correlation the

Stratonovich interpretation is probably the more appropriate when approximating physical noise having nonzero correlation time with white noise (see [135]). A more thorough discussion of these two interpretations is given in [129, 135].

In Paper II and also in the papers Paper III-Paper V and Paper IX the Stratonovich interpretation is always applied. The reasons of this choice are the convenience of having standard calculus and the fact that this approach is the more appropriate when approximating physical noise with nonzero correlation time with white noise.

Having made this choice it is a fairly simple matter [133] to write down the governing equation for the probability density $P(B, \dot{B}, t)$. The governing equation is in general called the *Fokker-Planck equation* and it here takes the form

$$\frac{dP}{dt} = -\dot{B}P_B - \frac{\Delta}{B^3}P_{\dot{B}} + \frac{\gamma}{B^4}P_{\dot{B}\dot{B}}, \tag{2.20}$$

where γ is proportional to D. Since it is a difficult task to analyze the Fokker-Planck equation (2.20) we choose a different approach. Instead of the stochastic equation Eq.(2.17) we can introduce a simpler stochastic equation which leads to the same Fokker-Planck equation (2.20) and in this manner yields an equivalent description of the process. This equivalent stochastic equation is

$$\ddot{B} = \frac{\Delta}{B^3} + \frac{h(t)}{B^2}, \tag{2.21}$$

where the noise, h, is simply δ-correlated

$$\langle h(t)\rangle = 0, \quad \langle h(t)h(t')\rangle = 2\gamma\delta(t-t'). \tag{2.22}$$

We have now developed the tools to complete the analytical analysis of the noise effects on the coherence time of the Townes soliton (denoted the ground state soliton (GS) in Paper II); this soliton is characterized by yielding $\Delta = 0$ in Eq.(2.21). In Paper II a perturbation approach is used to solve Eq.(2.21) in this simplified case. The result is

$$\langle B^2(t)\rangle \simeq B^2(0) + \frac{16D}{3s_3^2 B^4(0)}t^3. \tag{2.23}$$

Clearly this leads to the result

$$t_{\rm coh} \propto D^{\perp 1/3} \propto T^{\perp 1/3}, \tag{2.24}$$

which is in good agreement with the numerical result summarized by Eq.(2.12). The numerical result Eq.(2.12) and the analytical result Eq.(2.24) are compared in Fig.2.2 (Fig. 4 of Paper II).

A similar method is used in Paper III to investigate the effects on the collapse caused by the noise term. In this paper a slight generalization is made since the collapse is investigated in the framework of the equation

$$i\phi_t + \nabla^2\phi + |\phi|^{2\sigma}\phi + \eta(x,t)\phi = 0. \tag{2.25}$$

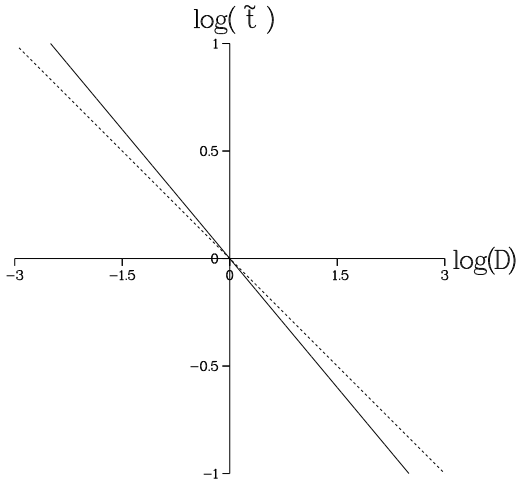

Figure 2.2: Coherence time as function of the noise variance, D, from the numerical solution of Eq.(2.13) (solid curve), and from Eq.(2.24) (dashed curve). $\tilde{t}$ is the normalized coherence time, $\tilde{t} = t_{\rm coh}(D)/t_{\rm coh}(D=1)$.

Only the *critical collapse* ($d\sigma = 2$) is investigated. Also in Paper III the collective coordinate approach is applied and the result is of course an equation of similar form as Eq.(2.17). Using similar arguments as in Paper II it can be found that the equivalent (i.e. having the same Fokker-Planck equation) but simpler equation for the width B is

$$\ddot{B} = \frac{\Delta}{B^3} + \frac{h(t)}{B^\rho}, \tag{2.26}$$

where the power ρ equals $\frac{5}{2}$ and 2 in one and two dimensions, respectively. In contrast to the Paper II where $\Delta = 0$, Paper III investigates collapse implying that $\Delta < 0$. Equation (2.26) is investigated numerically as well as analytically. The analytical methods are tightly related to the *slaving principle* of Haken [130, 131]. Intuitively the presence of the noise has the effect of at least slowing down the collapse process since the noise previously has been seen to destroy the coherence of an excitation. This intuition is confirmed by the analytical as well as the numerical results. Furthermore, it appears that the collapse process can be arrested provided the noise is strong enough. The critical strength (variance D) of the noise above which the collapse is arrested is shown to obey

$$D \propto |\Delta|^{3/2} \propto N^{3\sigma/2} \tag{2.27}$$

in both one and two dimensions. However, the magnitude of the critical variance depends on the dimension, such that the critical variance is much larger in one

dimension that in two dimensions. The results are compared to direct numerical simulations of Eq.(2.25) and the agreement is found to be good.

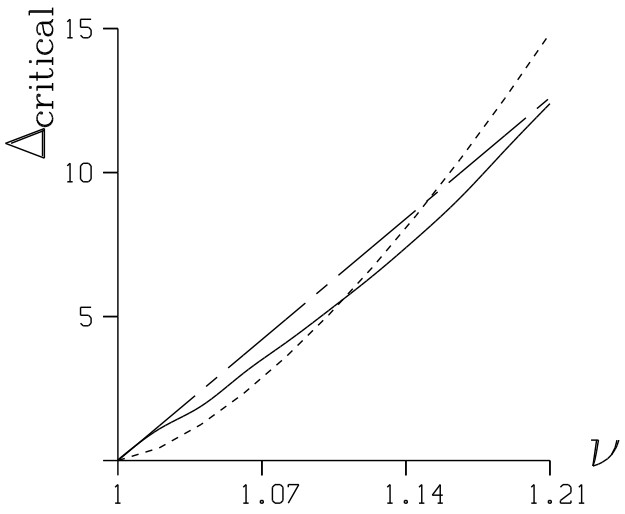

Figure 2.3: Critical variance versus normalized norm. Results (Solid line) obtained from direct numerical solution of Eq.(2.25). Analytical prediction (dashed line) and linear fit (chain dashed) Eq.(2.28).

The results of the papers Paper I, Paper II and Paper III are summarized in the physical context of Scheibe aggregates in Paper IV. The main results given as Eq.(2.27) (more detailed in Eq.(25)) is in Paper IV approximated by

$$D = \alpha(\nu - 1) \tag{2.28}$$

where $\alpha \simeq 60$ is a fitting parameter and $\nu = N/N_s$ is the norm of the excitation normalized to the norm N_s of the simple localized solution.

The fit is shown in Fig.2.3 (Fig. 1 of Paper IV which is a modification of Fig. 3 of Paper III) which also shows the relevant Eq.(2.27) result of Paper III. This leads to a relation which defines in terms of the physical parameters the temperature regions where collapse is possible. The separating curve in a V/J_0-T plane is given by the relation

$$\frac{V}{J_0} = \frac{N_s}{1 - T/T_0}, \tag{2.29}$$

with

$$T_0 = \frac{3\pi\alpha}{2N_s}\frac{\omega_0}{\lambda}\frac{\hbar\omega_0}{k_B}. \tag{2.30}$$

In Fig.2.4 (Fig. 2 of Paper IV) V/J_0, given by Eq.(2.29), is plotted versus

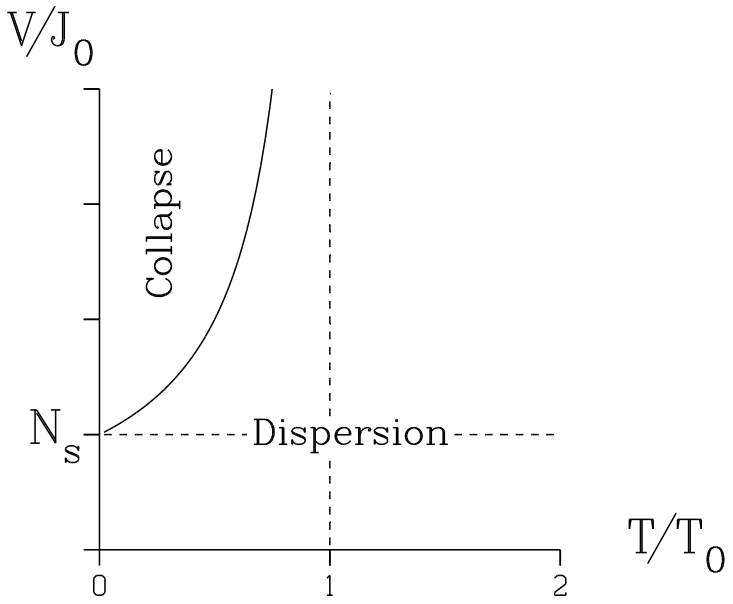

Figure 2.4: V/J_0 versus T/T_0, Eq.(2.29), separating regions of collapse and incoherence.

T/T_0 showing the curve which separates three regions in the V/J_0-T parameter plane:

(i) Above the curve collapse takes place, and the collapse time of the initial localized distribution given in Paper III increases with temperature.

(ii) For $V/J_0 > N_s$ at $T = 0$ we have collapse. However, at finite temperature, below the curve, there is no collapse and the coherence time, measured as given by Eq.(2.24) decreases with temperature.

(iii) For $V/J_0 < N_s$, the initial distribution always disperses in agreement with the discussion in Sec.1.3.2.

The physical parameters for the monolayer oxacyanine Scheibe aggregate used in Möbius and Kuhn's experiments [59] and [60] are not well-known. However, common values for the phonon frequency, ω_0, and the line width of the infra-red absorption spectrum, λ, are of the order $10^{12}\mathrm{s}^{\perp 1}$ and $10^{11}\mathrm{s}^{\perp 1}$, respectively. From Eq.(2.30) with $\alpha \simeq 60$ and $N_s = 11.7$ follows $T_0 \simeq 1850\mathrm{K}$. According to Eq.(2.29) we would get collapse at room temperature, $T = 300\mathrm{K}$, if $V/J_0 > 14$. The order of magnitude of the static dipole-dipole interaction energy is $J_0 \simeq 10^{\perp 21}\mathrm{J}$. The nonlinearity parameter $V = \chi^2/(M\omega_0^2)$ depends

strongly on the exciton-phonon coupling parameter, χ, which is not known for the Scheibe aggregate. Clearly, the nonlinear elastic properties of the Scheibe aggregate corresponds to an enhanced effective value of the coupling parameter. Taking e.g. $\chi \simeq 0.3 \times 10^{\perp 9}$N we get $V \simeq 7.5 \times 10^{\perp 20}$N and $V/J_0 \simeq 75$, indicating that the initial state collapses. According to the results of Paper III the collapse time then increases with temperature.

The Möbius-Kuhn coherent exciton, excited by the incident photon, is modelled by the generalized version of the Townes soliton. If the initial data are subjected to the dynamics of the two-dimensional nonlinear Schrödinger equation we conclude that a possible choice of parameters leads to collapse of the excitation. By the collapse the localization is concentrated on fewer molecules. The intensity then becomes so high that the effect of loss mechanisms must be included. In our model the collapse time increases with temperature.

It is noted that Möbius and Kuhn [60] deduce from their experimental observations that the life time of the coherent exciton increases linearly with temperature and a connection between the collapse time and the life time seems therefore to be a possible explanation of the measured behavior.

2.3 Effects of nonlinear damping

The previous section sketched how the model Eqs.(2.5) and (2.6) of the coupled exciton-phonon system could be reduced to one equation (2.9) describing the exciton wave function. The reduced equation included a noise term but not a damping term and therefore the damping of the phonon system was merely represented via the strength of the noise and not by an explicit damping term. This fact was an effect of the approximation applied in the reduction to a single equation. The drawback of this approximation is therefore that it prevents the exciton system from reaching thermal equilibrium.

This approximation is improved in Paper V such that the governing equation for the exciton wave function reads

$$i\hbar\phi_t + J_0 l^2 \nabla^2 \phi + V l^2 |\phi|^2 \phi - V \frac{\lambda}{\omega_0^2} l^2 \phi (|\phi|^2)_t + l^2 \sigma \phi = 0, \tag{2.31}$$

which in the more convenient dimensionless form becomes

$$i\phi_t + \nabla^2 \phi + |\phi|^2 \phi - \Lambda \phi (|\phi|^2)_t + \sigma \phi = 0 \tag{2.32}$$

where the nonlinear damping parameter Λ is

$$\Lambda = \lambda J_0 / \hbar \omega_0^2. \tag{2.33}$$

Equation (2.32) is a modified NLS equation, which has the surprising property that is still conserves the norm given in Eq.(1.16). However, the ordinary NLS Hamiltonian Eq.(1.17) will in general no longer be conserved. Instead we

find that

$$\frac{dH}{dt} = \int\int \sigma(x,y,t)(|\phi|^2)_t \, dx\, dy - \Lambda \int\int [(|\phi|^2)_t]^2 \, dx\, dy. \tag{2.34}$$

Thus, the two terms provide energy input and energy dissipation to the exciton system, making an energy balance possible. Consequently, there is a possibility for the system to reach thermal equilibrium.

Analyzing the effect of the nonlinear damping term $\Lambda\phi(|\phi|^2)_t$ we again apply a collective coordinate approach using a slightly generalized trial function

$$\phi(r,t) = A(t) f(r/B(t)) \exp[i\alpha(t) r^2], \tag{2.35}$$

where A is the complex amplitude and $f(r)$ is a suitable profile function (for example $\mathrm{sech}(r)$).

This leads to the following equation for the width, B, of the excitation

$$B^3 \ddot{B} = \Delta - ? \frac{\dot{B}}{B} - \frac{8\pi}{s_3} \int_0^\infty \left(1 + \frac{r}{B} \frac{f'(r/B)}{f(r/B)}\right) \times \left[f\left(\frac{r}{B}\right)\right]^2 \sigma(r,t) r \, dr, \tag{2.36}$$

where Δ and s_3 (for $f(r) = \mathrm{sech}(r)$) is defined in connection with Eq.(2.17). The damping coefficient ? is proportional to $N\Lambda$. The precise value depends on f and the relation is given in Paper V. In analogy with the treatment of the underdamped case in Paper II and Paper III, we find that it is possible to transform Eq.(2.36) into a simpler stochastic differential equation without changing the Fokker-Planck equation for the system. This equation, which therefore yields an equivalent description of the process, has the form

$$\ddot{B} = \frac{\Delta}{B^3} - ? \frac{\dot{B}}{B^4} + \frac{h(t)}{B^2}, \tag{2.37}$$

where h is Gaussian white noise with the variance $2D$. The variance $2D$ is proportional to the variance of the noise in Eq.(2.32), again the precise value depends on f and is given in Paper V.

The first notable property of Eq.(2.37) is that even without the noise term $h \equiv 0$ we find that collapse will not occur in a strict sense, since the solution will be defined for all t. Instead we find that $B(t)$ will tend exponentially to zero for large t,

$$B(t) \sim e^{\perp(|\Delta|/\Gamma)t}, \quad t \to \infty, \tag{2.38}$$

so that the process can be considered as a collapse process with an infinite collapse time. We coin the term *pseudocollapse* for this type of behavior. Illustrating the difference between the damped and the undamped cases we show

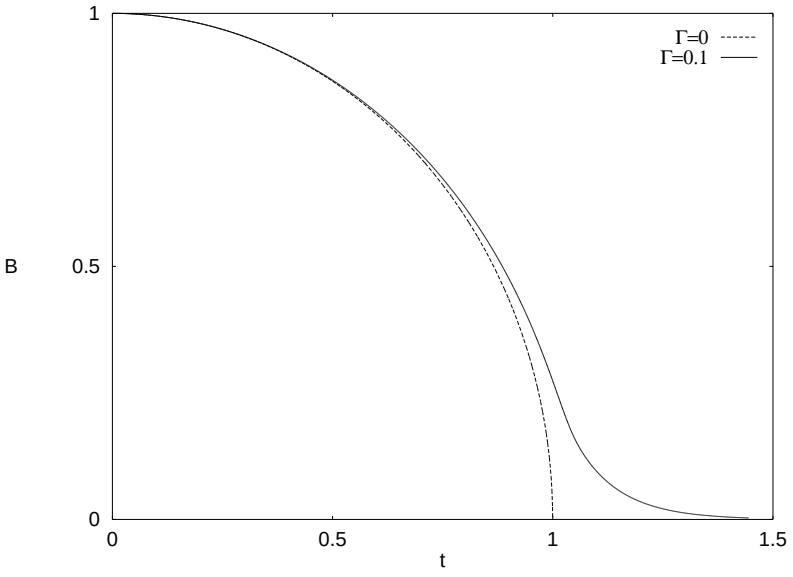

Figure 2.5: Width B as a function of time t in the absence of noise. Dashed line shows the analytical solution of Eq.(2.37) with $? = 0$ and for $B(0) = |\Delta| = 1$, $\dot{B}(0) = 0$; solid line shows the numerical solution of Eq.(2.37) with $? = 0.1$.

Fig.2.5 (Fig. 1 of Paper V). From this figure it can be seen that the initial stages of the pseudocollapse resemble a pure collapse as long as the damping is small. We therefore define the *pseudocollapse time* as the time where the asymptotic behavior (2.38) sets in. The numerical simulations of Eq.(2.37) show that the (pseudo)collapse process still can be arrested by the noise in the presence of the nonlinear damping. Furthermore the presence of the nonlinear damping does not cause any significant change in the critical noise variance $D_{\rm crit}$ needed to arrest the (pseudo)collapse. This is true as long as $|\Delta| \gg ?^2$ that is as long as the excitation norm is large (or the nonlinear damping small). Under this constraint the relation found in Paper IV (Eq.(2.27)) between critical variance $D_{\rm crit}$ and the norm ($|\Delta|$) is still valid and the critical variance is basically independent of the nonlinear damping $?$. When $|\Delta| \gg ?^2$ does not hold we observe (see Fig. 3 of Paper V) that the critical variance $D_{\rm crit}$ is an increasing function of $?$.

The averaged $\langle B(t)\rangle$ behavior of $B(t)$ is shown in Fig.2.6 (Fig.4 of Paper V) for the parameter values $B(0) = |\Delta| = 1$, $? = 0.1$, and several different values of the noise variance. It can be seen that for $D < D_{\rm crit} \simeq 0.15$, the effect of the noise is to delay the pseudocollapse in terms of the ensemble average of the width, in agreement with the result of Paper IV for the undamped case. We observe for $D > D_{\rm crit}$ a nonmonotonic behavior of $\langle B(t)\rangle$.

Finally, Paper V presents some indications that there exists at least an asymptotic balance between the energy input and the energy dissipation in the

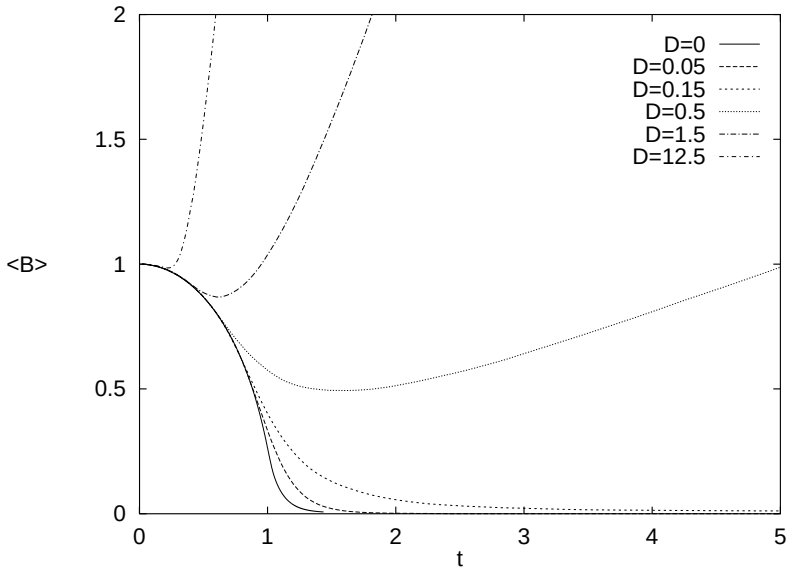

Figure 2.6: Ensemble average of the width $\langle B \rangle$ as a function of time t for different noise variances. From bottom to top we have $D = 0$, 0.05, 0.15, 0.5, 1.5, and 12.5, respectively. In all cases $B(0) = |\Delta| = 1$, and ? $= 0.1$

system. However, only indications and no proof of this statement is given. It would have been convenient to have some numerical results obtained directly from the reduced system (2.32). The first step of accomplishing this is presented in Paper IX, but here the investigations are carried out in the one-dimensional discrete version of Eq.(2.32). Since the discreteness causes the appearance of some new phenomena we postpone the discussion of the results to chapter 4 which is devoted to the discreteness effects.

2.4 Effects of impurities

The experimental investigations of the energy transport on the aggregates [59, 60] were made by doping the aggregates with guest (acceptor) molecules which effectively quenches the fluorescence of the host molecules. This effective quench was accomplished even at a molar ratio host:acceptor 10^4. Clearly, these acceptor molecules will act as impurities even when the acceptors are as scarce as mentioned above. It is therefore important to stress that although the nonlinear model developed in Paper I-Paper V is intended as initial steps in the process of explaining energy transfer from host molecules to impurity (acceptor) molecules, the model does not directly take impurity effects into account, but concentrates on the creation and dynamics of the exciton. However, the presence of impurities can drastically influence the excitation dynamics as was

shown for the one-dimensional NLS equation in Refs. [44, 99, 136]. In Paper VI and Paper VII, which are going to be discussed below, the effects of the presence of localized impurities in the two-dimensional case are investigated.

Paper VI gives the derivation of the governing equation for the exciton wave function, when the exciton is moving in an aggregate doped with acceptor molecules having a larger (or smaller) excitation energy than the host molecules. The governing equation is shown to be a NLS equation with a localized potential

$$i\hbar\phi_t + l^2 J_0 \nabla^2 \phi + l^2 V |\phi|^2 \phi = E(x,y)\phi, \tag{2.39}$$

where the notation is explained in connection with Eq.(2.9). $E(x,y)$ determines an energetic profile for an excitation in the vicinity of an impurity molecule. As discussed in Paper VI this profile will be rather complicated in real systems. Since we want to consider some general features of excitation dynamics in the vicinity of an impurity we shall for the sake of simplicity assume that $E(x,y)$ is an axially symmetric Gaussian function

$$E(r) = E_0 \exp\left(-\frac{r^2}{r_0^2}\right), \tag{2.40}$$

where E_0 is the strength of the impurity and r_0 is the radius. In dimensionless variables we thus have

$$i\phi_t + \nabla^2 \phi + |\phi|^2 \phi = U(r)\phi, \tag{2.41}$$

$$U(r) = \epsilon \exp(-r^2), \tag{2.42}$$

where the dimensionless parameter $\epsilon = (E_0 r_0^2)/(Jl^2)$ characterizes the strength of the impurity.

In a large part of Paper VI we consider the excitation in the vicinity of an impurity center such that the approximation $U(r) \simeq \epsilon(1 - r^2)$ is permissible. Additionally we allow for generality the strength $\epsilon = \epsilon(t)$ to be time dependent. After two independent transformations, where the first separates the internal and external dynamics of the excitation, while the second (called the Talanov transformation or lens transformation [111, 137, 138]) allows a detailed investigation of the internal dynamics, the following equations for the center of mass $R = \int r^2 |\phi(r)|^2 dr$ and the width B are obtained

$$\ddot{R} - 4\epsilon(t) R = 0, \tag{2.43}$$

$$\Delta = \frac{1}{2} B^3 \ddot{B} - \epsilon(t) B^4. \tag{2.44}$$

where Δ is a constant playing the same role as the Δ in Eq.(2.17), even though it appears in a slightly different manner in the present context (see Paper VI page 2954 which is page 135 of the Thesis for details). It is seen that the

equation (2.43) for the center of mass R is the equation for a linear time dependent oscillator. The equation (2.44) for the width belongs to the class of so-called Ermarkov-Pinney equations [139, 140] (see also [141] pp 28 and references therein).

As given by Pinney [140] the solution to Eq.(2.44) is

$$B(t) = \left\{ u^2(t) + \frac{4\Delta}{W^2} v^2(t) \right\}^{1/2}, \tag{2.45}$$

where $W = \dot{u}v - u\dot{v} =$ constant is the Wronskian and u, v are two linearly independent solutions of the linear equation

$$\ddot{y} - 4\epsilon(t)y = 0, \tag{2.46}$$

which coincides with Eq.(2.43) for the center of mass.

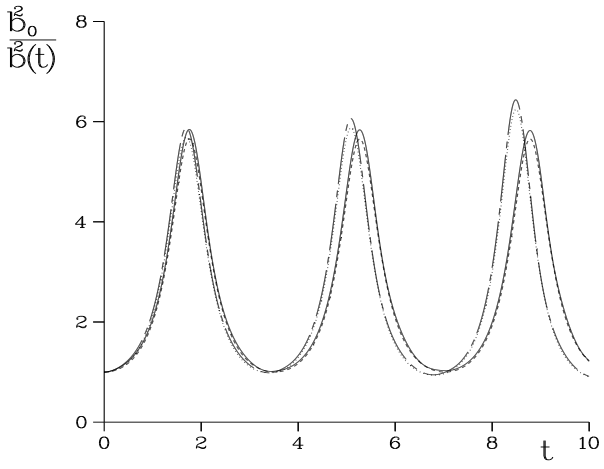

Figure 2.7: Comparison of the numerical solution to Eq.(2.42) (solid lines) and the results of the analytical approach with $\epsilon(t)$ given by Eq.(2.47) (dashed line) and Eq.(2.48) (dotted line), respectively.

In Paper VI two different choices of $\epsilon(t)$ are investigated. First a constant is chosen

$$\epsilon(t) = -\frac{\Omega_0^2}{4}, \tag{2.47}$$

which turns Eq.(2.43) into a simple harmonic oscillator which is easily solved and which also makes it possible to write down the solution of Eq.(2.44) in exact

form. Secondly, Paper VI investigates the effects of

$$\epsilon(t) = -\frac{\Omega_0^2}{4}(1 + \lambda \cos \Omega t), \tag{2.48}$$

which turns Eq.(2.43) into a Mathieu equation. The Mathieu equation is known to show two kinds of asymptotic behavior. Depending on the parameters (Ω_0, λ) the solution of the Mathieu equation can be either bounded or unbounded as time tends to infinity. The latter behavior is ascribed to the so-called parametric resonance effect. In the range of the first resonance $|\Omega - 2\Omega_0| < \Omega_0\lambda/2$ an approximate solution is given in [142]. The solution also allows us to give the behavior of the width B through Eq.(2.45). In Fig.2.7 (Fig. 1 of Paper VI) we show examples of the time evolution of B for ϵ chosen according to Eq.(2.47), and Eq.(2.48), and we also compare the results to direct numerical solution of Eq.(2.42). As is seen Eq.(2.44) describes the situation very well. Since the equation (2.43) is exact within the parabolic approximation of the impurity no comparison to results of direct simulations is needed.

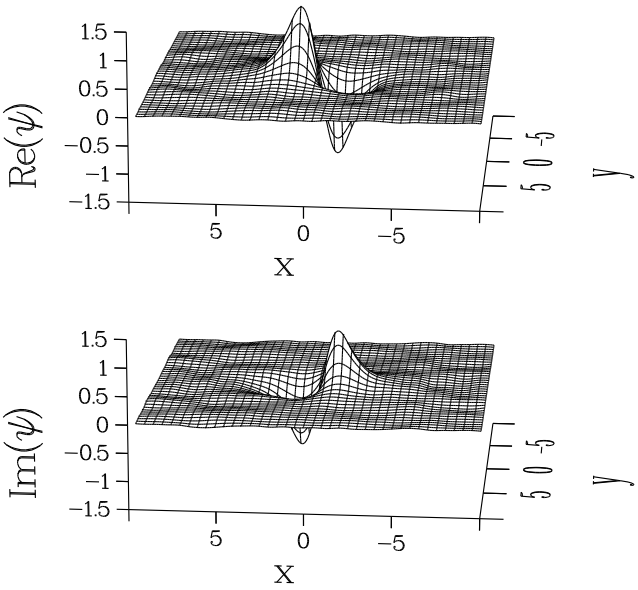

Figure 2.8: The real and imaginary parts of the dipole-like excitation at $N = 11.7$ for $\epsilon = 5.0$ at $t = 40$.

In the remaining part of Paper VI and in further detail in Paper VII we

discuss the possibility of having dipole-like excitations in the two-dimensional NLS equation. In [143] (also mentioned in [27]) a stationary solitary solution with a dipolar shape was shown to exist in the two-dimensional NLS equation. However, preliminary analyses seem to indicate that this excitation is at most marginally stable. In the presence of a Gaussian impurity Eq.(2.40) the situation improves such that a dipole-like excitation centered around the impurity exists and is stable. The excitation however performs small amplitude oscillations transferring small amounts of energy across the impurity center. The dipole-like excitation is found numerically in Paper VI and Paper VII and is shown in Fig.2.8 (Fig.6 of Paper VI and Fig.2 of Paper VII). Paper VI and Paper VII also analyze the creation and the oscillations of this excitation using collective coordinate approach. This approach will not be reviewed here since it is quite elaborate. However, we will mention the main results of the approach. (1) A threshold value of the impurity strength ϵ is found. Below this threshold value the creation of a dipole-like excitation is impossible. (2) The frequency of the energy transfer across the impurity center is found in terms of the impurity strength ϵ and the excitation width.

2.5 Conclusion

In summary we have in this chapter shown how to derive the equations describing the exciton and phonon dynamics on molecular aggregates, and we have shown how these equations reduce to a two-dimensional NLS equation augmented by a noise term (Paper I). The analysis of this equation and the results on how the noise determines the coherence time of a localized excitation (Paper II), and on how the noise affects the collapse process (Paper III and Paper IV) have been reviewed. It has been shown how to refine the model such that thermal equilibrium of the exciton system is possible (Paper V), and the changes of the above mentioned results have been summarized. Finally, we have shown how to modify the NLS equation to account for impurities (acceptors) in the molecular aggregates (Paper VI) and we have shown how such impurities modify the exciton dynamics (Paper VI) and how a Gaussian impurity can support dipole-like excitations (Paper VI and Paper VII). Parts of the material reviewed in this chapter can also be found in the publications [16, 18–23] which display different parts of the material from various points of view.

Chapter 3

Discrete models

3.1 Introduction

Discrete nonlinear Schrödinger systems are the topic of this chapter. We shall in the first section briefly describe some general and well known properties of the two most common discretizations of the continuum NLS equation. Additionally we will briefly discuss some analytical methods of treating these discrete problems. After this general description of the discrete systems we will move on to review the work contained in Paper VIII and Paper IX on the one-dimensional discrete nonlinear Schrödinger systems. Finally, the results of Paper X on the two-dimensional discrete NLS equation will be reviewed.

3.2 Discrete nonlinear Schrödinger equations

As explained in Sec.1.3.1 the one-dimensional NLS equation provides one of the few example of completely integrable nonlinear partial differential equations. Since most work in nonlinear wave propagation at some stage involves a numerical study, the issue of the discretization of the NLS equation was addressed early by Ablowitz and Ladik [144]. These authors noticed that among a large number of possible discretizations of the continuum NLS equation the following leads to an integrable discrete model. The integrable version of the discrete NLS equation, hereafter called the Ablowitz-Ladik or AL equation takes the form

$$i\dot{\psi}_n + (1+\mu|\psi_n|^2)(\psi_{n\perp 1} + \psi_{n+1}) = 0, \tag{3.1}$$

where ψ_n is a complex valued amplitude and μ is the nonlinearity parameter. As the continuum NLS equation the AL equation possesses a discrete IST [144] and therefore it possesses an infinite number of conserved quantities [80, 145]. General solutions can be obtained on the infinite line [145] and also on a periodic

interval [146]. The one soliton solution on the infinite line is

$$\psi_n = \frac{\sinh\beta}{\sqrt{\mu}}\mathrm{sech}[\beta(n-ut)]e^{\perp i(\omega t \perp \alpha n)}, \tag{3.2}$$

$$\omega = -2\cos\alpha\cosh\beta, \tag{3.3}$$

$$u = \beta^{\perp 1}\sin\alpha\sinh\beta, \tag{3.4}$$

where $\beta \in [0,\infty)$ and $\alpha \in [-\pi,\pi)$. It is seen that the soliton (3.2) is a fairly straightforward discrete version of the continuum one soliton solution. The importance of the AL equation is mainly mathematical even though a few special physical cases have been shown [147] to be described by an equation having AL character. The properties of the AL discretization have also lead to the development of effective numerical schemes [148, 149] which have formed the core of the numerical scheme used in most of the numerical work on continuum equations presented in this Thesis. Since Paper X, discussed later in this chapter, partly deals with impurities, it is worth to mention that the addition of the term $\mathcal{E}(t)n\psi_n$, such that the equation becomes

$$i\dot{\psi}_n + (1+\mu|\psi_n|^2)(\psi_{n\perp 1} + \psi_{n+1}) + \mathcal{E}(t)n\psi_n = 0, \tag{3.5}$$

where $\mathcal{E}(t)$ is an arbitrary function of time, preserves the integrability [150–153]. This is similar to the equivalent continuum case which also is integrable [154].

There is one more discrete version of the NLS equation that is integrable. This version has been introduced by Izergin and Korepin [155] and described in the book by Faddeev and Takhtajan [156] (pp. 299-303). Although this version is a very complicated system with no apparent applications it can been claimed to be the most important discrete NLS equation since it has the same r-matrix as the standard continuum NLS equation (see [156]).

The following discrete and more obvious version of the NLS equation was studied later [157, 158]

$$i\dot{\psi}_n + (\psi_{n+1} + \psi_{n\perp 1}) + \gamma|\psi_n|^2\psi_n = 0. \tag{3.6}$$

This version, usually referred to as the discrete nonlinear Schrödinger (DNLS) equation, has a number of interesting properties, but it is not integrable [159]. Equation (3.6) is a special case of the equation usually referred to as the discrete self-trapping (DST) equation [160, 158]. The DST equation allows in contrast to the DNLS equation coupling between all oscillating sites, as in a typical molecule [161]. For an extensive list of references to work on the DST equation we refer to [162].

The AL equation and the DNLS equation are quite different: The AL equation, on one hand has, as already mentioned very interesting mathematical properties, but not very clear physical significance; the introduction of the DNLS equation, on the other hand, is primarily motivated physically. For example, an equation of this form did arise from the discussion in Sec.2.2 describing molecular aggregates. The DNLS equations also seems to arise naturally in context of energy localization in condensed matter and biological systems as well as in the

modelling of optical devices [38, 158, 163–169]. Finally, it is worth mentioning that the regular and irregular behavior of the DNLS system with a few degrees of freedom (usually less than four) has been thoroughly investigated [170].

Aiming at being as general as possible in what follows we now introduce the combined AL and DNLS (AL-DNLS) equation

$$i\dot{\psi}_n + (\psi_{n+1} + \psi_{n\perp 1})(1 + \mu|\psi_n|^2) + \gamma|\psi_n|^2\psi_n = 0. \tag{3.7}$$

This may seem as an obvious generalization to do but actually it was done only recently and strangely enough first in the quantum case by Salerno [171] and later it was reintroduced in the form of Eq.(3.7) by Cai, Bishop and Grønbech-Jensen [172]. However, Eq.(3.7) had previously been studied by Vakhnenko and Gaididei [173] who treated the DNLS term $\gamma|\psi_n|^2\psi_n$ as a perturbation to the integrable AL equation and derived, via the IST, the evolution equations for the soliton parameters. This result was recently rederived [174] and simultaneously a Lagrangian formalism yielding the IST perturbation results was established. Developing such a formalism is a rather nontrivial task due to the deformed Poisson structure (see later this section). Equation (3.7) has also recently [147] been shown to model an electrical lattice.

The two most important conserved quantities of Eq.(3.7) are the norm

$$N = \mu^{\perp 1}\sum_n \ln(1 + \mu|\psi_n|^2) \tag{3.8}$$

and the Hamiltonian

$$H = -\sum_n (\psi_n\psi^*_{n+1} + \psi^*_n\psi_{n+1}) - \frac{\gamma}{\mu}\sum_n |\psi_n|^2 + \frac{\gamma}{\mu^2}\sum_n \ln(1 + \mu|\psi_n|^2). \tag{3.9}$$

Equation (3.7) can be derived from the Hamiltonian (3.9) using the deformed Poisson brackets

$$\{\psi_n, \psi^*_m\} = i(1 + \mu|\psi_n|^2)\delta_{n,m}, \quad \{\psi_n, \psi_m\} = \{\psi^*_n, \psi^*_m\} = 0, \tag{3.10}$$

and the equation of motion

$$\dot{\psi}_n = \{H, \psi_n\}. \tag{3.11}$$

Notice that in the AL limit ($\gamma \to 0$) as well as in the DNLS limit ($\mu \to 0$) the equation (3.7) can be obtained in this manner. In the latter limit the Poisson brackets Eq.(3.10) become standard Poisson brackets and the norm Eq.(3.8) becomes the standard probability norm $N = \sum_n |\psi_n|^2$.

In continuation of the previous chapter we will mainly be interested in the occurrence and properties of localized excitations in these discrete equations. Quite a lot of research has been devoted to this topic in quite a lot of different physical contexts and nonlinear models, a few examples are [175–183]. The excitations which are spatially localized and time periodic have also been given a variety of names. Takeno and co-workers have coined the term *intrinsically localized modes*. These modes are localized modes similar to localized modes

in disordered media (*Anderson localization* for example [184]) or in aperiodic media [185] but intrinsic because no disorder, aperiodicity or impurities are needed for their existence. Interesting effects arise when disorder, aperiodicity or impurities and nonlinearity are present simultaneously [186–189, 17]. The term *discrete breathers* is another often used [190] term for these modes in analogy with the name given to spatially localized and time periodic solutions of certain nonlinear partial differential equations [89]. However it would be more appropriate to reserve this term for the, presumably more fundamental, excitations which are spatially localized but quasiperiodic in time [191, 192]. Recently it has been shown [193] that the intrinsically localized modes in the leading order are solitons in the narrow mathematical sense, which also makes the name *solitonlike excitations* (see [189] and Paper VIII) appropriate.

Hennig *et al.* [194] applied the substitution

$$\psi_n(t) = \phi_n \exp(-i\omega t) \tag{3.12}$$

to transform Eq.(3.7) into

$$\phi_{n+1} = -\frac{\omega + \gamma|\phi_n|^2}{1 + \mu|\phi_n|^2}\phi_n - \phi_{n\perp 1} \tag{3.13}$$

which is a map determining the complex amplitude of the stationary state Eq.(3.12). This map is in Ref. [194] used to investigate several interesting aspects of the combined AL-DNLS equation; e.g. the regions in the parameter space (μ, γ, ω) where the trajectories of Eq.(3.13) are regular and irregular respectively. The authors also applied the concept of the *anti integrable limit* (or more appropriately *anti continuous limit* [183]) introduced by Aubry and Abramovici [195–197] investigating the existence of breathers (intrinsically localized modes) in Eq.(3.7). The idea of applying Eq.(3.13) to investigate the intrinsically localized modes of Eq.(3.7) is continued in Paper VIII which will be described in the next section.

3.3 Solitonlike solutions

This section shall review the results of Paper VIII, which deals with localized solutions or solitonlike solutions of the form Eq.(3.12) to the combined AL-DNLS equation (3.7). We shall particularly be interested in solutions exponentially localized and distinguish two situations: (1) $|\phi_n| > |\phi_{n+1}|$ for $n > 0$ and $|\phi_n| < |\phi_{n+1}|$ for $n < 0$ with $\lim_{|n|\to\infty} = 0$ corresponding to a bright solitonlike solution and (2) $|\phi_n| < |\phi_{n+1}|$ for $n > 0$ and $|\phi_n| > |\phi_{n+1}|$ for $n < 0$ with $\lim_{|n|\to\infty} = a > 0$ resulting in a dark solitonlike solution (for a description of dark solitons in the continuum NLS see [198] (IST) and [33] and references therein). It is easily shown that we without loss of generality can consider real-valued ϕ only. This allows us of to cast Eq.(3.13) into a two-dimensional map

$\mathcal{M}$ by identifying $x_n = \phi_n$ and $y_n = \phi_{n\perp 1}$

$$\mathcal{M}: \begin{cases} x_{n+1} &= -\dfrac{\omega + \gamma x_n^2}{1+\mu x_n^2} x_n - y_n \\ \\ y_{n+1} &= x_n \end{cases} . \tag{3.14}$$

This map can be shown to be a reversible area-preserving twist map [199].

In order to investigate stationary localized solutions in the form of the bright (dark) soliton, respectively, it suffices to study the fixed points (period-1 orbits) of the map $\mathcal{M}$. The fixed points, for which $\hat{x} = \hat{y}$, of this map are clearly located at

$$\hat{x}_0 = 0\,, \qquad\qquad \hat{x}_\pm = \pm\sqrt{-\frac{\omega+2}{\gamma+2\mu}}\,, \tag{3.15}$$

where $\hat{x}_\pm$ exists only if $\mathrm{sign}(\omega+2) = -\mathrm{sign}(\gamma+2\mu)$. The stability of the fixed points is governed by their value for the corresponding residues [141, 200]

$$\rho = 1/4\,[2 - \mathrm{Tr}\,(D\mathcal{M}(\hat{x}))]. \tag{3.16}$$

The tangent map $D\mathcal{M}$ is determined by

$$D\mathcal{M}(x) \;=\; \begin{pmatrix} \omega_n & -1 \\ 1 & 0 \end{pmatrix}\,, \tag{3.17}$$

with

$$\omega_n \;=\; -\frac{\omega + (3\gamma - \mu\omega)x_n^2 + \gamma\mu x_n^4}{(1+\mu x_n^2)^2}. \tag{3.18}$$

The residue corresponding to the fixed point at the origin is

$$\rho = \frac{1}{4}(\omega+2)\,. \tag{3.19}$$

For ω values within the range of the linear band, i.e. $|\omega| < 2$, $0 < \rho < 1$ holds and the origin is a stable elliptic fixed point encircled by stable elliptic type map orbits. For $|\omega| > 2$ (outside the range of the linear band) we distinguish the following two cases:

(i) $\omega < -2$, $\gamma + 2\mu > 0$:

In this case the residue is negative ($\rho < 0$), and hence the origin loses stability and is turned into an unstable hyperbolic point caused by a tangent bifurcation. This hyperbolic point is connected to itself by a homoclinic orbit created by the (invariant) unstable and stable manifold. As will be shown below the homoclinic orbit is manifested on the lattice chain as a *solitonlike solution*. For more information on homoclinic and heteroclinic connections of hyperbolic points Ref. [199] can be consulted.

The pair of points $\hat{x}_\pm$ on the symmetry line $x = y$ form stable elliptic fixed points.

(ii) $\omega > 2$, $\gamma + 2\mu < 0$:

The value for the residue at the origin has passed through the value of one, that is $\rho > 1$, connected with the onset of a period-doubling bifurcation, where the fixed point is converted into an unstable hyperbolic point with reflection. The newly created period-2 orbits are located on the line $x = -y$.

The homoclinic map orbit supports on the lattice chain a solitonlike solution which exists in the gap above the linear passing band and has alternating signs for adjacent amplitudes, i.e. $\mathrm{sign}(\phi_{n+1}) = -\mathrm{sign}(\phi_n)$ as a characteristic feature. This stationary localized structure has been called a *staggered soliton* [150, 172]. Correspondingly the soliton solution of case (i) is called unstaggered soliton. Note that upon sign change $\gamma \to -\gamma$ and $\omega \to -\omega$ the map has the symmetry property of $\mathrm{sign}(\phi_{n+1}) = -\mathrm{sign}(\phi_n)$ so that the unstaggered and staggered solitons replace each other.

A third case of unstable fixed points can also be attributed to the occurrence of a stationary localized structure on the nonlinear lattice, namely:

(iii) $|\omega| < 2$ and $\gamma + 2\mu < 0$:

Since the frequency is in the linear band the origin is still a stable elliptic fixed point whereas the pair of fixed points $\hat{x}_\pm$ on the line $x = y$ represents two unstable hyperbolic fixed points which are connected to each other via a (pair of) heteroclinic orbits. This heteroclinic map orbit represents a kink-like solution, also called a dark soliton. There exist staggered and unstaggered versions of this soliton, too.

Figure 3.1: The homoclinic orbits related to the staggered and unstaggered bright solitons, respectively. Parameters: $\gamma = 5$, $\mu = 1$, and $\omega = 2.25$.

Figure 3.2: The heteroclinic orbits related to the unstaggered dark soliton. Parameters: $\gamma = -3$, $\mu = 1$, and $\omega = -1$.

Since the nature of the solitonlike solutions depends on the stability of the fixed points we summarize their bifurcation behavior. The stability properties of the fixed point $(\hat{x}_0, \hat{y}_0)$ is

$$\begin{array}{lll} |\omega| & < 2, & \text{elliptic point,} \\ \omega & > 2, & \text{hyperbolic point with reflection,} \\ \omega & < -2, & \text{hyperbolic point .} \end{array} \tag{3.20}$$

From the stability analysis of the fixed point $(\hat{x}_\pm, \hat{y}_\pm)$ it can be seen that the dark soliton solution exist only for $\gamma < 0$ and not for vanishing γ. In other words AL dark solitons are excluded whereas the bright solitons exist in both extreme cases of $(\gamma \neq 0, \mu = 0)$ and $(\gamma = 0, \mu \neq 0)$. In Fig. 3.1 (Fig. 2(a) of Paper VIII) we show the staggered and unstaggered bright solitons superimposed on a single map plane. The transversal intersections of the stable and unstable manifolds of the hyperbolic point at the origin are invisible on the used scale. However, as we will see later we can prove the existence of these intersections analytically. Figure 3.2 (Fig. 2(b) of Paper VIII) illustrates the heteroclinic structure and here the chaotic layer connected with the heteroclinic connection of the two hyperbolic points are clearly visible. Thus points belonging to the stable manifold $\mathcal{W}^s(p)$ approach the fixed point p under map iteration $\mathcal{M}^n$ for $n \to \infty$, likewise points on the unstable manifold $\mathcal{W}^u(p)$ reach the fixed point p for $n \to -\infty$. Thus going along the invariant manifolds of the hyperbolic fixed point localized stationary solutions can be created. However, searching for solitonlike solutions, one has to be aware that the DNLS system is nonintegrable; a property which usually prevents systems from having solitonlike solutions, since

these are associated with an integrable system. As already mentioned the integrable AL equation possesses soliton solutions which are the discrete versions of the solitons of the (integrable) continuum nonlinear Schrödinger equation [144]. These discrete AL-solitons manifest in the integrable map as a perfect separatrix with coinciding stable and unstable manifolds. Since the DNLS system is nonintegrable we know that the separatrix is destroyed in the sense that the stable and unstable manifolds no longer coincide but rather intersect each other transversally in homoclinic points, creating complicated chaotic dynamics developing eventually Smale horseshoes [199]. Coste and Peyrard [201] as well as Wan and Soukoulis [202] dealt with the linkage between the homoclinic orbit of the DNLS map and localized states of the lattice. Coste and Peyrard draw the conclusion that 'perfect localization in a DNLS system is impossible' because of the residual stochasticity near the hyperbolic points. Instead of exhibiting a 'one-peak solution' as in an integrable system where a solution can approach a hyperbolic point as arbitrarily close as is wanted, they claim that in a nonintegrable system multi-peak solutions are expected to appear. Wan and Soukoulis came to the same conclusion regarding the DNLS system in the context of Holstein's polaron model.

Figure 3.3: The homoclinic tangle of the hyperbolic fixed point at the origin. The amplitudes resulting from the dynamical study are shown with diamonds. They appear at the transversal intersections of the invariant manifolds.

In contrast to the propositions in [201, 202], there exist stable stationary localized solutions to the DNLS associated with homoclinic and heteroclinic orbits of the related map. This is the case even though there exist neighboring map orbits which are strongly chaotic. The reason is that the localized states rely on the structural stability of homoclinic (heteroclinic) orbits, such that

their amplitudes are represented by a homoclinic (heteroclinic) orbit in the corresponding map plane of $\mathcal{M}$. A homoclinic point $(\phi^h_{n+1}, \phi^h_n) \equiv q$ is defined by $q \in \mathcal{W}^s \cap \mathcal{W}^u$ and $q \neq p$. Since q belongs both to the stable and the unstable manifold of p it follows that $\mathcal{M}^n(q) \to p$ as $n \to \pm\infty$.

In Fig.3.3 (Fig. 3(b) of Paper VIII) we show the homoclinic tangle, and the homoclinic points are clearly recognized. Points below the symmetry line $x = y$ are characterized by $\phi_{n+1} < \phi_n$ for $n > 0$, i.e. belong to $\mathcal{W}^s$. Each homoclinic point is mapped into another one and after only a few map iterations rapidly approaches the map origin where $\phi_n \to 0$.

Correspondingly, the homoclinic points above the line $x = y$ for which $\phi_n < \phi_{n+1}$ for $n > 0$ will be mapped into the map origin in course of the inverse map, i.e. belong to $\mathcal{W}^u$ reflecting the translational invariance of the discrete lattice under the operation $n \leftrightarrow -n$.

The knowledge about the homoclinic (heteroclinic) orbits can be used to initiate (stationary) breathers for the time-dependent DNLS dynamics. In order to invoke the homoclinic map orbit as an initial condition for the dynamics, a sufficiently accurate location of the orbit members (homoclinic intersection points) is demanded. There are several analytical methods which meet this demand, and we use an approach recently developed by Tabacman [203]. For a study of the soliton dynamics for the AL-DNLS Eq.(3.7) we use a lattice of chain length $N = 201$. We implement the analytically computed homoclinic orbit ϕ^h_n with $n \in [-N/2, N/2]$ as initial conditions $\mathrm{Re}[\psi_n(t = 0)] = \phi_n$ and $\mathrm{Im}[\psi_n(t = 0)] = 0$. The result for the breather is illustrated in Fig.3.4 (Fig. 4(a) of Paper VIII). The (dynamical) breather intensities $|\psi_n(t)|^2$ are inserted

Figure 3.4: Profile $|\psi_n(t)|^2$ of the stationary bright solitonlike solution of the AL-DNLS Eq.(3.7)

as diamonds on the map plane in Fig. 3.3 to show that they coincide with the homoclinic orbit. From Fig. 3.3 it is now apparent that the shown solitonlike solution is not the only one possible. The other possibility is to chose the homoclinic orbit which has one of its members on the line $x = y$. This will result in a solution which has its center between sites and is often called the *Page mode* [204]. Contrary to the Page mode the solution which is shown in Fig.3.4 has its center on a site and is often called the *Sievers-Takeno mode* [175]. The Page mode is usually dynamically unstable contrasting the Sievers-Takeno mode [116].

A tool to analyze the homoclinic tangle is the Melnikov function [199]. Glasser *et al.* [205] extended the Melnikov analysis to two-dimensional discrete maps $u_{n+1} = F(u_n) + \epsilon G(u_n)$ of the plane. Thus, the map is assumed to consist of a completely integrable part F and a small nonintegrable perturbation ϵG with $\epsilon \ll 1$. Furthermore, the unperturbed system of $\epsilon = 0$ possesses an unstable equilibrium characterized by coinciding stable and unstable manifolds forming a perfect unperturbed separatrix on which the solution is known explicitly. Based on geometric arguments a Melnikov function was developed in [205] measuring the distance between the stable and unstable manifolds under the action of the perturbation. For a perturbational treatment we consider the nonlinear term related with γ as a small (nonintegrable) perturbation of the integrable AL map ($\gamma = 0$, $\mu \neq 0$).

The Melnikov function $\Delta'(0)$ can be found exactly in terms of Jacobi Elliptic functions. It is a rather complex expression (see Paper VIII) so here we will only give an approximate expression

$$\Delta'(0) = -\frac{\epsilon\gamma}{\mu} A(\omega) \cos\left(\frac{4K}{\beta} t + \theta\right) + \mathcal{O}(k^2) \tag{3.21}$$

where

$$A(\omega) = \frac{2K^3 k^2}{\omega \beta^2} \sqrt{\coth^2 \beta + \frac{26K^2}{9\beta^2}} \sinh^4 \beta, \tag{3.22}$$

$$\tan\theta = \frac{3\beta \coth \beta}{4K}. \tag{3.23}$$

K and E are the complete elliptic integral of the second kind and the associated complete elliptic integral of the second kind, respectively. These integrals are related to β through $E(k)/K(k) = \pi/\beta$ where $\cosh \beta = -\omega/2$. The distance between successive zeros of the Melnikov function is given by

$$\Delta t = \frac{\pi\beta}{4K} \simeq \frac{1}{2} \ln\left(-\frac{\omega}{2} + \sqrt{\frac{\omega^2}{4} - 1} \right), \tag{3.24}$$

telling us that the distance between two adjacent intersections of the stable and unstable manifold depends solely on the breather frequency ω. The distance vanishes at the band edge of $\omega = -2$ and grows logarithmically when ω ranges further down in the gap.

Equation (3.21) shows that the separatrix splitting is proportional to the ratio $\gamma/(\omega\mu)$. The same ratio was found in [194] to bound the parameter region where the map (3.14) shows regular motion. Finally, from Eq. (3.21) it is obtained that the distance between successive transversal intersections of the stable and unstable manifolds only depends on ω and not directly on the nonlinearity parameters γ and μ. The nonlinearity parameters appear only in front of the Melnikov function (3.21) as a factor regulating the degree of the separatrix splitting. Apparently with higher nonintegrability parameter γ the splitting grows whereas the integrability parameter μ acts in the opposite direction, namely suppresses the splitting.

Using Eq.(3.24) we calculate in Paper VIII the energetic difference between the Sievers-Takeno mode and the Page mode. As suggested by other authors [206, 196] this is approximately the energy required for the excitation to move from one lattice site to the next. So the energetic difference is an estimate of the so-called *Peierls-Nabarro* barrier, which was first discussed in the theory of dislocations in solid state systems [207]. The Peierls-Nabarro barrier reflects the fact that the discreteness of the underlying lattice in solid state systems breaks the continuous translation invariance and generates a periodic potential which affetcs the dislocations. From the physical point of view, the amplitude of the Peierls-Nabarro potential barrier may be viewed as the minimum barrier which must be overcome to translate the dislocation by one lattice period. In the present context we can clearly ascribe the Peierls-Nabarro barrier to the nonintegrality imposed on the system by the DNLS term. Estimates based on IST perturbation theory of the Peierls-Nabarro barrier in the AL-DNLS equations has been given before [206, 174], however, this estimate is generally quite poor [208]. An analysis of the combined effects of the finiteness of the lattice and the discreteness in the DNLS is given in [14].

The method of using the homoclinic and heteroclinic intersections to design solitonlike solutions, may be developed further, to construct for example "multi humped" solutions similar to the N soliton solutions of the continuum NLS equation, using the secondary intersections of the tangling homoclinic orbits. This could probably be done using some recently developed Melnikov methods [209] to obtain the secondary intersections.

3.4 Noise effects on discrete solitonlike excitations

Chapter 2 reviews the work on the models derived as reductions of the coupled exciton system, and particularly Sec.2.3 reviews the results obtained when the reduced equation (see Eq.(2.31)) includes a nonlinear damping term. The equation (2.31) was a result of a continuum approximation. Since we now have obtained some knowledge on discrete effects it is the purpose of the present section to review the result of the work (given in Paper IX) on the one-dimensional

discrete version of Eq.(2.31)

$$i\dot{\psi}_n + J_0(\psi_{n+1} + \psi_{n\perp 1}) + \gamma|\psi_n|^2\psi_n - \eta\psi_n\frac{d}{dt}[|\psi_n|^2] + h_n(t)\psi_n = 0 \qquad (3.25)$$

where the last two terms describe nonlinear damping and multiplicative Gaussian white noise, respectively. The noise is assumed to have zero mean and variance $2D$, i.e.,

$$\langle h_n(t)\rangle = 0, \quad \langle h_n(t)h_{n'}(t')\rangle = 2D\delta(t-t')\delta_{n,n'}. \qquad (3.26)$$

For the discrete version Eq.(3.25) the norm conservation persists and a discrete analogue of Eq.(2.34) also in the discrete version provides the possibility of thermal equilibrium in the exciton system.

Paper IX presents numerical simulations of the dynamics of Eq.(3.25). In the simulations the exciton wave function is always normalized to have the norm $N = \sum_n |\psi_n| = 1$. This is done without loss of generality since results for any norm N can be obtained by rescaling $\gamma \to \gamma N$, $\eta \to \eta N$. Also without loss of generality we have fixed the energy (or time) scale by using $J_0 = 1$. The initial condition used in all simulations is the single site excitation at site n_0

$$\psi_n(0) = \delta_{n,n_0}. \qquad (3.27)$$

This choice of initial condition has, in the absence of noise and damping, previously [210–212] been used to show that the DNLS equation exhibits a *self-trapping transition* when $\gamma = \gamma_c \simeq 3.5$. That is, for $\gamma > \gamma_c$ the initial-site probability $|\psi_{n_0}|^2$ will always remain nonzero. Thus a breatherlike excitation exists. Since we here are interested in studying the effect of noise and damping on the localized excitation we consider only nonlinearities $\gamma \geq 5$, for which the trapped excitation has a highly discrete breatherlike nature. Figure 3.5 (Fig. 1 of Paper IX) illustrates how the presence of noise in Eq.(3.25) affects the breather. As is seen the main effect of the noise is initially to cause a slow decrease (which is almost linear with time) of the breather intensities. This slow decrease continues until the initial-site probability has reached approximately half of its initial value. At this point the breather is rapidly destroyed. The long time behavior is then diffusive (i.e. $|\psi_{n_0}|^2$ decays in average as $t^{\perp 1/2}$), as in the linear system, $\gamma = 0$.

Judging from the systematic numerical investigations of Paper IX, the behavior seen in Fig.3.5 appears to be generic. The lifetime of the breather is always finite, but increases when (a) the nonlinearity γ is increased, (b) the nonlinear damping η is increased, or (c) the noise variance D is decreased. To quantify these dependences the decay rate κ defined as the mean value of $(-d/dt)(|\psi_{n_0}|^2)$ is studied. As noted above the breather amplitude decrease linearly in time such that the lifetime t_L is related to the decay rate as $t_L \simeq 1/(2\kappa)$. The study of the decay rate shows that for not too strong noise the decay rate κ is proportional to the noise variance D. If the noise is too strong the diffusive spreading sets in immediately never allowing existence of a breatherlike excitation. Fixing D

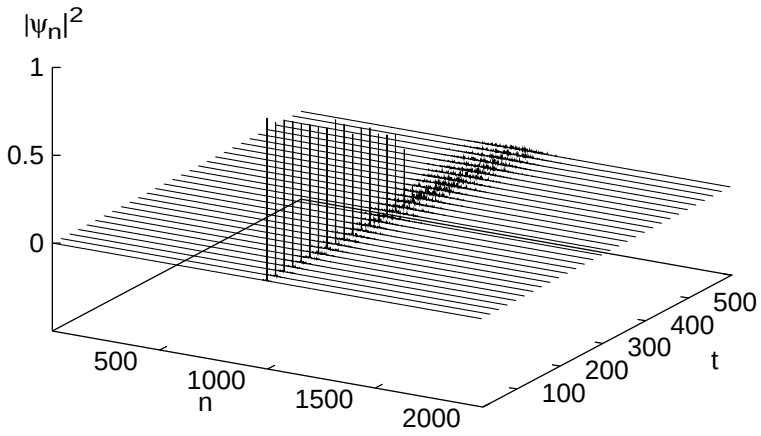

Figure 3.5: Time evolution of an initially single-site localized excitation. Parameter values are $\gamma = 10$, $\eta = 2$ and $D = 0.05$.

and η Paper IX also finds the decay rate to be proportional to $\gamma^{\perp 2}$, while no simple relation between the decay rate and the damping η is observed.

Paper IX also treats Eq.(3.25) analytically applying a collective coordinate method. We shall here omit the the details of this approach which involves a transformation to action angle variables and a derivation of a Fokker-Planck equation [133] for these variables. Based on this Fokker-Planck equation the approximate evolution of the initial-site probability is found to

$$\langle |\psi_0(t)|^2 \rangle \simeq \begin{cases} 1 - \frac{2J_0^2}{\gamma^2} - \frac{6DJ_0^2}{\gamma^2} t, & \frac{6\eta J^2}{\gamma} t \ll 1, \\ 1 - \frac{2J_0^2}{\gamma^2} - \frac{D}{\gamma\eta}, & \frac{6\eta J^2}{\gamma} t \gg 1. \end{cases} \tag{3.28}$$

We see that the collective-coordinate approach yields a qualitatively good agreement with the results of the numerical simulations as concerns the dependence of the decay rate of the breather on nonlinearity and the noise intensity: The coefficient $6DJ_0^2/\gamma^2$ for the linear term in the short time regime exhibits the proportionality to D/γ^2 that was observed numerically and the numerical prefactor is of the same order of magnitude. However, Eq.(3.28) predicts a stationary nonzero value of the initial-site intensity as $t \to \infty$ when $\eta \gtrsim D/\gamma$, while we have seen above that $|\psi_{n_0}|^2$ always decays to zero. The discrepancy is caused by the fact that the collective coordinate approach necessarily assumes conservation of the total norm of the breather. As is clear from Fig.3.5 there will in reality be created some radiation through the action of the noise, causing the norm of the breather to decay in with time.

As an interesting example Paper IX shows that if the lattice is truncated to consist of only two sites - a dimer - the stationary Fokker-Planck equation

can be solved exactly. Thus the stationary distribution function for the difference $z = |\psi_1|^2 - |\psi_2|^2$ in the occupation probability between the two sites can be found analytically. From this function, which is given in Eq.(49) of Paper IX, we observe that the shape of the stationary probability distribution changes qualitatively when the parameters D and η are varied. In one region of the parameter space the probability distribution is unimodal, having one single maximum at $z = 0$ corresponding to equal population between sites. In other regions the probability distribution is bimodal, having two equivalent maxima corresponding to an excess of population on either of the two sites and a local minimum at $z = 0$. Thus, changing the noise D a transition in the form of the probability distribution can be accomplished; this is a so-called *noise-induced phase transition* [135]. It is important to note that the state will not necessarily be trapped around one of the probability maxima even if the distribution is bimodal, since the noise can force frequent transitions between the sites. So although the self-trapping transition and the above described transition coincide in the noise free limit (shown in Paper IX), they are very different when noise is present.

3.5 Two-dimensional effects

In chapter 2 we approximated the discrete two-dimensional NLS like equations with the two-dimensional continuum equation, and previously in the present chapter we have studied the localized excitations of discrete one-dimensional NLS equations. To complete the picture we should study the localized excitations of discrete two-dimensional systems. This we will do in this section which gives a review of Paper X.

We simply study the two-dimensional version of the combined AL-DNLS equation Eq.(3.7)

$$\begin{aligned} i\dot{U}_{m,n} &+ \omega_{m,n}U_{m,n} - 4U_{m,n} + 2\,(1-\alpha)\,U_{m,n}|U_{m,n}|^2 \\ &+ (U_{m+1,n} + U_{m\perp 1,n} + U_{m,n+1} + U_{m,n\perp 1}) \\ &\times \left(1 + \frac{\alpha}{2}|U_{m,n}|^2\right) = 0, \end{aligned} \tag{3.29}$$

where the parameter α gives the relative strength of DNLS ($\alpha = 0$) and AL ($\alpha = 1$) types of nonlinearities, and $\omega_{m,n}$ describes an inhomogeneous frequency shift at site n, m such that impurity effects can easily be studied. Equation (3.29) possesses conserved quantities which are simple generalizations of those given in Eqs.(3.8) and (3.9). Also, Eq.(3.29) can be derived from the Hamiltonian using a deformed Poisson bracket similar to Eq.(3.10). It is expected that although the integrability is lost even for $\alpha = 1$ this case should be "more" well behaved than the case $\alpha = 0$.

In Paper X we study numerically the stationary states

$$U_{m,n} = F_{m,n}\exp(i\omega t) \tag{3.30}$$

of Eq.(3.29). In the one-dimensional DNLS equation (generalized to have nonlinearity $|\psi_n|^{2\sigma}\psi$) Laedke, Spatschek and Turitsyn [115] proved that the Vakhitov-Kolokolov criterion [118] Eq.(1.30) for the linear stability of the stationary excitations also applies to the discrete case. The criterion has not been proved to apply also to the case of Eq.(3.29), but it has been conjectured to hold also in this case by several authors [213, 214, 24]. For the pure DNLS case of Eq.(3.29) the validity of the Vakhitov-Kolokolov criterion has been proven in [214]. We

Figure 3.6: Norm N versus λ for $\alpha = 1$ (Ablowitz-Ladik case solid line), 0.5 (dashed line), 0.2 (dot-dashed line), and 0 (DNLS, dotted line)

plot in Fig. 3.6 (Fig. 1(a) of Paper X) the norm N versus the frequency $\lambda = \sqrt{\omega}$ for a particular grid size: 32×32, for different values of α. The value of the local maximum of N increases with α. On the other hand, the range in parameter λ corresponding to the negative slope of the curve $N(\lambda)$ is narrowing with the increasing of α. It means that in the case of Ablowitz-Ladik solitons the instability region is smaller. In the limit of large λ, $\partial N/\partial\lambda > 0$ for all α; i.e., the stability property of the "narrow" soliton solutions are independent of α.

The positive slope of $N(\lambda)$ near $\lambda = 0$ are boundary effects. Paper X shows this by investigating larger grid sizes. In the limit of infinite grids the influence of the boundary conditions becomes negligible and it is reflected in narrowing of the dip in the region of small λ with increasing number of grid points. The level of the flat plateau between the dip and the local maximum near $\lambda \approx 0.6$ approaches in an infinite lattice limit the asymptotic threshold value N_T corresponding to the continuum ground state soliton (the Townes soliton). The conjecture is therefore that only the smaller and the larger values of λ (for which $\partial N/\partial\lambda > 0$) corresponds to stable solutions, i.e. bistability occurs. We have obtained numerical support of that conjecture using the soliton solution as an

initial condition in simulations of the full dynamical equations (3.29).

Localization (quasi-collapse) and pinning (by the Peierls-Nabarro potential, see page 49) are important properties in applications. Paper X investigates the dynamics of initially localized excitations numerically using the initial condition

$$U(m,n,t=0) = A(m,n)\exp\left(i\kappa_m(m-\overline{m})+i\kappa_n(n-\overline{n})\right), \quad (3.31)$$

$$A(m,n) = A_0\exp\left(-\left(\frac{m-\overline{m}}{m_0}\right)^2-\left(\frac{n-\overline{n}}{n_0}\right)^2\right). \quad (3.32)$$

where $(\overline{m},\overline{n})$ is the initial position and $(m_0\,,n_0)$ the widths in the m and n directions, respectively. κ_m and κ_n define the initial velocities in the m and n directions, respectively. The investigations of the discrete localization dynamics shows a much richer variety than in the continuum case where there are merely two alternatives, collapse in finite time or dispersive spreading. The behavior of nonmoving ($\kappa_m=\kappa_n=0$) initial conditions is investigated in the homogeneous case as well as in the presence of impurities at the center of the initial excitation. Both the case $\omega_{\overline{m},\overline{n}}=-\omega<0$ and the case $\omega_{\overline{m},\overline{n}}=\omega>0$ are investigated. The general scenario is that the initially broad excitations collapse to a much narrower excitation essentially occupying the five central sites. However the excitation is periodically transferring energy between the central site and the four neighboring ones. The details of this transfer depend on $\omega_{\overline{m},\overline{n}}$. Since the excitation seems only to occupy the central five sites, an obvious analytical approximation is to only consider these five sites, which makes the model solvable due to the symmetry properties. However the results of this approximation turn out to be quite poor. The scenario is even more spectacular when the the excitation is given an initial velocity $\kappa_m=0$, $\kappa_n\neq 0$. An example of the evolution of a broad initial condition with a nonzero velocity is given in Fig. 3.7. Initially the excitation is able to move because it is broad and continuum like and experiences only a small Peierls-Nabarro barrier. However, the excitation collapses to a much more narrow peak as in the non-moving case. As the width of the peak decreases, the Peierls-Nabarro barrier experienced by this part of the excitations increase because of the discreteness of the lattice. Eventually the narrow peak is stopped, but the background which is still rather broad does not feel the Peierls-Nabarro barrier and therefore continues until a new peak is created. The number of peaks depends on the initial norm of the excitation, and the relation is discussed in detail in Paper X. The norm of the quasi-collapsed peak is close to the norm of the Townes soliton because it is initiated by a continuum two-dimensional collapse. Because of various asymmetries, the norm of the quasi-collapsed peak is only close to the norm of the Townes soliton, and can vary slightly depending on the initial process. Paper X also describes this pinning effect in presence of inhomogeneities in the lattices. In Ref. [24] the combined two-dimensional AL-DNLS equation is investigated in further detail.

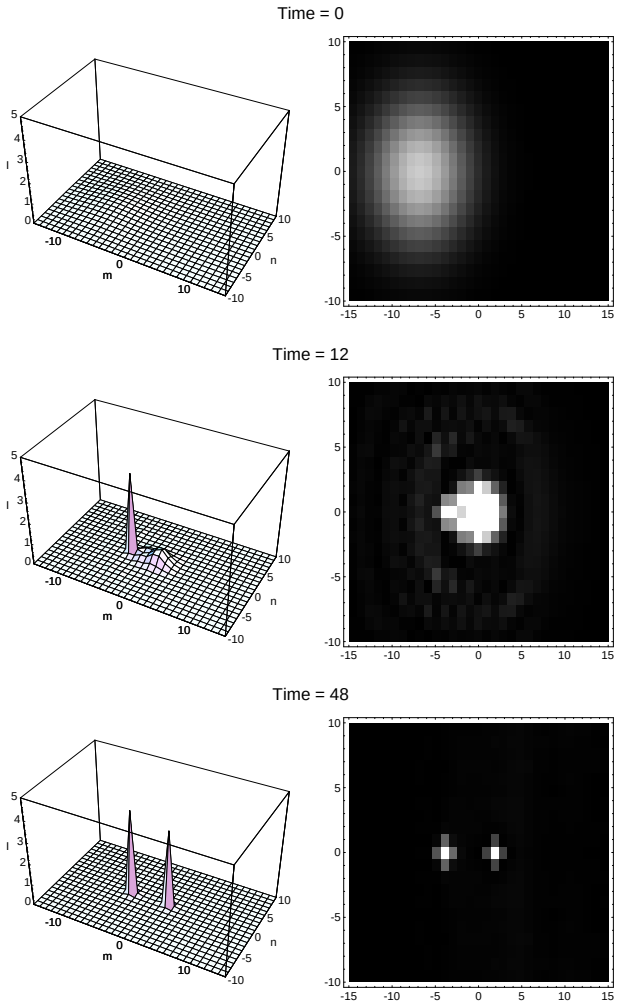

Figure 3.7: Evolution of the intensity of a moving solution in the homogeneous DNLS case. Initial condition Eq.(3.31), with $A_0 = 0.4$, $m_0 = n_0 = 8$, $\kappa_n = 0$, $\kappa_m = 0.1\pi$ and $(\overline{m}, \overline{n}) = (-7, 0)$; $t = 0$, 12, and 48.

3.6 Conclusion

In summary we have in the present chapter reviewed some of the properties of discrete NLS equations. Properties of the integrable discretization AL and of the more standard discretization DNLS have been described.

Reviewing Paper VIII, the relation between a discrete map and localized excitations of the combined AL-DNLS equations was described. The map was analyzed using traditional tools of nonlinear dynamics such as fixed point analysis and Melnikov analysis. The map also allowed us to describe the different parameter regions where bright (staggered or unstaggered) solitons and (staggered or unstaggered) dark solitons are possible. The Melnikov analysis allowed us to determine in a novel way the pinning energy of a discrete excitation.

The continuum model (of Paper V) with nonlinear damping and noise was studied in a discrete version. We showed in the process of reviewing Paper IX that the discrete breathers are always destroyed in the presence of the noise and that the life time of the breather essentially is inversely proportional to the noise variance and proportional to the square of the nonlinear coefficient.

Finally, the dynamics of localized excitations in the two-dimensional combined AL-DNLS equations was described reviewing Paper X. It was shown that the presence of the DNLS term expanded the window where the localized excitations where unstable. Furthermore, the propagation and the combined collapse-pinning effect was studied.

Parts of the material reviewed in this chapter can also be found in the publications [24–26] which display different parts of the material from various points of view.

Chapter 4

Nonlocal models

4.1 Introduction

This chapter will describe the extension of the already discussed continuum and discrete models to include long range interaction effects. First a short discussion of the possible physical origins of the long range interactions in various contexts will be given. Then we will move on to describe the effects of nonlocal dispersion in a continuum NLS equation, that will be a review of the work included in Paper XI. In the continuum model the nonlocal interaction will be assumed to depend exponentially on the distance. This assumption allow us to find the stationary solutions analytically.

After having discussed the results of the continuum system we will move on to describe the discrete systems as we are reviewing Paper XII. In the discrete case the nonlocal interaction will mainly be assumed to have a power law dependence on the distance; an assumption which is physically appropriate in the case of molecular aggregates for example. Finally, the chapter will show how a two-dimensional Kronig-Penney system can be described by a one-dimensional nonlocal equation. This is the result of Paper XIII where also the stationary states of the derived nonlocal equation are studied.

4.2 Physical origin

In the main body of the previous research on nonlinear systems in different physical contexts, the dispersive interaction was assumed to be short-ranged and therefore a nearest-neighbor approximation was used. Often the nearest-neighbor approximation has also been chosen because it can be easily treated, and suffices as a first approximation. However, there exist physical situations that are not appropriately described in the framework of this approximation. Excitation transfer in molecular crystals [50] and vibron energy transport in biopolymers [51] are due to transition dipole-dipole interaction with $1/r^3$ dependence on the distance, r. The DNA molecule contains charged groups, with

long-range Coulomb interaction $(1/r)$ between them. Systems where the dispersion curves of two elementary excitations are close or intersect the resulting dispersion curve saturates, which in effect leads to long-range transfer. Such a situation arises for excitons and photons in semiconductors and molecular crystals as the so-called polariton effects [50].

Nonlinear waves in a one-dimensional chain with Lennard-Jones $(2n, n)$ interatomic potential were studied by Ishimori [215] who showed that the dynamics is governed by the Benjamin-Ono equation in the case $n = 2$ or by the Korteweg-de Vries equation for $n \geq 4$. Solitons in implicit form were obtained [216] in a sine-Gordon system with long range interaction of the Kac-Baker type [217] and the dependence of the soliton width and energy on the radius of the long range interaction was analyzed. A sine-Gordon equation with a nonlocal character of the nonlinear term was postulated in [218] and novel soliton states, of topological charge zero, were found to exist at large interaction radius. The effects of long-range harmonic interaction in a chain with short-range anharmonicity was considered in [219], and it was demonstrated that the existence of two velocity dependent competing length scales leads to two types of solitons with characteristically different width and shapes for two velocity regions separated by a gap. Effects of long-range interactions of the Kac-Baker type were also studied in static and dynamic nonlinear Klein-Gordon models [220].

4.3 Continuum description

In order to investigate the dynamics of self-interacting quasiparticles in one-dimensional systems with long-range dispersive interactions we consider in Paper XI the Hamiltonian

$$\begin{aligned} H = & - \int_{\perp\infty}^{\infty} \left\{ \frac{1}{2} |\psi(x,t)|^4 \right. \\ & + \left. \int_{\perp\infty}^{\infty} J(x-y) (\psi^*(x,t)\psi(y,t) - |\psi(x,t)|^2) dy \right\} dx \end{aligned} \tag{4.1}$$

and the corresponding Lagrangian

$$L = \frac{i}{2} \int_{\perp\infty}^{\infty} \{\psi^*(x,t)\partial_t \psi(x,t) - c.c.\}\, dx - H. \tag{4.2}$$

The double integral in Eq.(4.1) describes the excitation transfer in the system. The matrix element of transfer, $J(x)$, is chosen to be of the Kac-Baker [217] form $J(x) = J \exp(-\alpha|x|)$, with α being the inverse radius of interaction, and J its intensity. The equation of motion for the excitation wave function then becomes the nonlocal nonlinear Schrödinger equation

$$i\psi_t + \int_{\perp\infty}^{\infty} J(x-y)\, (\psi(y,t) - \psi(x,t))\, dy + |\psi|^2 \psi = 0. \tag{4.3}$$

The kernel $J(x)$ in this integro-differential equation is the Green's function given by the equation $(\partial_x^2 - \alpha^2)J(x) = -2J\alpha\delta(x)$. Consequently Eq.(4.3) may be rewritten as

$$i\partial_t\psi + \frac{2J}{\alpha}\frac{\partial_x^2}{\alpha^2 - \partial_x^2}\psi + |\psi|^2\psi = 0. \tag{4.4}$$

The linear part of Eq.(4.4) corresponds to the dispersion law $\omega(k) = \frac{2J}{\alpha}\frac{k^2}{\alpha^2+k^2}$. Under the assumption $\alpha \to \infty$, $J \to \infty$, $J\alpha^{\perp 3} \to$ const. Eq.(4.4) reduces to the NLS Eq.(1.8). However, if the width of the excitations and the radius of interaction, $\alpha^{\perp 1}$, are of the same order, the nonlocal effects represented by the pseudo-differential operator in Eq.(4.4) become important.

In rescaled form Eq.(4.4) becomes

$$i\partial_t\phi + \frac{\partial_z^2}{1 - \partial_z^2}\phi + |\phi|^2\phi = 0, \tag{4.5}$$

and additionally

$$\int_{\perp\infty}^{\infty} |\phi(z,t)|^2 dz = \frac{\alpha^2}{2J}N \equiv \mathcal{N}, \tag{4.6}$$

where the norm N, like the Hamiltonian H, is a conserved quantity. Stationary solutions of Eq.(4.5) in the form

$$\phi(z) = F(z,\lambda)\exp(i\lambda^2 t) \tag{4.7}$$

can be obtained exactly since the resulting ordinary differential equation for F can be solved by quadrature. Therefore the norm $\mathcal{N}$ can also be expressed in terms of the frequency λ^2. In Figure 4.1 we show $\mathcal{N}$ versus λ and it shows in contrast to the ordinary NLS equation that the stationary solution exists only for $\mathcal{N} \leq \mathcal{N}_{\max} \simeq 1.128$, or $N \leq N_{\max} \simeq 2.255 J\alpha^{\perp 2}$. Therefore the nonlocal NLS equation has stationary solutions only in a finite interval of $\mathcal{N} \in [0, \mathcal{N}_{\max}]$. $\mathcal{N}_{\max}$ tends to infinity in the limit of the usual NLS equation. Figure 4.1 shows that with the norm $\mathcal{N}$ in the interval $[1.125, \mathcal{N}_{\max}]$ there are two values of λ for a given $\mathcal{N}$, i.e. two branches of stationary solutions exist in that interval. The first branch corresponds to the part of the $\mathcal{N}(\lambda)$ for which $\frac{d\mathcal{N}}{d\lambda} > 0$ and it exists for any $\mathcal{N} \leq \mathcal{N}_{\max}$. For $\mathcal{N} \ll \mathcal{N}_{\max}$ ($\lambda \ll 1/\sqrt{8}$) the solution reduces to the stationary solution of the usual NLS equation. The second branch with $\frac{d\mathcal{N}}{d\lambda} < 0$ exists only in the interval $[1.125, \mathcal{N}_{\max}]$. At $\mathcal{N} = \mathcal{N}_{\text{cusp}} = 1.125$ we obtain a solution of the form

$$\phi(z,t) = \left(\frac{3}{8}\right)^{1/2} \exp\left(i\frac{t}{8} - \frac{1}{3}|z|\right). \tag{4.8}$$

Due to the pointed maximum of this solution we called it a *cusp soliton*.

Paper XI applies a collective coordinate approach to investigate the stability of the stationary states. This method leads to the instability criterion $d\mathcal{N}/d\lambda < 0$ which agrees with the Vakhitov-Kolokolov criterion (see the discussion related to Eq.(1.30) page 16). It should however be emphasized that

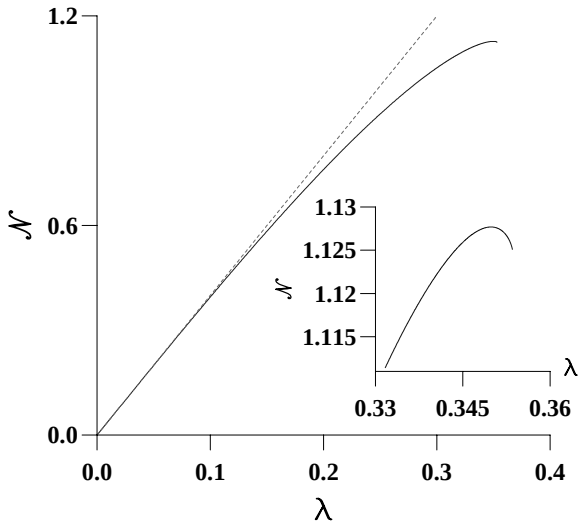

Figure 4.1: Norm $\mathcal{N}$ versus nonlinear frequency λ, for the stationary solutions. Dashed line: NLS Eq.(1.8). Solid line: nonlocal NLS Eq.(4.5). The inset shows the two branches at the maximal norm. The endpoint corresponds to the cusp soliton.

using the collective coordinate approach we can not prove stability but only instability can be proven. Numerical simulations support the conjecture that the Vakhitov-Kolokolov criterion is valid also in this nonlocal case. Plotting the Hamiltonian H versus the norm $\mathcal{N}$ shows the bifurcation diagram of the so called *catastrophe manifold* [221]. The bifurcation diagram has a *swallow tail* structure, and using the conjectures of catastrophe theory [221] on this diagram leads to the same stability criterion as suggested above. A similar discussion for a two-dimensional NLS equation is given by Laedke *et al.* [214]. This means that the branch in Fig.4.1 with $d\mathcal{N}/d\lambda < 0$ is unstable and in particular the cusp soliton is unstable. The instability expresses itself by the creation of a collapse like phenomenon in the evolution of a slightly perturbed state from the unstable branch. The collapse is clearly due to the saturation of the dispersion in the high end of the spectrum enabling high sharp peaks to develop without excessive energy consumption.

In contrast to the ordinary NLS equation, Eq.(4.3) is not Galilean invariant, causing radiation losses when the solitons are propagated. This radiation is investigated analytically and numerically in Paper XI where also the dominant wave number of the radiation is found to be inversely proportional to the propagation velocity. Thus no radiation is present when the soliton is non-moving. This is in contrast to the case of high order dispersion caused by terms like $i\phi_{xxx}$ or ϕ_{xxxx} in the ordinary NLS equation. These case were studied numerically and analytically by several authors [222] who found that the soliton will always

radiate in the presence of the high order dispersion.

4.4 Discrete description

The paper Paper XII investigates the impact of nonlocal dispersive coupling on discrete NLS systems. In the discrete case the coupling is chosen to have a power $r^{\perp s}$ dependence on the distance r; this choice is based on the physical relevance of such a coupling. However, investigations [223] have shown that the exact form of the coupling only affects the behavior quantitatively. Kac-Baker and the power $r^{\perp s}$ dependence have been observed [223] to yield exactly the equivalent qualitative features. The model studied in Paper XII is

$$i\dot{\psi}_n + \sum_{m(m\neq n)} |m-n|^{\perp s}(\psi_m - \psi_n) + |\psi_n|^{2\sigma}\psi_n = 0 \tag{4.9}$$

where the generalized nonlinearity $|\psi_n|^{2\sigma}\psi_n$ is reintroduced from Eq.(1.28). The parameter s is introduced to cover different physical situations from nearest-neighbor approximations $s = \infty$, dipole-dipole interaction $s = 3$, to the long-range Coulomb interaction $s = 1$. The introduction of the two tunable (s and σ) properties illuminates both the competition between nonlinearity and dispersion and the interplay of long range interactions and lattice discreteness. Equation (4.9) can be derived from the Hamiltonian

$$H = T + U_\sigma, \tag{4.10}$$

where

$$T = \frac{1}{2} \sum_{n,m(n\neq m)} |m-n|^{\perp s} |\psi_m - \psi_n|^2, \tag{4.11}$$

is the dispersive energy of the excitation and

$$U_\sigma = -\frac{1}{(\sigma+1)} \sum_n |\psi_n|^{2(\sigma+1)} \tag{4.12}$$

is the potential energy of the excitation. We are interested in stationary solutions of Eq. (4.9) of the form

$$\psi_n = \phi_n \exp(i\Lambda t) \tag{4.13}$$

with a real valued shape function ϕ_n and a nonlinear frequency Λ. The functions ϕ_n are determined by

$$\Lambda\phi_n = \sum_{m(m\neq n)} |n-m|^{\perp s}(\phi_m - \phi_n) + \phi_n^{(2\sigma+1)}. \tag{4.14}$$

In contrast to the continuum model of Sec.4.3 the discrete model (4.9) cannot be solved analytically. Therefore we apply a variational approach with the trial function

$$\phi_n = \left(N \frac{\sinh\alpha}{\cosh\{\alpha(2\delta-1)\}} \right)^{\frac{1}{2}} \exp(-\alpha|n-\delta|) \tag{4.15}$$

where α is a trial parameter and δ is the position of the center of the localized state which without loss of generality can be restricted to $0 \leq \delta < 1$ for the infinite chain. The ansatz (4.15) is chosen to automatically satisfy the normalization condition $\sum_n \phi_n^2 = N$ reducing the variational approach to determining α by $dH/d\alpha = 0$. Performing some rather lengthy manipulations (see Paper XII for details) we can minimize the energy of the state (4.15) and thereby implicitly find the dependence N on Λ for the stationary state. Applying this result we shall study for in detail the stationary states of the system, considering the following two types of stationary states: on-site (Sievers-Takeno mode) ($\delta = 0$) and inter-site (Page mode) ($\delta = 1/2$) separately. All results are for cubic nonlinearity, $\sigma = 1$.

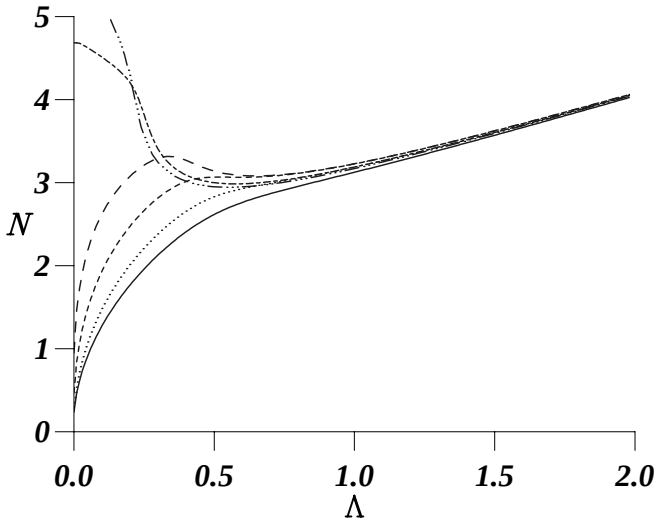

Figure 4.2: Norm N of on-site states ($\delta = 0$) versus the nonlinear frequency Λ numerically obtained from Eq.(4.14) for $s = \infty$ (solid), 4 (dotted), 3 (short-dashed), 2.5 (long-dashed), 2 (short-long-dashed), 1.9 (dashed-dotted)

I. On-site localized states: $\delta = 0$.

Figure 4.2 (Fig. 2 of Paper XII) shows direct numerically obtained dependence $N(\Lambda)$. A monotonic function is obtained for $s > s_{cr}$, but for $s_{cr} > s > 2$ the dependence becomes nonmonotonic with a local maximum and a local minimum. These extrema coalesce at $s \simeq 2.72$ (from the analytical approach) and $s = s_{cr} \simeq 3.03$ (from the numerical solution of Eq.(4.14)). For $s < 2$ the local maximum disappears. Thus the main features of all DNLS models with a power law dispersive interaction decreasing faster than $|n-m|^{\perp s_{cr}}$ coincide qualitatively with the features obtained in the nearest-neighbor approximation

where only one on-site stationary state exists for any norm. However, in the case of the nonlocal NLS equation (4.9) with $2 < s < s_{cr}$ there exist for each N in the interval $[N_l(s), N_u(s)]$ three stationary states with nonlinear frequencies $\Lambda_1(N) < \Lambda_2(N) < \Lambda_3(N)$. In particular, this means that in the case of dipole-dipole interaction ($s = 3$) multiple solutions exist. This property of the system is very similar to the bistability phenomenon observed in the two-dimensional case described in Sec. 3.5. Also in the nearest-neighbor case of Eq.(4.9) the bistability phenomenon exists [116, 117] when the degree of nonlinearity σ exceeds some critical value.

Investigating the stability properties of the different stationary states, we use the approach developed in [116] and find that the positive definiteness of the dispersion term T given by Eq.(4.11) and the form of the nonlinear term U permit generalization of the result of Laedke, Spatschek and Turitsyn [116] to this nonlocal case. According to this result the necessary and sufficient stability criterion for on-site stationary states is again similar to that of Vakhitov-Kolokolov Eq.(1.30). Thus in the notation of the present section

$$\frac{dN}{d\Lambda} = \frac{d}{d\Lambda} \sum_n \phi_n^2 > 0. \tag{4.16}$$

Therefore we can conclude that in the interval $[N_l(s), N_u(s)]$ there are only two linearly stable stationary states ($\Lambda_1(N)$ and $\Lambda_3(N)$). The third state is unstable since $\frac{dN}{d\Lambda} < 0$ at $\Lambda = \Lambda_2$.

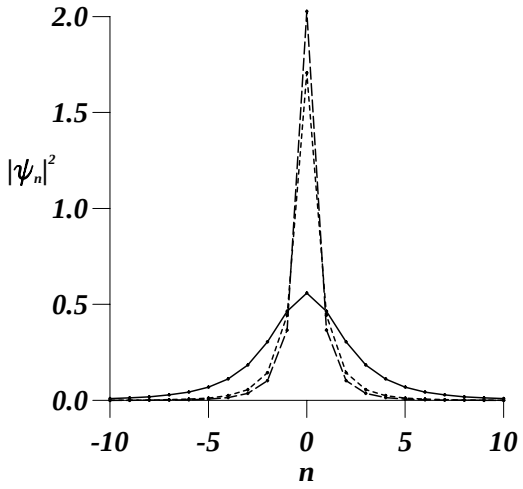

Figure 4.3: Shapes of the three stationary states for $s = 2.5$ and $N = 3.1$. The stable: $\Lambda = 0.21$ (long-dashed), $\Lambda = 0.74$ (solid). The unstable: $\Lambda = 0.57$ (short-dashed).

Figure 4.3 shows that the three solutions differ significantly. The low frequency states are wide and continuum-like while the high frequency solutions

represent intrinsically localized states with a width of a few lattice spacings. For $s \gtrsim 2$ the inverse widths of the stable stationary states are respectively

$$\alpha_1 \approx (\frac{N}{8J})^{\frac{1}{(s-2)}} = (\frac{N}{8J})^{\frac{\ln l}{1-2\ln l}}, \quad \alpha_3 \approx \ln(\frac{N}{J}) \tag{4.17}$$

where $l = \exp(1/s)$ is the characteristic range of the dispersive interaction. It follows from these expressions that the existence of two so different soliton states for one value of the norm, N, is due to the presence of two different length scales in the system: the usual scale of the NLS model which is related to the competition between nonlinearity and dispersion (expressed in terms of the ratio N/J) and the range of the dispersive interaction l.

Paper XII finds that the particular value $s = 2$ separates two different kinds of behavior: for $s > 2$, $H \to 0$ while for $1 < s < 2$, $H \to \infty$ as $N \to 0$ and the stable continuum-like soliton disappears. This is confirmed by our simulation (see Fig. 4.2), which also indicates that the low frequency solitons in this case ($s < 2$) have algebraic tails i.e., for $s = 1.9$, $\log \phi_n \simeq 6.3 - 2 \log n$ when $n \gg 1$. The existence of excitations with algebraic tails or the so-called *algebraic solitons* in models with nonlocal interaction is well known [224]. Algebraic solitons have also recently [225, 108, 226] been found in generalized Schrödinger equations with two competing nonlinearities. However, as in the nonlocal case these solitons are unstable [226].

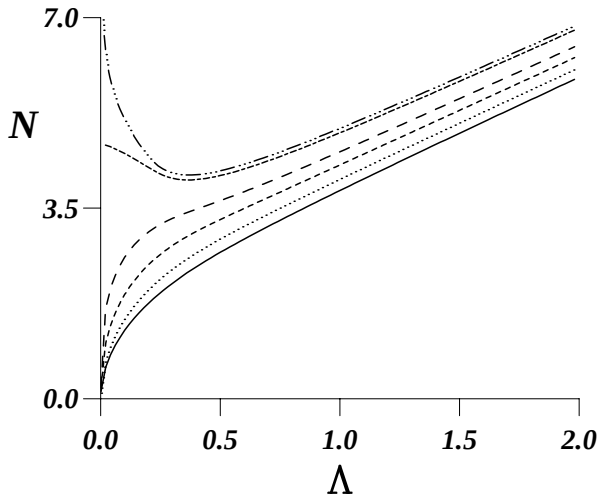

Figure 4.4: Norm N of inter-site states ($\delta = 1/2$) versus the nonlinear frequency Λ numerically obtained from Eq.(4.14) for $s = \infty$ (solid), 4 (dotted), 3 (short-dashed), 2.5 (long-dashed), 2 (short-long-dashed), 1.9 (dashed-dotted)

II. Inter-site localized states: $\delta = 1/2$.

In Fig. 4.4 we plot the norm, N, as a function of nonlinear frequency Λ for inter-site localized states obtained from numerical solution of Eq.(4.14). The analytical results for $\delta = 1/2$ are in qualitative agreement with numerical results but the quantitative agreement is not as good as in the on-site soliton case. The dependence displayed in Fig. 4.4 is similar to the dependence $N(\Lambda)$ obtained for on-site localized states (Fig. 4.2); the main distinction being that the inter-site states are much less sensitive to the long range character of the dispersion.

For the parity conserving (even) perturbations the stability condition of inter-site stationary states is the same as (4.16) but these excitations are unstable with respect to parity nonconserving perturbations. Typically the evolution of these excitations will result in that an initially inter-site state is transformed into an intrinsically localized on-site state with a time-dependent width.

Now we turn to discussing stationary states of the discrete NLS model given by Eq.(4.9) with arbitrary power nonlinearity. The main properties of the system remain unchanged but the critical value of the dispersion parameter s_{cr} is now a function of σ. The results of analytical consideration confirmed by the

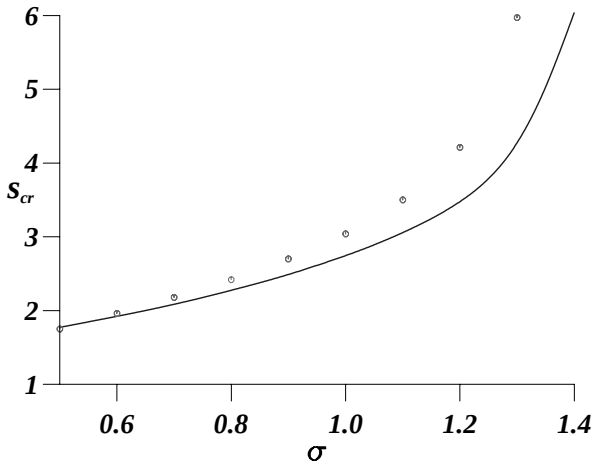

Figure 4.5: Critical dispersion parameter, $s_{\rm cr}$, versus the power nonlinearity, σ. Analytical dependence (solid), numerical dependence (circles). Only results for inter-site states are shown.

simulation (Fig. 4.5) show that s_{cr} increases when σ increases. In particular for $\sigma \geq 1.4$ (the value at which discrete symmetric ground states can be unstable in the nearest-neighbor approximation [116] whereas Malomed and Weinstein [117] found the critical value to $\sigma \simeq 1.32$ due to the approximative character of their

variational approach) the bistability in the nonlinear energy spectrum occurs even for $s \geq 6$. As discussed in Sec.1.3.2 the behavior of the one-dimensional system with quintic nonlinearity ($\sigma = 2$) is qualitatively the same as the behavior of the two-dimensional systems with cubic nonlinearity. Then, it may be expected that the bistability phenomenon takes place in two-dimensional NLS models with quadrupole-quadrupole interaction ($s = 5$).

Finally, Paper XII shows analytically that only for $s > 3$ the localized states of Eq.(4.9) are exponentially localized. When the dispersion parameter s is in the range $2 < s < 3$ the localized states are merely algebraically localized with the long distance behavior $\phi_n \propto |n|^{\perp 2}$. This behavior is found for the low frequncy states as well as for the high frequency states.

4.5 Two-dimensional Kronig-Penney model

This section will describe the results of Paper XIII on a two-dimensional nonlinear Kronig-Penney model. Our interest in the Kronig-Penney model [227] arises from its application in describing electromagnetic wave propagation through dielectric media. Particularly, we are interested in electromagnetic wave propagation in dielectric superlattices. In the approximation where only the scalar nature of the electromagnetic field is taken into account, the wave propagation is resembled by the dynamics of a particle in a crystal lattice [228, 229]. As a result of the periodicity photonic bands and gaps arises, giving the system the name *photonic band-gap materials*.

In the case of periodic nonlinear superlattices consisting of alternating layers of two dielectrics, it is usually assumed that the nonlinearity of one of the dielectrics is much larger than the nonlinearity of the other, so that the latter can be considered linear. If the thickness of the nonlinear layer is small compared to the thickness of the linear, the problem can be described by the nonlinear Kronig-Penney model

$$i\psi_t + \nabla^2\psi + \sum_n \delta(x - x_n)|\psi|^2\psi = 0, \tag{4.18}$$

corresponding to a focusing medium with a Kerr nonlinearity. Here $x_n = n\,\ell$ is the coordinate of the n-th nonlinear layer and ℓ is the distance between adjacent nonlinear layers. Wave propagation in the framework of the one-dimensional nonlinear Kronig-Penney model was studied in detail in Ref. [228–231], but in these works the coupling between the longitudinal and transversal degrees of freedom was ignored. It was shown that the transmission properties depend critically on the injected wave power. Additionally, it was shown that these systems exhibit bistability and multistability.

In Paper XIII we consider two-dimensional effects in the nonlinear Kronig-Penney model given by Eq.(4.18) where the complex amplitude depends on the coordinate x transversal to the nonlinear layers and the longitudinal coordinate z.

Similarly to the approach used in Refs. [230] and [231], we can solve these equations in the linear medium and thereby express the field $\psi(x,z;t)$ for $n\ell \leq x \leq (n+1)\ell$, in terms of the complex amplitudes, $\psi_n(z,t) \equiv \psi(x_n,z;t)$ at the nonlinear layers,

$$\begin{aligned}\psi(x,z;t) &= \frac{\sinh(\hat{\kappa}((n+1)\ell - x))}{\sinh(\hat{\kappa}\ell)}\,\psi_n(z,t) \\ &+ \frac{\sinh(\hat{\kappa}(x - n\ell))}{\sinh(\hat{\kappa}\ell)}\,\psi_{n+1}(z,t), \end{aligned} \tag{4.19}$$

where the complex amplitude $\psi_n(z,t)$ satisfies the following set of pseudo-differential equations

$$\frac{\bar{}\,\hat{\kappa}}{\sinh \ell\hat{\kappa}}(\psi_{n+1} + \psi_{n\perp 1}) - \frac{2\hat{\kappa}}{\tanh \ell\hat{\kappa}}\,\psi_n + |\psi_n|^2\,\psi_n = 0, \tag{4.20}$$

with periodic boundary conditions $\psi_{n+\upsilon} = \psi_n$ where υ is the number of layers. In Eqs.(4.19) and (4.20) the operator $\hat{\kappa}$ is defined as

$$\hat{\kappa}\psi = \sqrt{-i\partial_t - \partial_z^2}\,\psi. \tag{4.21}$$

More information on how to interpret this operator can be found in Paper XIII.

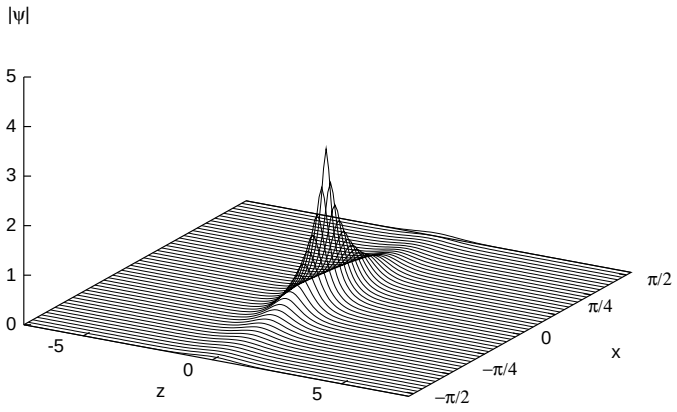

Figure 4.6: Stationary state localized in the longitudinal direction with $\lambda^2 = 5.0$ The spacing between the nonlinear layers is $\ell = \pi$ so the nonlinear layers are positioned at $x = ..., -\pi, 0, \pi, ...\psi(x+\ell,z,t) = \psi(x,z,t)$.

Paper XIII hereafter uses techniques similar to those of Paper XI to investigate solutions of the form

$$\psi_n(z,t) = \phi_n(z)\, e^{i\lambda^2 t} \tag{4.22}$$

where λ^2 is the nonlinear frequency and $\phi_n(z)$ the amplitude in the n-th nonlinear layer. Since Eq.(4.20) is Galilean invariant, standing excitations can always be Galileo boosted to any velocity in the z-direction. It is found that indeed such solutions are possible (an example is shown in Fig.4.6 (Fig.2 of Paper XIII)) but there is a maximum norm $N_m = N(\lambda_m)$ above which no solutions of the kind (4.22) can exist. It is also shown that these solutions are linearly stable with respect to perturbations in the z direction as long as $\lambda < \lambda_m$. However there is also a source of instability in perturbations along the x direction and therefor the stationary solution are only stable as long as the following inequality is satisfied

$$\lambda^2 \;<\; \frac{1}{\ell^2}\min\{\frac{4}{3}\sin^2(\frac{\pi}{\upsilon}), \lambda_m^2\}. \tag{4.23}$$

In particular, this means that the stationary state $\psi_n(z,t) = e^{i\lambda^2 t}\phi(z)$ is neither stable in the case of only one nonlinear layer ($\ell \to \infty$) nor in the quasi-continuum limit ($\upsilon \to \infty$).

Finally, Paper XIII shows that the system described by Eq.(4.18) also supports states which are localized in both spatial directions and not uniform from nonlinear layer to nonlinear layer as the example shown in Fig.(4.6).

4.6 Conclusion

The present chapter has reviewed the work described in the papers Paper XI, Paper XII and Paper XIII which all deal with nonlinear equation with nonlocal dispersion.

A short description of the physical origin of the long range interaction was given. As a first step a continuum NLS equation with nonlocal dispersion was studied. The equation being continuum allowed the stationary states to be found analytically. This model showed that there is an upper limit for the norm in the presence of the long range interaction term, and as a special case this model has a cusp soliton as an analytical solution.

The chapter continued the discussion of the nonlocal effects by considering a power law transfer mechanism in discrete NLS models. This was shown to lead to bistable stationary states due to the presence of different length scales of the problem. The bistability displayed itself by allowing a broad state and a very narrow state to exist, with the same norm. Both on-site states (Sievers-Takeno modes) and inter-site (Page modes) where shown to exists, and the inter-site state appeared to be less sensitive to the long range interaction. However, as in the case of the nearest-neighbor coupling, the inter-site state was shown to be unstable with respect to parity disturbing perturbations.

Finally, the chapter showed how the two-dimensional Kronig-Penney problem of electromagnetic wave propagation in nonlinear superlattices can be regarded as a nonlocal problem. The localized states of this problem were then studied from this perspective.

Bibliography

[1] O. Bang, P. L. Christiansen, F. If, K. Ø. Rasmussen, and Yu. B. Gaididei, Phys. Rev. E **49**, 4627 (1994).

[2] O. Bang, P. L. Christiansen, F. If, K. Ø. Rasmussen, and Yu. B. Gaididei, Appl. Anal. **57**, 3 (1995).

[3] K. Ø. Rasmussen, Yu. B. Gaididei, O. Bang, and P. L. Christiansen, Phys. Lett. A **204**, 121 (1995).

[4] P. L. Christiansen, K. Ø. Rasmussen, O. Bang, and Yu. B. Gaididei, Physica D **87**, 321 (1995).

[5] P. L. Christiansen, Yu. B. Gaididei, M. Johansson, K. Ø. Rasmussen, and I. I. Yakimenko, Phys. Rev. E **54**, 924 (1996).

[6] Yu. B. Gaididei, K. Ø. Rasmussen, and P. L. Christiansen, Phys. Rev. E **52**, 2951 (1995).

[7] Yu. B. Gaididei, K. Ø. Rasmussen, and P. L. Christiansen, Phys. Lett. A **203**, 175 (1995).

[8] D. Hennig, K. Ø. Rasmussen, H. Gabriel, and A. Bülow, Phys. Rev. E **54**, 5788 (1996).

[9] P. L. Christiansen, Yu. B. Gaididei, M. Johansson, and K. Ø. Rasmussen, Phys. Rev. B **55**, 5759 (1997).

[10] P. L. Christiansen, K. Ø. Rasmussen, Yu. B. Gaididei, V. K. Mezentsev, and J. Juul Rasmussen, Phys. Rev. B **54**, 900 (1996).

[11] Yu. B. Gaididei, S. F. Mingaleev, P. L. Christiansen, and K. Ø. Rasmussen, Phys. Lett. A **222**, 152 (1996).

[12] Yu. B. Gaididei, S. F. Mingaleev, P. L. Christiansen, and K. Ø. Rasmussen, Phys. Rev. E **55**, (1997).

[13] Yu. B. Gaididei, P. L. Christiansen, K. Ø. Rasmussen, and M. Johansson, Phys. Rev. B **55**, 13365 (1997).

[14] K. Ø. Rasmussen, D. Cai, A. R. Bishop, and N. Grønbech-Jensen, Phys. Rev. E **55**, 6141 (1997).

[15] K. Ø. Rasmussen, O. Bang, and P. L. Christiansen, Phys. Lett. A **184**, 241 (1994).

[16] K. Ø. Rasmussen, Yu. B. Gaididei, O. Bang, and P. L. Christiansen, Math. Comp. Sim. **40**, 339 (1996).

[17] D. Hennig, K. Ø. Rasmussen, G. P. Tsironis, and H. Gabriel, Phys. Rev. E **52**, R4628 (1995).

[18] Yu. B. Gaididei, S. F. Mingaleev, I. I. Yakimenko, P. L. Christiansen, M. Johansson, and K. Ø. Rasmussen, Phys. Scr. **T67**, 151 (1996).

[19] O. Bang, P. L. Christiansen, K. Ø. Rasmussen, and Yu. B. Gaididei, in *Nonlinear excitations in biomolecules*, edited by M. Peyrard (Les Editions de Physique and Springer, Berlin, 1995), p. 317.

[20] P. L. Christiansen, K. Ø. Rasmussen, O. Bang, and Yu. B. Gaididei, in *Fluctuation phenomena: Disorder and Nonlinearity*, edited by A. R. Bishop, S. Jiménez, and L. Vázquez (World Scientific, Singapore, 1994), p. 38.

[21] P. L. Christiansen, K. Ø. Rasmussen, M. Johansson, Yu. B. Gaididei, and O. Bang, in *Nonlinear Klein-Gordon and Schrödinger systems: Theory and Applications*, edited by L. Vázquez, L. Streit, and V. M. Pérez-García (World Scientific, Singapore, 1996), p. 215.

[22] Yu. B. Gaididei, K. Ø. Rasmussen, P. L. Christiansen, and S. F. Mingaleev, in *Proceedings of the Conference on Nonlinear Coherent Structures in Physics and Biology*, edited by D. B. Duncan and J. C. Eilbeck (Published on WWW. http://www.ma.hw.ac.uk/solitons/procs, Heriot-Watt University, Edinburgh, 1995).

[23] P. L. Christiansen, M. Johansson, K. Ø. Rasmussen, Yu. B. Gaididei, and I. I. Yakimenko, in *Proceedings of the 9'th Conference of the European Consortium for Mathematics in Industry*, edited by M. Brøns (Teubner, Stuttgart, 1997), to appear.

[24] P. L. Christiansen, Yu. B. Gaididei, V. K. Mezentsev, S. L. Musher, K. Ø. Rasmussen, J. Juul Rasmussen, I. V. Ryzhenkova, and S. K. Turitsyn, Phys. Scr. **T67**, 160 (1996).

[25] K. Ø. Rasmussen, P. L. Christiansen, M. Johansson, Yu. B. Gaididei, and S. F. Mingaleev, in *Fluctuations, Nonlinearity and Disorder*, edited by G. P. Tsironis (Elsevier in Physica D, Amsterdam, 1997), to appear.

[26] K. Ø. Rasmussen, P. L. Christiansen, M. Johansson, and Yu. B. Gaididei, in *Nonlinear Dynamics of Heterogeneous and Microstructured solids*, edited by J. Engelbrecht (Proceedings of the Estonian National Academy of Science, Tallin, 1997), to appear.

[27] L. Bergé, M. R. Schmidt, J. Juul Rasmussen, P. L. Christiansen, and K. Ø. Rasmussen, J. Opt. Soc. Am , submitted 1996.

[28] A. C. Newell and J. V. Moloney, *Nonlinear Optics* (Addison-Wiley, Amsterdam, 1992).

[29] G. G. Luther, A. C. Newell, and J. V. Moloney, Physica D **74**, 59 (1994).

[30] L. Bergé and J. Juul Rasmussen, Phys. Plasma **3**, 824 (1996).

[31] J. K. Ranka, R. W. Schirmer, and A. L. Gaeta, Phys. Rev. Lett. **77**, 3783 (1996).

[32] A. Hasegawa and F. Tappert, Appl. Phys. Lett. **23**, 142 (1973); *ibid.* **23**, 171 (1973).

[33] H. Hasegawa and Y. Kodama, *Solitons in Optical Communications* (Claredon Press, Oxford, 1995).

[34] Y. Kodama and A. Hasegawa, IEEE J. Ouantum Electron. **23**, 5610 (1987).

[35] M. Gedalin, T. C. Scott, and Y. B. Band, Phys. Rev. Lett. **78**, 448 (1997).

[36] E. M. Gromov, Phys. Lett. A **227**, 678 (1997).

[37] L. Bergé, J. Juul Rasmussen, and J. Wyller, J. Phys. A: Math. Gen. **29**, 3581 (1996).

[38] D. N. Christodoulides and R. I. Joseph, Opt. Lett. **13**, 794 (1988).

[39] A. B. Aceves, C. De Angelis, G. G. Luther, A. M. Rubenchik, and S. K. Turitsyn, Physica D **87**, 262 (1995).

[40] A. B. Aceves, G. G. Luther, C. De Angelis, A. M. Rubenchik, and S. K. Turitsyn, Phys. Rev. Lett. **75**, 73 (1995).

[41] T. Taniuti, Prog. Theor. Phys. Suppl. **55**, 1 (1974).

[42] T. Taniuti and N. Yajima, J. Math. Phys. **10**, 1369 (1969); N. Asano and T. Taniuti and N. Yajimai *ibid.* **10**, 2020 (1969).

[43] V. E. Zakharov, Zh. Eksp. Teor. Fiz. **62**, 1745 (1972), [Sov. Phys. JETP **35**, 908 (1972)].

[44] Y. S. Kivshar and B. A. Malomed, Rev. Mod. Phys. **61**, 763 (1989).

[45] N. W. Ashcroft and N. D. Mermin, *Solid State Physics* (Saunders College Publishing, Orlando, 1976).

[46] T. Holstein, Ann. Phys. **8**, 325 (1959).

[47] D. W. Brown, K. Lindenberg, and B. West, Phys. Rev. B **37**, 2946 (1988).

[48] V. M. Kenkre, Physica D **68**, 153 (1993).

[49] A. Davydov, Phys. Scr. **20**, 387 (1979).

[50] A. S. Davydov, *Solitons in Molecular Systems* (D. Reidel Publishing Company, Dordrecht, 1985).

[51] A. C. Scott, Phys. Rep. **217**, 1 (1992).

[52] in *Davydovs' Soliton Revisited*, edited by P. L. Christiansen and A. C. Scott (Plenum, New York, 1990).

[53] M. Lakshmanan, Phys. Lett. A **61**, 53 (1977).

[54] E. H. Lieb, Phys. Rev. **130**, 1616 (1963).

[55] G. Scheibe, Angew. Chem. **49**, 563 (1936).

[56] G. Feher and M. Y. Okamura, in *The photosynthetic bacteria*, edited by R. K. Clayton and W. F. Sirtronm (Plenum, New York, 1978), p. 349.

[57] I. Langmuir, J. Am. Chem. Soc. **39**, 1848 (1917); K. B. Blodgett, *ibid.* **57**, 1007 (1935).

[58] H. Bücher and H. Kuhn, Chem. Phys. Lett. **6**, 183 (1970).

[59] D. Möbius and H. Kuhn, Isr. J. Chem. **18**, 375 (1979).

[60] D. Möbius and H. Kuhn, J. Appl. Phys. **64**, 5138 (1988).

[61] H. P. Dorn and A. Müller, Appl. Phys. B **43**, 167 (1987).

[62] S. De Boer and D. A. Wiersma, Chem. Phys. Lett. **165**, 45 (1990).

[63] T. Itoh, T. Ikehara, and Y. Iwabuchi, J. Lumin **45**, 29 (1990).

[64] J. Feldman, G. Peter, E. O. Göbel, P. Dawson, K. Moore, C. Foxon, and R. J. Elliott, Phys. Rev. Lett. **59**, 2337 (1987).

[65] L. M. Blinov, Russ. Chem. Rev. **52**, 713 (1983).

[66] R. H. Tredgold, Rep. Prog. Phys. **50**, 1609 (1987).

[67] F. C. Spano and S. Mukamel, J. Chem. Phys. **91**, 683 (1989).

[68] F. C. Spano, J. R. Kuklinski, and S. Mukamel, Phys. Rev. Lett. **65**, 211 (1990).

[69] E. A. Bartnik, K. J. Blinowska, and J. A. Tuszyński, Phys. Lett. A **159**, 67 (1991).

[70] E. A. Bartnik, K. J. Blinowska, and J. A. Tuszyński, Nanobiology **1**, 239 (1992).

[71] E. A. Bartnik, K. J. Blinowska, and J. A. Tuszyński, Phys. Lett. A **169**, 46 (1992).

[72] E. A. Bartnik and J. A. Tuszyński, Phys. Rev. E **48**, 1516 (1993).

[73] G. C. Huth, F. Gutmann, and G. Vitiello, Phys. Lett. A **140**, 339 (1989).

[74] P. L. Christiansen, S. Pagano, and G. Vitiello, Phys. Lett. A **154**, 381 (1991).

[75] P. L. Christiansen, O. Bang, S. Pagano, and G. Vitiello, Nanobiology **1**, 229 (1992).

[76] A. S. Davydov, J. Theor. Biol. **38**, 559 (1973).

[77] F. Calogero, in *What Is Integrability?*, edited by V. E. Zakharov (Springer-Verlag, Berlin, 1991).

[78] C. S. Gardner, J. M. Green, M. D. Kruskal, and R. M. Miura, Phys. Rev. Lett. **19**, 1095 (1967).

[79] P. D. Lax, Commun. Pure Appl. Math. **21**, 467 (1968).

[80] V. E. Zakharov and A. B. Shabat, Zh. Eksp. Teor. Fiz. **61**, 118 (1971), [Sov. Phys. JETP **34**, 62 (1972)].

[81] M. J. Ablowitz, D. J. Kaup, A. C. Newell, and H. Segur, Phys. Rev. Lett. **31**, 125 (1973).

[82] M. J. Ablowitz, D. J. Kaup, A. C. Newell, and H. Segur, Stud. Appl. Math. **53**, 249 (1974).

[83] A. C. Scott, F. Y. F. Chu, and D. W. McLaughlin, Proc. IEEE **61**, 1443 (1973).

[84] G. L. Lamb, *Elements of Soliton Theory* (Wiley, New York, 1980).

[85] M. J. Ablowitz and H. Segur, *Solitons and the Inverse Scattering Transform* (SIAM, Philadelphia, 1981).

[86] F. Calogero and A. Degasperis, *Spectral Transforms and Solitons* (North-Holland, Amsterdam, 1982).

[87] R. K. Dodd, J. C. Eilbeck, J. D. Gibbon, and H. C. Morris, *Solitons and Nonlinear Wave Equations* (Academic Press, London, 1982).

[88] A. C. Newell, *Solitons in Mathematics and Physics* (SIAM, Philadelphia, 1985).

[89] P. Drazin and R. Johnson, *Solitons: an introduction* (Cambridge University Press, Cambridge, 1989).

[90] J. Satsuma and N. Yajima, Prog. Theo. Phys. Suppl. **284**, 284 (1974).

[91] D. J. Kaup, SIAM J. Appl. Math. **31**, 121 (1976).

[92] V. I. Karpmann, Zh. Eksp. Teor. Phys. **25**, 296 (1977), [JETP Lett. **25**, 271 (1977)].

[93] V. I. Karpmann and E. M. Maslov, Zh. Eksp. Teor. Fiz. **73**, 537 (1977), [Sov. Phys. JETP **46**, 281 (1977)].

[94] D. J. Kaup and A. C. Newell, Proc. R. Soc. London, Ser. A **361**, 413 (1978).

[95] A. Bondeson, M. Lisak, and D. Anderson, Phys. Scr. **20**, 479 (1979).

[96] G. B. Whitham, *Linear and Nonlinear Waves* (Wiley, New York, 1974).

[97] R. Blaha, E. W. Laedke, and K. H. Spatschek, in *Nonlinear Dispersive Waves*, edited by L. Debnath (World Scientific, Singapore, 1991).

[98] B. A. Malomed, Wave Motion **9**, 401 (1987).

[99] R. Scharf and A. R. Bishop, Phys. Rev. E **47**, 1375 (1993).

[100] J. G. Caputo, N. Flytzanis, and M. P. Sørensen, J. Opt. Soc. Am. B **12**, 139 (1995).

[101] B. Bendow, P. D. Gianino, and N. Tzoar, J. Opt. Soc. Am. **6**, 656 (1981).

[102] M. Desaix, D. Anderson, and M. Lisak, J. Opt. Soc. Am. B **8**, 2082 (1991).

[103] L. Bergé, Phys. Lett. A **189**, 290 (1994).

[104] M. Desaix, D. Anderson, and M. Lisak, Phys. Rev. E **50**, 2253 (1994).

[105] A. Berntson, D. Anderson, and M. Lisak, Phys. Scr. **52**, 544 (1995).

[106] V. V. Afanasjev, Phys. Rev. E **52**, 3153 (1995).

[107] V. M. Pérez-García, M. A. Porras, and L. Vázquez, Phys. Lett. A **202**, 176 (1995).

[108] D. E. Pelinovsky, V. Afanasjev, and Yu. S. Kivshar, Phys. Rev. E **53**, 1940 (1996).

[109] L. Bergé, J. Juul Rasmussen, E. A. Kuznetsov, E. G. Shapiro, and S. K. Turitsyn, J. Opt. Soc. Am. B **13**, 1879 (1996).

[110] R. I. Chiao, E. Garmire, and C. H. Townes, Phys. Rev. Lett. **13**, 479 (1964).

[111] G. Fibich, V. M. Malkin, and G. C. Papanicolaou, Phys. Rev. A **52**, 4218 (1995).

[112] V. E. Zakharov, V. V. Sobolev, and V. S. Synakh, Zh. Eksp. Teor. Fiz. **60**, 136 (1971), [Sov. Phys. JETP **33**, 77 (1971)].

[113] V. E. Zakharov and V. S. Synakh, Zh. Eksp. Teor. Fiz. **68**, 940 (1975), [Sov. Phys. JETP **41**, 465 (1975)].

[114] A. W. Snyder and D. J. Mitchell, Opt. Lett. **18**, 101 (1993).

[115] O. Bang, J. Juul Rasmussen, and P. L. Christiansen, Nonlinearity **7**, 205 (1994).

[116] E. W. Laedke, K. H. Spatschek, and S. K. Turitsyn, Phys. Rev. Lett. **73**, 1055 (1994), [E. W. Laedke, O. Kluth and K. H. Spatschek, Phys. Rev. E **54**, 4299 (1996)].

[117] B. Malomed and M. I. Weinstein, Phys. Lett. A **220**, 91 (1996).

[118] M. G. Vakhitov and A. A. Kolokolov, Izv. Vyssh. Uch. Zav. Radiofizika **16**, 1020 (1973), [Radiophys. Quantum Electron. **16**, 783 (1973)].

[119] M. I. Weinstein, Comments Pure Appl. Math. **39**, 51 (1986).

[120] O. Bang, Ph.D. thesis, Laboratory for Mathematical Physics, The Technical University of Denmark, 1993.

[121] J. Juul Rasmussen and K. Rypdal, Phys. Scr. **33**, 481 (1986); K. Rypdal and J. Juul Rasmussen, **33**, 498 (1986).

[122] M. V. Goldman and D. R. Nicholson, Phys. Rev. Lett. **41**, 406 (1978).

[123] S. N. Vlasov, V. A. Petrishchev, and V. I. Talanov, Izv. Vys. Uchebn. Zaved. Radiofiz. **14**, 1353 (1971), [Radiophys. Quantum Electron. **14**, 1062 (1974)].

[124] E. A. Kuznetsov, J. Juul Rasmussen, K. Rypdal, and S. K. Turitsyn, Physica D **87**, 273 (1995).

[125] E. A. Kuznetsov, Chaos **6**, 381 (1996).

[126] M. I. Weinstein, Commun. Math. Phys. **87**, 567 (1983).

[127] J. Ginibre and G. Velo, J. Funct. Anal. **32**, 33 (1979).

[128] A. S. Davydov, *Quantum Mechanics* (Pergamon, Oxford, 1965).

[129] C. W. Gardiner, *Handbook of Stochastic Methods* (Springer-Verlag, Berlin, 1983).

[130] H. Haken, *Synergetics* (Springer-Verlag, Berlin, 1978).

[131] H. Haken, *Advanced Synergetics* (Springer-Verlag, Berlin, 1983).

[132] P. Langevin, Comptes. Rendues **146**, 530 (1908).

[133] H. Risken, *The Fokker-Planck Equation* (Springer-Verlag, Berlin, 1984).

[134] D. Anderson, M. Bonnedal, and M. Lisak, Phys. Fluids **22**, 1838 (1979).

[135] W. Horsthemke and R. Lefevre, *Noise-Induced Transitions* (Springer-Verlag, Berlin, 1984).

[136] Y. Nogami and F. M. Toyama, Phys. Rev. E **49**, 4497 (1994).

[137] D. W. McLaughlin, G. C. Papanicolaou, C. Sulem, and P. L. Sulem, Phys. Rev. A **34**, 1200 (1986).

[138] J. T. Manassah, Opt. Lett. **17**, 1259 (1992).

[139] V. P. Ermakov, Univ. Izv. Kiev **20**, 1 (1880).

[140] E. Pinney, Proc. Amer. Math. Soc. **1**, 681 (1950).

[141] A. J. Lichtenberg and M. A. Lieberman, *Regular and Stochastic Motion* (Springer-Verlag, Berlin, 1983).

[142] L. D. Landau and E. M. Lifshitz, *Mechanics* (Pergamon, Oxford, 1960).

[143] J. S. Hesthaven, J. P. Lynov, A. H. Nielsen, J. Juul Rasmussen, M. R. Schmidt, E. A. Shapiro, and S. K. Turitsyn, Phys. Fluids **7**, 2220 (1995).

[144] M. J. Ablowitz and J. F. Ladik, J. Math. Phys. **17**, 1011 (1976).

[145] M. J. Ablowitz and J. F. Ladik, Stud. Appl. Math. **65**, 213 (1976).

[146] N. N. Bogolyubov and A. K. Prikarpatskii, Dokl. Akad. Nauk SSSR **262**, 1103 (1982), [Sov. Phys. Dokl. **27**, 113 (1976)].

[147] P. Marquié, J. M. Bilbault, and M. Remoissenet, Phys. Rev. E **51**, 6127 (1995).

[148] T. R. Taha and M. J. Ablowitz, J. Comp. Phys. **55**, 192 (1984).

[149] T. R. Taha and M. J. Ablowitz, J. Comp. Phys. **55**, 203 (1984).

[150] R. Scharf and A. R. Bishop, Phys. Rev. A **43**, 6535 (1991).

[151] V. V. Konotop, Phys. Rev. E **47**, 1423 (1993).

[152] V. Konotop, O. A. Chubykalo, and L. Vázquez, Phys. Rev. E **48**, 563 (1993).

[153] D. Cai, A. R. Bishop, N. Grønbech-Jensen, and M. Salerno, Phys. Rev. Lett. **74**, 1186 (1995).

[154] H. H. Chen and C. S. Lui, Phys. Rev. Lett. **37**, 693 (1976); Phys. Fluids **21**, 377 (1978).

[155] A. G. Izergin and V. E. Korepin, Dokl. Akad. Nauk SSSR **259**, 76 (1981).

[156] L. D. Faddeev and L. A. Takhtajan, *Hamiltonian Methods in the Theory of Solitons* (Springer-Verlag, Berlin, 1986).

[157] A. C. Scott and L. MacNeil, Phys. Lett. **98**, 87 (1983).

[158] J. C. Eilbeck, P. S. Lomdahl, and A. C. Scott, Physica D **16**, 318 (1985).

[159] B. M. Herbst and M. J. Ablowitz, Phys. Rev. Lett. **62**, 2065 (1989).

[160] J. C. Eilbeck, P. S. Lomdahl, and A. C. Scott, Phys. Rev. B **30**, 4703 (1984).

[161] A. C. Scott, P. S. Lomdahl, and J. C. Eilbeck, Chem. Phys. Lett. **113**, 29 (1985).

[162] Complete collection of the papers which cite J. C. Eilbeck, P. S. Lomdahl and A. C. Scott, Physica D, **16**, 318, (1985), collected by J. C. Eilbeck and available on the www address: http://www.ma.hw.ac.uk/ chris/dst/dst.bib.

[163] A. B. Aceves, C. De Angelis, A. M. Rubenchik, and S. K. Turitsyn, Opt. Lett. **19**, 329 (1994).

[164] A. B. Aceves, C. De Angelis, S. Trillo, and S. Wabnitz, Opt. Lett. **19**, 332 (1994).

[165] V. M. Kenkre and D. K. Campbell, Phys. Rev. B **34**, 4959 (1986).

[166] A. S. Davydov and N. I. Kislukha, Phys. Status Solidi B **59**, 465 (1973).

[167] N. Finlayson and G. I. Stegman, Appl. Phys. Lett. **56**, 2276 (1990).

[168] Y. Chen, A. W. Snyder, and D. J. Mitchell, Electron. Lett. **26**, 77 (1990).

[169] M. I. Molina, W. D. Deering, and G. P. Tsironis, Physica D **66**, 135 (1993).

[170] S. M. Jensen, IEEE J. Quantum Electron. **QE-18**, 1580 (1982); J. H. Jensen, P. L. Christiansen, J. N. Elgin, J. D. Gibbon and O. Skovgaard; S. De Filippo, G. M. Fusci and M. Salerno, Physica D **26**, 411 (1987); *ibid.* **29**, 421 (1988); S. De Filippo and M. Salerno, Phys. Lett. A **142**, 479 (1989); L. Cruzeiro-Hansson, H. Feddersen, R. Flesch, P. L. Christiansen, M. Salerno and A. C. Scott, Phys. Rev. B **42**, 522 (1990); D. Hennig, J. Phys. A: Math. Gen. **25**, 1247 (1992); D. Hennig, Physica D **64**, 121 (1993); D. Hennig, H. Gabriel, M. F. Jørgensen, P. L. Christiansen and C. B. Clausen, Phys. Rev. E, **51**, 2807 (1995); D. Hennig and H. Gabriel J. Phys. A: Math. Gen. **28**, 3749 (1995).

[171] M. Salerno, Phys. Rev. A **46**, 6856 (1992).

[172] D. Cai, A. R. Bishop, and N. Grønbech-Jensen, Phys. Rev. Lett. **72**, 591 (1994).

[173] A. A. Vakhnenko and Yu. B. Gaididei, Teor. Mat. Fiz. **68**, 350 (1986), [Theor. Math. Phys. **68**, 873 (1987)].

[174] D. Cai, A. R. Bishop, and N. Grønbech-Jensen, Phys. Rev. E **53**, 4131 (1996).

[175] A. J. Sievers and S. Takeno, Phys. Rev. Lett. **61**, 970 (1988).

[176] J. B. Page, Phys. Rev. B **41**, 7835 (1990).

[177] S. R. Bickham, S. A. Kiselev, and A. J. Sievers, Phys. Rev. B **47**, 14206 (1993).

[178] T. Dauxois, M. Peyrard, and C. R. Willis, Physica D **57**, 267 (1992); Phys. Rev. E **48**, 4768 (1993).

[179] Yu. S. Kivshar, Phys. Rev. E **48**, 4123 (1993).

[180] S. Flach, C. R. Willis, and E. Olbrich, Phys. Rev. E **49**, 836 (1994).

[181] S. Flach and C. R. Willis, Phys. Lett. A **181**, 232 (1993).

[182] C. Claude, Yu. S. Kivshar, K. H. Spatschek, and O. Kluth, Phys. Rev. B **47**, 14228 (1992).

[183] S. Aubry, Physica D **86**, 284 (1995).

[184] P. W. Anderson, Phys. Rev. **109**, 1492 (1958); Rev. Mod. Phys. **50**, 191 (1978).

[185] M. Johansson, Ph.D. thesis, Department of Physics and Measurement Technology, Linköping University, 1995.

[186] S. A. Gredeskul and Y. S. Kivshar, Phys. Rep. **216**, 1 (1992).

[187] M. I. Molina and G. P. Tsironis, Phys. Rev. Lett. **73**, 464 (1994).

[188] D. L. Shepelyansky, Phys. Rev. Lett. **70**, 1787 (1993).

[189] M. Johansson and R. Riklund, Phys. Rev. B **49**, 6587 (1994).

[190] D. K. Campbell and M. Peyrard, in *Chaos*, edited by D. K. Campbell (Am. Inst. of Phys., New York, 1990), p. 305.

[191] D. Cai, A. R. Bishop, and N. Grønbech-Jensen, Phys. Rev. E **52**, R5784 (1995); *ibid.* **53**, 1202 (1996).

[192] M. Johansson and S. Aubry, Nonlinearity , in press.

[193] V. V. Konotop and S. Takeno, Phys. Rev. E **54**, 2010 (1996).

[194] D. Hennig, N. G. Sun, H. Gabriel, and G. P. Tsironis, Phys. Rev. E **52**, 255 (1995).

[195] S. Aubry and G. Abramovici, Physica D **43**, 199 (1990).

[196] S. Aubry, Physica D **71**, 196 (1994).

[197] R. S. MacKay and S. Aubry, Nonlinearity **7**, 1623 (1994).

[198] V. E. Zakharov and A. B. Shabat, Sov. Phys. JETP **37**, 823 (1973).

[199] S. Wiggins, *Introduction to Applied Nonlinear Dynamical Systems and Chaos* (Springer-Verlag, Berlin, 1990).

[200] J. Greene, J. Math. Phys. **20**, 1183 (1979).

[201] J. Coste and J. Peyrard, Phys. Rev. B **39**, 13086 (1989).

[202] Y. Wan and C. M. Soukoulis, Phys. Rev. A **41**, 800 (1990).

[203] E. Tabacman, Physica D **85**, 548 (1995).

[204] K. W. Sandusky, J. P. Page, and K. E. Schmidt, Phys. Rev. B **46**, 6161 (1992).

[205] M. L. Glasser, V. G. Papageorgiou, and T. C. Bountis, SIAM J. Appl. Math. **49**, 692 (1989).

[206] Y. S. Kivshar and D. K. Campbell, Phys. Rev. E **48**, 3077 (1993).

[207] R. F. Peierls, Proc. R. Soc. London **52**, 34 (1940); F. R. N. Nabarro *ibid.* **59**, 256 (1947).

[208] K. Ø. Rasmussen, D. Cai, A. R. Bishop, and N. Grønbech-Jensen (unpublished).

[209] R. Camassa, G. Kovačič, and S. Tin, , preprint; G. Haller, preprint.

[210] M. I. Molina and G. P. Tsironis, Physica D **65**, 267 (1993).

[211] L. J. Bernstein, K. W. DeLong, and N. Finlayson, Phys. Lett. A **181**, 135 (1993).

[212] M. Johansson, M. Hörnquist, and R. Riklund, Phys. Rev. B **52**, 231 (1995).

[213] V. K. Mezentsev, S. L. Musher, I. V. Ryzhenkova, and S. K. Turitsyn, Pis'ma Zh. Eksp. Teor. Fiz. **60**, 815 (1994), [JETP Lett., **60**, 829 (1994)].

[214] E. W. Laedke, K. H. Spatshek, V. K. Mezentsev, S. L. Musher, I. V. Ryzhenkova, and S. K. Turitsyn, Pis'ma Zh. Eksp. Teor. Fiz. **62**, 652 (1995), [JETP Lett. **62**, 677 (1995)].

[215] Y. Ishimori, Prog. Theor. Phys. **68**, 402 (1982).

[216] P. Woafo, J. R. Kenne, and T. C. Kofane, J. Phys. Condens. Matter **5**, L123 (1993).

[217] G. A. Baker Jr, Phys. Rev. **122**, 1477 (1961); M. Kac and E. Helfand, J. Math. Phys., **4**, 1078 (1963).

[218] L. Váquez, W. A. B. Evans, and G. Rickayzen, Phys. Lett. A **189**, 454 (1994).

[219] Yu. Gaididei, N. Flytzanis, A. Neuper, and F. G. Mertens, Phys. Rev. Lett. **75**, 2240 (1995).

[220] O. M. Braun, Yu. S. Kivshar, and I. I. Zelenskaya, Phys. Rev. B **41**, 7118 (1990); A. Dikande and T. C. Kofane, Physica D **83**, 450 (1995); G. L. Alfimov, V. M. Eleonskii, N. E. Kulagin, and N. V. Mitskevich, Chaos **3**, 405 (1993).

[221] F. V. Kusmartsev, Phys. Rep. **183**, 1 (1989).

[222] P. K. A. Wai, H. H. Chen, and Y. C. Lee, Phys. Rev. A **41**, 426 (1990); H. H. Kuehl and C.Y. Zhang, Phys. Fluids B, **2**, 889 (1990); V. I. Karpman, Phys. Rev. E, **47**, 2073 (1993); V. I. Karpman, Phys. Lett. A **181**, 211 (1993).

[223] K. Ø. Rasmussen, Yu. B. Gaididei, S. F. Mingaleev, and P. L. Christiansen (unpublished).

[224] Y. Matsuno, Int. J. Mod. Phys. B **17**, 1985 (1995).

[225] K. Hayata and M. Koshiba, Phys. Rev. E **51**, 1499 (1995).

[226] R. W. Micallef, V. V. Afanasjev, Yu. S. Kivshar, and J. D. Love, Phys. Rev. E **54**, 2936 (1996).

[227] R. de L. Kronig and W. G. Penney, Proc. R. Soc. London, Ser. A **130**, 499 (1931).

[228] D. Hennig, H. Gabriel, G. P. Tsironis, and M. Molina, Appl. Phys. Lett. **64**, 2934 (1994).

[229] D. Hennig, N. G. Sun, G. P. Tsironis, and S. Pnevmatikos, *Stationary properties of one-dimensional nonlinear lattices* (Erasmus Monograph 'Mathematics and Fundamental Applications', Heraklion, 1995).

[230] Q. Li, C. T. Chan, K. M. Ho, and C. M. Soukoulis, Phys. Rev. B **53**, 15577 (1996); E. Lidorikis, Q. Li and C. M. Soukoulis; *ibid.* **54**, 10249 (1996).

[231] N. G. Sun and G. P. Tsironis, in *Photonic Band Gap Materials*, edited by C. M. Soukoulis (Kluwer, London, 1996), p. 535.